UNIVERSITÉ DE MONTRÉAL

SIMULATION OF A CIRCULATING FLUIDIZED BED COMBUSTOR USING ASPEN PLUS

Par

Rahmat SOTUDEH GHAREBAAGH

DÉPARTEMENT DE GÉNIE CHIMIQUE

ÉCOLE POLYTECHNIQUE

MÉMOIRE PRÉSENTÉ EN VUE DE L'OBTENTION

DU GRADE DE MAÎTRE ÈS SCIENCES APPLIQUÉES (M.Sc.A.)

AVRIL 1994

© droits réservés de Rahmat SOTUDEH GHAREBAAGH 1994.

National Library of Canada
Bibliothèque nationale du Canada

Acquisitions and Bibliographic Services Branch
Direction des acquisitions et des services bibliographiques

395 Wellington Street
Ottawa, Ontario
K1A 0N4

395, rue Wellington
Ottawa (Ontario)
K1A 0N4

Your file Votre référence

Our file Notre référence

The author has granted an irrevocable non-exclusive licence allowing the National Library of Canada to reproduce, loan, distribute or sell copies of his/her thesis by any means and in any form or format, making this thesis available to interested persons.

L'auteur a accordé une licence irrévocable et non exclusive permettant à la Bibliothèque nationale du Canada de reproduire, prêter, distribuer ou vendre des copies de sa thèse de quelque manière et sous quelque forme que ce soit pour mettre des exemplaires de cette thèse à la disposition des personnes intéressées.

The author retains ownership of the copyright in his/her thesis. Neither the thesis nor substantial extracts from it may be printed or otherwise reproduced without his/her permission.

L'auteur conserve la propriété du droit d'auteur qui protège sa thèse. Ni la thèse ni des extraits substantiels de celle-ci ne doivent être imprimés ou autrement reproduits sans son autorisation.

ISBN 0-315-93370-4

Canada

om Rahmat SOTUDEH GHAREBAAGH

ssertation Abstracts International est organisé en catégories de sujets. Veuillez s.v.p. choisir le sujet qui décrit le mieux votre èse et inscrivez le code numérique approprié dans l'espace réservé ci-dessous.

Génie chimique

SUJET

0542

CODE DE SUJET

U·M·I

atégories par sujets

IUMANITÉS ET SCIENCES SOCIALES

MMUNICATIONS ET LES ARTS

chitecture 0729
aux-arts 0357
bliothéconomie 0399
néma 0900
mmunication verbale 0459
mmunications 0708
nse 0378
stoire de l'art 0377
urnalisme 0391
sique 0413
iences de l'information 0723
éâtre 0465

UCATION

énéralités 515
dministration 0514
t 0273
ollèges communautaires 0275
ommerce 0688
onomie domestique 0278
lucation permanente 0516
lucation préscolaire 0518
lucation sanitaire 0680
nseignement agricole 0517
nseignement bilingue et multiculturel 0282
nseignement industriel 0521
nseignement primaire. 0524
nseignement professionnel 0747
nseignement religieux 0527
nseignement secondaire 0533
nseignement spécial 0529
nseignement supérieur 0745
valuation 0288
nances 0277
ormation des enseignants 0530
istoire de l'éducation 0520
ngues et littérature 0279
Lecture 0535
Mathématiques 0280
Musique 0522
Orientation et consultation 0519
Philosophie de l'éducation 0998
Physique 0523
Programmes d'études et enseignement 0727
Psychologie 0525
Sciences 0714
Sciences sociales 0534
Sociologie de l'éducation 0340
Technologie 0710

LANGUE, LITTÉRATURE ET LINGUISTIQUE

Langues
- Généralités 0679
- Anciennes 0289
- Linguistique 0290
- Modernes 0291

Littérature
- Généralités 0401
- Anciennes 0294
- Comparée 0295
- Médiévale 0297
- Moderne 0298
- Africaine 0316
- Américaine 0591
- Anglaise 0593
- Asiatique 0305
- Canadienne (Anglaise) 0352
- Canadienne (Française) 0355
- Germanique 0311
- Latino-américaine 0312
- Moyen-orientale 0315
- Romane 0313
- Slave et est-européenne 0314

PHILOSOPHIE, RELIGION ET THÉOLOGIE

Philosophie 0422
Religion
- Généralités 0318
- Clergé 0319
- Études bibliques 0321
- Histoire des religions 0320
- Philosophie de la religion 0322

Théologie 0469

SCIENCES SOCIALES

Anthropologie
- Archéologie 0324
- Culturelle 0326
- Physique 0327

Droit 0398
Économie
- Généralités 0501
- Commerce-Affaires 0505
- Économie agricole 0503
- Économie du travail 0510
- Finances 0508
- Histoire 0509
- Théorie 0511

Études américaines 0323
Études canadiennes 0385
Études féministes 0453
Folklore 0358
Géographie 0366
Gérontologie 0351
Gestion des affaires
- Généralités 0310
- Administration 0454
- Banques 0770
- Comptabilité 0272
- Marketing 0338

Histoire
- Histoire générale 0578
- Ancienne 0579
- Médiévale 0581
- Moderne 0582
- Histoire des noirs 0328
- Africaine 0331
- Canadienne 0334
- États-Unis 0337
- Européenne 0335
- Moyen-orientale 0333
- Latino-américaine 0336
- Asie, Australie et Océanie 0332

Histoire des sciences 0585
Loisirs 0814
Planification urbaine et régionale 0999
Science politique
- Généralités 0615
- Administration publique 0617
- Droit et relations internationales 0616

Sociologie
- Généralités 0626
- Aide et bien-être social 0630
- Criminologie et établissements pénitentiaires 0627
- Démographie 0938
- Études de l' individu et de la famille 0628
- Études des relations interethniques et des relations raciales 0631
- Structure et développement social 0700
- Théorie et méthodes. 0344
- Travail et relations industrielles 0629

Transports 0709
Travail social 0452

SCIENCES ET INGÉNIERIE

CIENCES BIOLOGIQUES

griculture
- Généralités 0473
- Agronomie. 0285
- Alimentation et technologie alimentaire 0359
- Culture 0479
- Élevage et alimentation 0475
- Exploitation des pâturages 0777
- Pathologie animale 0476
- Pathologie végétale 0480
- Physiologie végétale 0817
- Sylviculture et faune 0478
- Technologie du bois 0746

iologie
- Généralités 0306
- Anatomie 0287
- Biologie (Statistiques) 0308
- Biologie moléculaire 0307
- Botanique 0309
- Cellule 0379
- Écologie 0329
- Entomologie 0353
- Génétique 0369
- Limnologie 0793
- Microbiologie 0410
- Neurologie 0317
- Océanographie 0416
- Physiologie 0433
- Radiation 0821
- Science vétérinaire 0778
- Zoologie 0472

Biophysique
- Généralités 0786
- Medicale 0760

SCIENCES DE LA TERRE

Biogéochimie 0425
Géochimie 0996
Géodésie 0370
Géographie physique 0368
Géologie 0372
Géophysique 0373
Hydrologie 0388
Minéralogie 0411
Océanographie physique 0415
Paléobotanique 0345
Paléoécologie 0426
Paléontologie 0418
Paléozoologie 0985
Palynologie 0427

SCIENCES DE LA SANTÉ ET DE L'ENVIRONNEMENT

Économie domestique 0386
Sciences de l'environnement 0768
Sciences de la santé
- Généralités 0566
- Administration des hipitaux 0769
- Alimentation et nutrition 0570
- Audiologie 0300
- Chimiothérapie 0992
- Dentisterie 0567
- Développement humain 0758
- Enseignement 0350
- Immunologie 0982
- Loisirs 0575
- Médecine du travail et thérapie 0354
- Médecine et chirurgie 0564
- Obstétrique et gynécologie 0380
- Ophtalmologie 0381
- Orthophonie 0460
- Pathologie 0571
- Pharmacie 0572
- Pharmacologie 0419
- Physiothérapie 0382
- Radiologie 0574
- Santé mentale 0347
- Santé publique 0573
- Soins infirmiers 0569
- Toxicologie 0383

SCIENCES PHYSIQUES

Sciences Pures

Chimie
- Généralités 0485
- Biochimie 487
- Chimie agricole 0749
- Chimie analytique 0486
- Chimie minérale 0488
- Chimie nucléaire 0738
- Chimie organique 0490
- Chimie pharmaceutique 0491
- Physique 0494
- PolymÇres 0495
- Radiation 0754

Mathématiques 0405
Physique
- Généralités 0605
- Acoustique 0986
- Astronomie et astrophysique 0606
- Electronique et électricité 0607
- Fluides et plasma 0759
- Météorologie 0608
- Optique 0752
- Particules (Physique nucléaire) 0798
- Physique atomique 0748
- Physique de l'état solide 0611
- Physique moléculaire 0609
- Physique nucléaire 0610
- Radiation 0756

Statistiques 0463

Sciences Appliqués Et Technologie

Informatique 0984
Ingénierie
- Généralités 0537
- Agricole 0539
- Automobile 0540
- Biomédicale 0541
- Chaleur et ther modynamique 0348
- Conditionnement (Emballage) 0549
- Génie aérospatial 0538
- Génie chimique ..... 0542 ✓
- Génie civil 0543
- Génie électronique et électrique 0544
- Génie industriel 0546
- Génie mécanique 0548
- Génie nucléaire 0552
- Ingénierie des systèmes 0790
- Mécanique navale 0547
- Métallurgie 0743
- Science des matériaux 0794
- Technique du pétrole 0765
- Technique minière 0551
- Techniques sanitaires et municipales 0554
- Technologie hydraulique 0545

Mécanique appliquée 0346
Géotechnologie 0428
Matières plastiques (Technologie) 0795
Recherche opérationnelle 0796
Textiles et tissus (Technologie) 0794

PSYCHOLOGIE

Généralités 0621
Personnalité 0625
Psychobiologie 0349
Psychologie clinique 0622
Psychologie du comportement 0384
Psychologie du développement 0620
Psychologie expérimentale 0623
Psychologie industrielle 0624
Psychologie physiologique 0989
Psychologie sociale 0451
Psychométrie 0632

Name _____

Dissertation Abstracts International is arranged by broad, general subject categories. Please select the one subject which most nearly describes the content of your dissertation. Enter the corresponding four-digit code in the spaces provided.

_____ SUBJECT TERM

| | | | | SUBJECT CODE

U·M·I

Subject Categories

THE HUMANITIES AND SOCIAL SCIENCES

COMMUNICATIONS AND THE ARTS
Architecture 0729
Art History 0377
Cinema 0900
Dance 0378
Fine Arts 0357
Information Science 0723
Journalism 0391
Library Science 0399
Mass Communications 0708
Music 0413
Speech Communication 0459
Theater 0465

EDUCATION
General 0515
Administration 0514
Adult and Continuing 0516
Agricultural 0517
Art 0273
Bilingual and Multicultural 0282
Business 0688
Community College 0275
Curriculum and Instruction 0727
Early Childhood 0518
Elementary 0524
Finance 0277
Guidance and Counseling 0519
Health 0680
Higher 0745
History of 0520
Home Economics 0278
Industrial 0521
Language and Literature 0279
Mathematics 0280
Music 0522
Philosophy of 0998
Physical 0523
Psychology 0525
Reading 0535
Religious 0527
Sciences 0714
Secondary 0533
Social Sciences 0534
Sociology of 0340
Special 0529
Teacher Training 0530
Technology 0710
Tests and Measurements 0288
Vocational 0747

LANGUAGE, LITERATURE AND LINGUISTICS
Language
- General 0679
- Ancient 0289
- Linguistics 0290
- Modern 0291

Literature
- General 0401
- Classical 0294
- Comparative 0295
- Medieval 0297
- Modern 0298
- African 0316
- American 0591
- Asian 0305
- Canadian (English) 0352
- Canadian (French) 0355
- English 0593
- Germanic 0311
- Latin American 0312
- Middle Eastern 0315
- Romance 0313
- Slavic and East European 0314

PHILOSOPHY, RELIGION AND THEOLOGY
Philosophy 0422
Religion
- General 0318
- Biblical Studies 0321
- Clergy 0319
- History of 0320
- Philosophy of 0322

Theology 0469

SOCIAL SCIENCES
American Studies 0323
Anthropology
- Archaeology 0324
- Cultural 0326
- Physical 0327

Business Administration
- General 0310
- Accounting 0272
- Banking 0770
- Management 0454
- Marketing 0338

Canadian Studies 0385
Economics
- General 0501
- Agricultural 0503
- Commerce-Business 0505
- Finance 0508
- History 0509
- Labor 0510
- Theory 0511

Folklore 0358
Geography 0366
Gerontology 0351
History
- General 0578
- Ancient 0579
- Medieval 0581
- Modern 0582
- Black 0328
- African 0331
- Asia, Australia and Oceania 0332
- Canadian 0334
- European 0335
- Latin American 0336
- Middle Eastern 0333
- United States 0337

History of Science 0585
Law 0398
Political Science
- General 0615
- International Law and Relations 0616
- Public Administration 0617

Recreation 0814
Social Work 0452
Sociology
- General 0626
- Criminology and Penology 0627
- Demography 0938
- Ethnic and Racial Studies 0631
- Individual and Family Studies 0628
- Industrial and Labor Relations 0629
- Public and Social Welfare 0630
- Social Structure and Development 0700
- Theory and Methods 0344

Transportation 0709
Urban and Regional Planning 0999
Women's Studies 0453

THE SCIENCES AND ENGINEERING

BIOLOGICAL SCIENCES
Agriculture
- General 0473
- Agronomy 0285
- Animal Culture and Nutrition 0475
- Animal Pathology 0476
- Food Science and Technology 0359
- Forestry and Wildlife 0478
- Plant Culture 0479
- Plant Pathology 0480
- Plant Physiology 0817
- Range Management 0777
- Wood Technology 0746

Biology
- General 0306
- Anatomy 0287
- Biostatistics 0308
- Botany 0309
- Cell 0379
- Ecology 0329
- Entomology 0353
- Genetics 0369
- Limnology 0793
- Microbiology 0410
- Molecular 0307
- Neuroscience 0317
- Oceanography 0416
- Physiology 0433
- Radiation 0821
- Veterinary Science 0778
- Zoology 0472

Biophysics
- General 0786
- Medical 0760

EARTH SCIENCES
Biogeochemistry 0425
Geochemistry 0996
Geodesy 0370
Geology 0372
Geophysics 0373
Hydrology 0388
Mineralogy 0411
Paleobotany 0345
Paleoecology 0426
Paleontology 0418
Paleozoology 0985
Palynology 0427
Physical Geography 0368
Physical Oceanography 0415

HEALTH AND ENVIRONMENTAL SCIENCES
Environmental Sciences 0768
Health Sciences
- General 0566
- Audiology 0300
- Chemotherapy 0992
- Dentistry 0567
- Education 0350
- Hospital Management 0769
- Human Development 0758
- Immunology 0982
- Medicine and Surgery 0564
- Mental Health 0347
- Nursing 0569
- Nutrition 0570
- Obstetrics and Gynecology 0380
- Occupational Health and Therapy 0354
- Ophthalmology 0381
- Pathology 0571
- Pharmacology 0419
- Pharmacy 0572
- Physical Therapy 0382
- Public Health 0573
- Radiology 0574
- Recreation 0575
- Speech Pathology 0460
- Toxicology 0383

Home Economics 0386

PHYSICAL SCIENCES

Pure Sciences
Chemistry
- General 0485
- Agricultural 0749
- Analytical 0486
- Biochemistry 0487
- Inorganic 0488
- Nuclear 0738
- Organic 0490
- Pharmaceutical 0491
- Physical 0494
- Polymer 0495
- Radiation 0754

Mathematics 0405
Physics
- General 0605
- Acoustics 0986
- Astronomy and Astrophysics 0606
- Atmospheric Science 0608
- Atomic 0748
- Electronics and Electricity 0607
- Elementary Particles and High Energy 0798
- Fluid and Plasma 0759
- Molecular 0609
- Nuclear 0610
- Optics 0752
- Radiation 0756
- Solid State 0611

Statistics 0463

Applied Sciences
Applied Mechanics 0346
Computer Science 0984
Engineering
- General 0537
- Aerospace 0538
- Agricultural 0539
- Automotive 0540
- Biomedical 0541
- Chemical 0542
- Civil 0543
- Electronics and Electrical 0544
- Heat and Thermodynamics 0348
- Hydraulic 0545
- Industrial 0546
- Marine 0547
- Materials Science 0794
- Mechanical 0548
- Metallurgy 0743
- Mining 0551
- Nuclear 0552
- Packaging 0549
- Petroleum 0765
- Sanitary and Municipal 0554
- System Science 0790

Geotechnology 0428
Operations Research 0796
Plastics Technology 0795
Textile Technology 0994

PSYCHOLOGY
General 0621
Behavioral 0384
Clinical 0622
Developmental 0620
Experimental 0623
Industrial 0624
Personality 0625
Physiological 0989
Psychobiology 0349
Psychometrics 0632
Social 0451

UNIVERSITÉ DE MONTRÉAL

ÉCOLE POLYTECHNIQUE

Ce mémoire intitulé:

SIMULATION OF A CIRCULATING FLUIDIZED BED COMBUSTOR USING ASPEN PLUS

présenté par: Rahmat SOTUDEH GHAREBAAGH

en vue de l'obtention du grade de: Maître ès Science Appliquées (M.Sc.A)

a été dûment accepté par le jury d'examen constitué de:

M. GUY Christophe, Ph.D., président

M. LEGROS Robert, Ph.D., membre et directeur de recherche

M. PARIS Jean, Ph.D., membre et co-directeur de recherche

M. ANTHONY Ben, Ph.D., Membre externe (CANMET- Ottawa)

SOMMAIRE

Les ressources pétrolières mondiales sont en voie de tarissement. On évalue à un demi-siècle encore l'exploitation de ces ressources jusqu'à leur épuisement total. Au cours des dernières années, le pétrole a été substitué par une autre source d'énergie en exploitant les importantes réserves de charbon. Le Canada occupe un rang privilégié par rapport aux pays possédant une telle ressource fossile. Même si la teneur en soufre contenu dans le charbon canadien est élevée, la possibilité d'exploitation peut dans un proche avenir s'avérer compétitive sur le marché mondial.

Il existe une nouvelle technologie, dite propre, pour la combustion du charbon en lit fluidisé circulant permettant une réduction considérable des émissions de SO_2 et NO_x. Le SO_2, par exemple, est capturé sous forme solide par du calcaire ou de la dolomite ajouté dans l'alimentation. Au Canada, il existe un certain intérêt pour le développement d'une telle technologie reliée à la combustion du charbon. Au niveaux mondial, on trouve le même intérêt avec de nombreux des projets de construction de Lits Fluidisés Circulants (LFCs) aux Etats-Unis, en Italie, en France, en Allemagne, en Angleterre, au Danemark, en Suède et ailleurs.

Depuis quelques années, on mène beaucoup d'activités de recherche dans le domaine de la modélisation des LFCs afin d'améliorer les efficacités des installations existantes et mieux contrôler les émissions gazeuses. Cet intérêt est due au fait que les LFCs sont considérés comme une technologie efficace qui vise à remplacer les méthodes traditionnelles de combustion dans les applications thermiques de grande puissance.

L'objectif de ce projet est d'effectuer la simulation d'un lit fluidisé circulant (LFC) à l'aide du simulateur de procédés ASPEN PLUS (système avancé pour le génie des procédés) et valider le modèle par les données expérimentales de l'unité pilote à LFC de CANMET existante à Ottawa.

ASPEN PLUS est un excellent outil pour la simulation et l'analyse des procédés en génie chimique qui a été testé depuis longtemps. ASPEN PLUS est un programme de simulation modulaire qui a une libraire d'opération unitaire. Puisqu'il n'existe pas d'opération unitaire dans ASPEN PLUS pour représenter le LFC, on doit développer notre module avec la combinaison des opérations unitaires existantes dans ASPEN PLUS après avoir respectés les aspects hydrodynamiques et réactionnels propres aux LFCs. Donc, nous avons envisagé d'implanter les modules des réacteurs existants sur ASPEN PLUS pour simuler le fonctionnement d'une unité pilot à LFC.

On se propose donc de développer et mettre en oeuvre un modèle de simulation du réacteur pilote de CANMET qui utilise de façon la plus appropriée les capacités d'ASPEN PLUS et incorpore les effets de l'hydrodynamique du réacteur. Normalement, pour simuler le comportement d'un lit fluidisé circulant, il faut intégrer le modèle hydrodynamique et les modèles réactionnels. L'essentiel de ce présent travail consistait à développer des modules mathématiques, programmables en code Fortran, et à les implanter sur ASPEN PLUS pour la caractérisation hydrodynamique, la capture de SO_2 et la cinétique de combustion du char.

Pour modéliser le LFC, on divise le tube de montée en deux parties: la partie dense et la partie diluée. Chacune des parties est se site de certaines réactions de combustion du charbon. En fait, quatre étapes de réactions ont été considérées pour la combustion du charbon :

1- Dévolatilisation et combustion des volatiles

2- Combustion du carbone fixe "char"

3- Formation des NO_x

4- Absorption du SO_2 par l'absorbant

Il faut bien mentionner que toutes les réactions peuvent se produire dans les deux zones du lit, sauf la première réaction qui a lieu uniquement dans la partie dense.

L'approche utilisée pour la simulation du LFC est de diviser le lit en une série de réacteurs. Dans chaque réacteur, des réactions différentes se produisent. Avant d'effectuer ces réactions, il est nécessaire de décomposer le charbon en ses différents composés dans un réacteur RYIELD, afin de les faire réagir séparément. Ce bloc calcule le débit de chacun des composés. Le deuxième réacteur, "RSTOIC ", est utilisé pour la combustion des volatiles et les réactions correspondantes sont les suivantes :

$C + \frac{1}{2}O_2 \Rightarrow CO$	Taux de conversion de carbone=0.3132
$S + O_2 \Rightarrow SO_2$	Taux de conversion de soufre =1.00
$H_2 + \frac{1}{2}O_2 \Rightarrow H_2O$	Taux de conversion d'hydrogène=1.00

Ces taux de conversion sont considérés comme des hypothèses simplificatrices du

problème.

Le courant de sortie du deuxième réacteur est dirigé vers le réacteur parfaitement mélangé RCSTR. Dans ce bloc, les réactions suivantes se produisent :

$$C + \frac{1}{2}O_2 \Rightarrow CO$$

$$CO + \frac{1}{2}O_2 \Rightarrow CO_2$$

Pour simuler ces réactions dans le réacteur RCSTR, un modèle cinétique, en code fortran, a été développé. Le modèle fourni au bloc les données nécessaires pour calculer les conversions du C et du CO.

Un réacteur REQUIL est utilisé pour modéliser la formation de NO_x. Dans ce bloc, les réactions suivantes atteignent l'équilibre:

$$\frac{1}{2}N_2 + \frac{1}{2}O_2 \Rightarrow NO$$

$$\frac{1}{2}N_2 + O_2 \Rightarrow NO_2$$

$$N_2 + \frac{1}{2}O_2 \Rightarrow N_2O$$

Les phénomènes concernant l'absorption de SO_2 dans le LFC ont été modélisés avec un réacteur RSTOIC. Les réactions suivantes se produisent dans ce bloc:

$CaCO_3 \Rightarrow CaO + CO_2$ (Taux de conversion de $CaCO_3$=1.00)

$$CaO + SO_2 + \frac{1}{2}O_2 \Rightarrow CaSO_4$$

Les taux de conversion de la deuxième réaction ont été déterminés à partir d'une cinétique de capture du SO_2 sur des particules de CaO. Cette cinétique fut codée en Fortran et permet de calculer la conversion pour la réaction simulée par le réacteur RSTOIC.

La partie diluée du lit fluidisé a été divisée en trois sections. Dans chaque section, trois phénomènes se produisent. Nous avons considéré que la première étape de la combustion (dévolatilisation et combustion des volatiles) se passe exclusivement dans la partie dense. Pour la fin de la modélisation de la combustion dans chaque zone, on utilise les trois derniers réacteurs appliqués pour la partie dense. Comme le calcaire est une matière non stable, on suppose que la calcination a lieu uniquement dans la partie dense du LFC. L'ordre des réacteurs est comme suit : RCSTR, REQUIL et RSTOIC.

Une des hypothèses simplificatrices de notre simulation est de considérer un écoulement piston pour le gaz et le solide dans la partie diluée. Nous avons modélisé cet effet en utilisant trois réacteurs RCSTR. Chaque section et la partie dense du LFC est caractérisée à l'aide d'une fraction de vide moyenne qui a été exprimée à l'aide d'un modèle hydrodynamique. Le modèle hydrodynamique est incorporé comme bloc Fortran à la simulation.

Le courant de matière de sortie du lit est dirigé dans un séparateur pour soutirer entièrement le solide présent dans le flux de gaz. Ce solide, par la suite, est envoyé dans

un autre séparateur "FSPLIT". La majorité de ce solide est envoyée à la partie dense du LFC et constitue le courant de recirculation du solide dans le LFC. Le reste du solide quitte le système. La valeur typique du taux de recirculation du solide pour le LFC est de 50 kg/(m^2.sec).

Les propriétés physico-chimiques nécessaires pour calculer les différents paramètres dans la simulation ont été obtenues dans la littérature. Les données expérimentales de l'unité pilote à LFC de CANMET à Ottawa ont été utilisées pour valider le modèle. Pour s'assurer une validation du programme de simulation, les valeurs obtenues sur l'unité pilote pour 14 cas différents de conditions opératoires ont été utilisés. Les prédictions du modèle se sont avérées en très bon accord avec les données expérimentales de l'unité.

Notre module de la simulation prédit bien les profils d'oxygène et de monoxyde de carbone, mais l'unité pilote existante à Ottawa ne permet pas d'obtenir ces profils. Par conséquence, il n'a pas été possible de valider les profils prédits par le module de façon quantitative. Durant des essais de combustion dans un LFC qui ont été eu lieu à l'Université de la Colombie Britannique, les profils de concentration d'oxygène et de monoxyde de carbone ont été mesurés. De façon qualitative, la comparaison entre les prédictions du modèle et les profils expérimentaux est raisonnablement concordante.

Finalement, avec l'aide d'ASPEN PLUS, nous avons simulé certains mécanismes physico-chimiques ayant lieu à l'intérieur du LFC. L'évaluation du modèle montre qu'il peut répond aux objectifs initialement fixés.

ABSTRACT

The objective of this project is the development of a design simulation program for Circulating Fluidized Bed coal Combustors (CFBCs) using the ASPEN PLUS simulator. ASPEN PLUS has been widely accepted in the chemical industry as a design tool because of its ability to simulate various chemical processes. Furthermore, ASPEN PLUS has the flexibility to allow the insertion of Fortran codes into the flowsheet computations. For these reasons, ASPEN PLUS was chosen as a framework for the development of a CFBC process simulation. Generally, chemical reactions such as the combustion of coal take place in a wide variety of process and reactor types. In ASPEN PLUS, six models are available for chemical reactor simulations involving solids. However, since there is no CFBC model provided by ASPEN PLUS, we must develop our own using the tools offered by ASPEN PLUS. In order to accurately simulate CFBCs, two models must be developed simultaneously: a hydrodynamic model and a combustion model.

The hydrodynamic model allows the distribution of gas and solids in the CFBC to be determined. Simplifying assumptions were made regarding the hydrodynamic of a CFBC. Our model considers that the CFBC is divided into two regions: a lower region and an upper region. The boundary between these regions is determined by the secondary injection point.

The combustion model allows for the determination of the chemical changes and the heat

released during combustion. The following basic steps of the coal combustion process are considered in the model:

1- Devolatilization and volatile combustion

2- Char combustion

3- NO_x formation

4- SO_2 absorption (Limestone-sulphur dioxide reactions).

To simulate the operation of a CFBC, several ASPEN PLUS unit operation blocks are combined together. To model the lower region, five ASPEN PLUS unit operation blocks, comprising RYIELD (Yield reactor), RSTOIC (Stoichiometric reactor), RCSTR (Continuous stirred tank reactor), REQUIL(Equilibrium reactor) and another RSTOIC are applied in the order listed. To model the upper region, the dilute bed is divided into 3 sections. Three ASPEN PLUS unit operation blocks, RCSTR, REQUIL and RSTOIC are applied in each section. It is assumed that steps 2,3 and 4 in the coal combustion process occur in each section of the upper region and they are modelled using RCSTR, REQUIL and RSTOIC, respectively. For the RCSTR in the lower region and in each section of the upper region, the kinetic models are developed using the data and models from the literature. The developed kinetic models must be inserted into the flowsheet as a subroutine for all unit operation blocks where they are required. A mathematical model has been developed for the absorption of SO_2 in the bed. A mathematical model has also been developed to calculate the mean void fraction in the lower region and in each section of the upper region. All models, which are developed as fortran code, are then nested

in the ASPEN PLUS input file so that the CFBC simulation program may be executed.

The physico-chemical properties needed to compute the various parameters in the simulation model were taken from the literature. Experimental data from a pilot plant at Energy Research laboratories, CANMET-Ottawa, were used to validate our simulation. The predicted results by the model are realistic and favourably agree with the experimental data. The accuracy of data published in the literature regarding the CO combustion rate was also justified. The end product of this study is the first process simulation program for a CFBC unit using ASPEN PLUS.

ACKNOWLEDGEMENT

I would like to express my sincere thanks and appreciation to my supervisors Professor R. Legros, J.Paris and J. Chaouki for their continuous support and invaluable guidance; under their constant enthusiasm and encouragement this work was accomplished.

My thanks are also extended to Dr. F. Preto for his help and generosity in Ottawa.

The members of the exam committee, Professor C. Guy and Dr. B. Anthony, are also acknowledged for their evaluation of this work.

I especially want to thank my colleagues of the Simulation Group of the Chemical Engineering Department for their generous help and understanding.

I am greatly indebted to my friends, especially R. Macline, for their helpful discussion and assistance throughout the course of this study.

My Special thanks are also due to my parents, brothers and sister for all their love and support.

To my wife and my little Hadi, I express my deepest gratitude; without their understanding, patience and prayers, the dream would never have come to reality.

This work was supported by CANMET, I am grateful for this financial support.

TABLE OF CONTENTS

PAGE

Sommaire..... iv

Abstract.....x

Acknowledgement..... xiii

Table of Contents..... xiv

List of Figures..... xviii

List of Tables..... xix

List of Appendices..... xxi

List of Symbols..... xxii

INTRODUCTION..... 1

CHAPTER 1 REACTION MODELS AND CHEMISTRY

1.1 COAL COMBUSTION CHEMISTRY..... 6

1.2 REACTION MODELS..... 11

1.2.1 Devolatilization and volatile combustion..... 12

1.2.2 Char combustion..... 13

1.2.3 NO_x formation..... 14

1.2.4 SO_2 capture..... 14

CHAPTER 2 HYDRODYNAMIC MODELLING

2.1 INTRODUCTION..... 15

2.2 MODEL FORMULATION..... 16

2.2.1 Lower region of the CFBC..... 17

2.2.2 upper region of the CFBC..... 18

CHAPTER 3 DEVELOPMENT OF A CFBC SIMULATION MODEL

3.1 PREVIOUS WORK..... 24

3.1.1 The work of Young on AFBC..... 24

3.1.2 CFBC simulation work at CERCHAR..... 25

3.1.3 CFBC simulation in Calgary..... 26

3.1.4 Lumped modelling approach for a CFBC..... 27

3.2 GENERAL HYPOTHESES OF THE SIMULATION MODEL... 27

3.2.1 Hydrodynamic..... 27

3.2.2 Combustion..... 29

3.3 STEPS INVOLVED IN THE SIMULATION OF A CFBC

USING ASPEN PLUS..... 31

3.4 MODEL DEVELOPMENT AND SIMULATION FLOWSHEET 32

3.4.1 Lower sub-flowsheet..... 38

3.4.1.1 Block RYIELD..... 38

3.4.1.2 Block RSTOIC..... 39

3.4.1.3 Block RCSTR..... 40

3.4.1.4 Block REQUIL..... 48

3.4.1.5 Block RSTOIC..... 49

3.4.2 Upper sub-flowsheet..... 59

3.4.2.1 Block RCSTR..... 61

3.4.2.2 Block REQUIL..... 62

3.4.2.3 Block RSTOIC..... 62

3.4.3 Sep sub-flowsheet..... 69

3.4.3.1 Block CYCLONE..... 70

3.4.3.2 Block FSPLIT..... 70

3.5 VALUE OF FIXED PARAMETERS USED IN THE SIMULATION..... 71

CHAPTER 4 SIMULATION RESULTS AND MODEL VALIDATION

4.1 BLACK BOX APPROACH..... 77

4.1.1 Model hypotheses..... 77

4.1.2 Simulation results..... 78

4.2 SLPC-1 APPROACH..... 79

4.2.1 Simulation diagram for the CANMET CFBC unit..... 79

4.2.2 Simulation convergence..... 82

4.2.3 Simulation results..... 83

4.3 CARBON MONOXIDE COMBUSTION RATE..... 85

4.4 MODEL VALIDATION..... 87

4.4.1 Simulation result analysis..... 104

4.4.1.1 CO_2 content in the flue gas..... 104

4.4.1.2 NO_x emission levels..... 104

4.4.1.3 CO emission levels..... 106

4.4.1.4 SO_2 emission levels..... 107

4.4.1.5 Combustion efficiency..... 109

4.4.1.6 O_2 and CO concentration profiles

within the CFBC..... 110

4.4.1.7 Conclusion..... 114

CHAPTER 5 CONCLUSIONS AND RECOMMENDATION FOR FUTURE WORK

5.1 CONCLUSIONS..... 115

5.2 RECOMMENDATION FOR FUTURE WORK..... 117

REFERENCES..... 118

APPENDICES..... 124

LIST OF FIGURES

1.1 A Schematic of a Circulating Fluidized Bed Combustor..... 3

2.1 Mean Voidage of the Dense Bed of the CFBC as a Function of Superficial Gas Velocities..... 17

2.2 The Variation of Void Fraction with Height in the CFBC..... 23

3.1 A simulation Diagram for the CFBC..... 37

3.2 Direction for Making simulation in the Entire CFBC..... 60

4.1 A Comprehensive Simulation Diagram for the CFBC..... 81

4.2 Comparison Between the Predicted and Experimental NO_x..... 105

4.3 The Predicted and Experimental NO_x in different S/P ratios..... 106

4.4 Comparison Between the Predicted and Experimental CO..... 107

4.5 Comparison Between the Predicted and Experimental SO_2..... 108

4.6 Comparison Between the Predicted and Experimental Combustion Efficiency..... 109

4.7 Typical Concentration Profiles for Oxygen and Carbon Monoxide within the CFBC..... 111

4.8 O_2 Concentration Profile as a Function of Height within the CFBC..... 111

4.9 CO Concentration Profile as a Function of Height within the CFBC..... 112

4.10 O_2 Concentration Profile within the CFBC..... 113

4.11 CO Concentration Profile within the CFBC..... 113

LIST OF TABLES

1.1 Coal Classification Based on the Heating Value and the Fixed Carbon Content..... 7

3.1 The reactor Models Specification Utilized in the Simulation..... 32

3.2 Design Data..... 71

3.3 Physico-chemical Properties used in the Simulation..... 72

3.4 Coal Analysis..... 73

3.5 Particle Size Distribution of Coal Particles..... 74

3.6 Particle Size Distribution of Sorbent Particles..... 75

4.1 BLACK BOX simulation results..... 78

4.2 The Comparison Between Simulation Results for BLACK BOX Approach and SLPC-1 Approach..... 84

4.3 The CFBC Operating Conditions..... 88

4.4 Parameters Utilized to Compare Predicted and Experimental Results Using the CANMET Runs Operating Conditions..... 89

4.5 Comparison Between SLPC-1 Simulation Results for RUN1 and Experimental Data..... 90

4.6 Comparison Between SLPC-1 Simulation Results for RUN2 and Experimental Data..... 91

4.7 Comparison Between SLPC-1 Simulation Results for RUN3 and Experimental Data..... 92

4.8 Comparison Between SLPC-1 Simulation Results for RUN4A and Experimental Data..... 93

4.9 Comparison Between SLPC-1 Simulation Results for RUN4B and Experimental Data..... 94

4.10 Comparison Between SLPC-1 Simulation Results for RUN5 and Experimental Data..... 95

4.11 Comparison Between SLPC-1 Simulation Results for RUN6 and Experimental Data..... 96

4.12 Comparison Between SLPC-1 Simulation Results for RUN7 and Experimental Data..... 97

4.13 Comparison Between SLPC-1 Simulation Results for RUN8 and Experimental Data..... 98

4.14 Comparison Between SLPC-1 Simulation Results for RUN9 and Experimental Data..... 99

4.15 Comparison Between SLPC-1 Simulation Results for RUN10 and Experimental Data..... 100

4.16 Comparison Between SLPC-1 Simulation Results for RUN11 and Experimental Data..... 101

4.17 Comparison Between SLPC-1 Simulation Results for RUN12A and Experimental Data..... 102

4.18 Comparison Between SLPC-1 Simulation Results for RUN12B and Experimental Data..... 103

LIST OF APPENDICES

A.1 ASPEN PLUS Input file..... 124

A.2 User-supplied kinetic subroutine..... 137

A.3 Fortran codes listing..... 145

A.4 A typical calculation for r_c..... 162

A.5 CANMET 0.8 MWth Unit Description..... 164

LIST OF SYMBOLS

A: Cross-sectional area of bed, m^2

a : Decay constant, m^{-1}

a_1 : Parameter defined in Eq. (3.26), sec^{-1}

a_s : External surface area per unit volume of char, m^{-1}

C : Combustion gas concentration, kmole/m^3

C_{O2} : Concentration of oxygen, kmole/m^3

C_{SO2} : SO_2 concentration in the surrounding gas, kmole/m^3

D_C : Cyclone diameter, m

D_{eff}: Effective diffusivity of O_2 in porous char, m^2/sec

D_P : Average sorbent surface particle diameter, cm

D_r : Riser diameter, m

d_p : Average particle diameter of bed particles, m

E_1 : Apparent activation energy, J/kmole

F(y) : Yield distribution vector

F_{air-1} : Mass flowrate of primary air, kg/hr

F_{air-2}: Molar flowrate of secondary air, kg/hr

F_C : Mass flowrate of coal, kg/sec

$F_{char,1}$: Flux of the char particles entering the dense bed, kg/sec

$F_{char,ni}$: Flux of the char particles entering the ni^{th} interval, kg/sec

F_{coal} : Mass flowrate of coal, kg/hr

F_L : Mass flowrate of limestone in the feed,kg/sec

F_{Lime} : Mass flowrate of limestone in the feed,kg/hr

F_r : Froude number

$F_{solid,1}$: Flux of solids entering the dense bed, m^3/sec

$F_{solid,ni}$: Flux of solids entering the nith interval, m^3/sec

F_{tr} : Particle Froude number

f_{CO} : Mole fraction of CO

f_{O2} : Mole fraction of O_2

f_{H2O} : Mole fraction of H_2O

G_s : Net solids circulation flux, kg/m^2_{riser}.sec

g : Acceleration due to gravity, m/sec^2

K : Dimensionless group

K_C : Overall rate constant,m/sec

k_{01} : Pre-exponential factor,m/sec

$k_{11,1}$: Volumetric rate constant for the char combustion,sec^{-1}

$k_{21,ni}$: Volumetric rate constant for the char combustion in the nith interval of the upper region,sec^{-1}

k_{cd} : Diffusion rate constant,m/sec

k_{cr} : Chemical reaction rate constant,m/sec

k_V : Volumetric rate constant,kmole/(m^3-sec)

L_1 : Height of the bed,m

L_1 : Height of dense bed,m

M_{char} : Total mass of the char particles in the bed, kg

$M_a(R_i)$: Reaction matrices in the absorption process

$M_d(R_i)$: Reaction matrices in the devolatiliztion process

m_{char} : Weight of a single particle, kg

$N_{char,1}$: Number of char particles in the dense bed

N_C : Char reaction rate,kmole/ m^2.sec

n_{air-1}: Molar flowrate of primary air,kmole/sec

n_{air-2}: Molar flowrate of secondary air,kmole/sec

n_c : Number of discrete intervals for the coarse particles

n_f : Number of discrete intervals for the fines particles

n_L : Number of size intervals for the sorbent particles

ni : Interval number in the upper region of the CFBC

P : Bed pressure, atm

$P_K(r_C(K))$: Weight fraction vector of char particles in the recirculation stream

$P_{K,0}(r_C(K))$: Weight fraction vector of char particles in the feed

$P_m(R_S(m))$: Weight fraction vector of sorbent particles in the feed

$P_{m,0}(R_S(m))$: Initial weight fraction vector of sorbent particles

R : Universal gas constant, (1.987 kcal/(kmole/.sec))

R_1 : Universal gas constant, (82.06 m.cm^3/(gmole.K))

R_{char} : Rate expression for char combustion per particle, kmole/(sec.particle)

R_g : Universal gas constant,J/(kmole-K)

R_S : Mean sorbent particle radius,cm

$R_s(m)$: Sorbent particle radius vector,cm

$R_{SO2,ni,2}$: Rate of SO_2 per unit volume of the nith interval in the upper region,kmole/m^3.sec

$R_{SO2,1}$: Rate of SO_2 generation per unit volume of dense bed,kmole/m^3.sec

$r_{11,1}$: Char combustion rate per unit volume of the dense bed, kmole/(m^3.sec)

$r_{11,i}$: Char combustion rate, kmole/m^3.sec

$r_{12,i}$: CO combustion rate, kmole/m^3.sec

r_C : Mean coal particle radius, m

$r_C(K)$: Coal particle radius vector, m

r_{CO} : Reaction rate per unit volume of the dense bed, kmole/(m^3.sec)

$r_{21,ni}$: Char combustion rate per unit volume of the nith interval of the dilute bed, kmole/(m^3.sec)

$r_{CO,ni}$: CO combustion rate per unit volume of the nith interval,kg/(m^3.sec)

$r_{SO2,ni,2}$: Mole of SO_2 removed per unit volume of the nith interval,kmole/(m^3.sec)

$r_{SO2,1}$: Rate of removal of SO_2 per unit volume of dense bed,kmole/(m^3.sec)

T_b : Bed temperature, K

T_p : Temperature of the char particles, K

T_{solid} : Mean residence time of solids in the dense bed, sec

t : Time, sec

$t_{ni,2}$: mean residence time of sorbent particles in the nith interval,sec

t_1: mean residence time of sorbent particles in the lower region of bed,sec

U_1 : Superficial gas velocity,m/sec

U_2 : Superficial gas velocity in the dilute bed, m/sec

U_t : Terminal velocity of particles, m/sec

V_C : Volume of the lower region, m^3

V_{CaO}: Molar volume of CaO,m^3/kmole

W_s : Sulphur weight fraction in the dry based coal

$X_{C,d}$: Fractional conversion of carbon in the volatile combustion

$X_{H2,d}$:Fractional conversion of hydrogen in the volatile combustion

$X_{S,,d}$: Fractional conversion of sulphur in the volatile combustion

X_{CaCO3} : Fractional conversion of $CaSO_4$ in the dense bed

X_{CaO}: Fractional conversion of CaO in the dense bed

$X_{CaO,ni,2}$: Fractional conversion of CaO in the ni^{th} interval

X_{CaO} : Fractional conversion of CaO in the dense bed

$Y_{SO2,L1}$: Mole fraction of SO_2 in the dense bed

$Y_{SO2,ni-1,u}$: Mole fraction of SO_2 entering the ni^{th} interval of the upper region

$Y_{SO2,ni,u}$: Mole fraction of SO_2 in the ni^{th} interval

Z : Distance above the lower region,m

Z_{ac} : Length of the acceleration zone,m

Z_{ni} : Corresponding distance for the ni^{th} interval above the lower region,m

Z_{ni-1} : Corresponding distance for the $ni-1^{th}$ interval above the lower region,m

Greek letters

α: External mass transfer coefficient,cm/sec

β : Attrition constant

ΔL : Hight of the nith interval

σ_{SP} : Volume fraction occupied by sorbent particles

ϵ_C : Char porosity

ϵ_I: Porosity of particle after the calcination

$\epsilon_{d,avg}$: Mean voidage of the lower region

$\epsilon_{u,ni,avg}$: Mean axial voidage in the nith interval of the upper region of the CFBC

$\epsilon_{u,3,avg}$: Mean axial voidage in the fully developed zone

ϵ_u : Axial voidage in the acceleration zone

ϵ^* : Axial voidage at saturated conditions

η_{O2} : Effectiveness factor

$\eta_{SO2,ni-1}$: Fractional sulphur capture in the bed with the height of L_1+Z_{ni-1}

$\eta_{SO2,i}$: Fractional conversion of SO_2 in the nith interval of the bed

μ : Viscosity of gaseous combustion product, kg/m.sec

ρ_{char} : Density of char particles,kg/m^3

ρ_g : Density of gaseous combustion product, kg/m^3

ρ_L : Density of limestone particles,kg/m^3

ρ_s : Density of bed solids particles, kg/m^3

ϕ_s: Sphericity

INTRODUCTION

Canada has tremendous coal reserves in its western and maritime provinces. These reserves are sufficiently large to supply Canadians with energy for many years to come. Coal has the potential to satisfy the increasing rate of the world's energy demand. The energy associated with coal is released as the result of a molecular combination which produces more stable components. There are many methods for coal combustion including some traditional ones. Among the newer methods, the fluidized bed combustion received much attention during the 1960's. Circulating Fluidized Bed Combustion (CFBC) technology is being considered as an improvement over the traditional methods associated with the coal combustion. CFBC is a low cost system, easily operated, which can be used to obtain energy from even high sulphur coal in an environmentally acceptable manner. Development of atmospheric CFBC is now passing the fundamental research and experiment stages.

To simulate a CFBC, the reaction models must be treated simultaneously with the hydrodynamic parameters respecting the physico-chemical properties and the operating conditions. In CFBCs, crushed coal, limestone or dolomite and ash particles are fluidized by the combustion air entering the bottom of the bed and the secondary air injection point. The bed into which the coal particles are burning, is in direct contact with the water tubes along the entire riser height, producing very high heat transfer rates, thus enabling a reduction in the size of the unit. In CFBCs, a large portion of the particles exit the bed with the flue gas due to the high superficial gas velocities utilized. These particles are then carried to the cyclone located at the riser outlet. Herein, the particles are separated from the exhaust and recycled into the CFBC to promote complete combustion of the coal. The combustion temperature in the bed is maintained at 850-900°C, which is lower than

the softening temperature of the ash. CFBCs can be operated at ambient pressure or in a pressurized condition. Figure 1.1 shows a schematic of a CFBC.

Combustion efficiency is affected by bed temperature, gas velocity, bed geometry and excess air. In coal combustion, the main interest lies in the heat released during combustion while other factors such as emission control are also of great importance.

The combustion of sulphur containing coal produces nitrogen oxides (NO_x) and sulphur dioxide (SO_2) which are air pollutants. The quantity of NO_x produced depends on the nitrogen content of the fuel, the combustion temperature and the amount of oxygen available for combustion. NO_x forms nitrous and nitric acids with moisture in the air and contributes to environmental pollution. SO_2 produces sulphuric and sulphurous acids in the presence of moisture. These acids constitute the main components of acid rain which contaminates the water source and the ground. To control any further environmental deterioration, the emission of combustion products must seriously be reduced. Furthermore, the combustion of coal results in a variety of other air pollutants. These pollutants are classified as follows (Meyers, 1981):

1- Particulate: (fly ash and carbon particles)

2- Gases: NO_x, CO, N_2O and SO_2

3- Organic Material: hydrocarbons, PCDD and PCDF

4- Trace elements

In the production of electricity from fossil fuels, the engineer must keep all the above factors in mind.

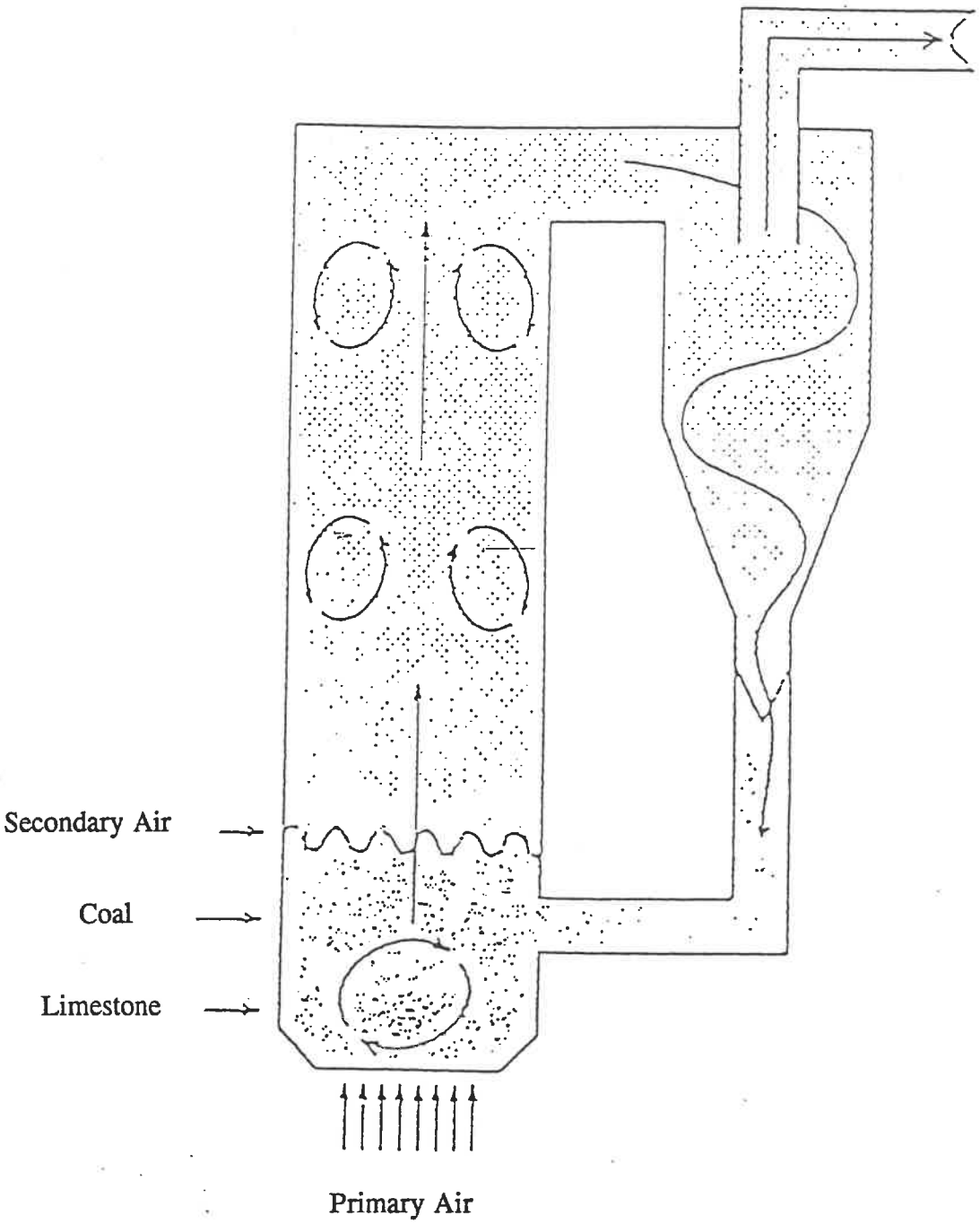

Figure 1.1 A Schematic of a Circulating Fluidized Bed Combustor

The CFBC exhibits several advantages over solid combustion methods especially when high sulphur coal is used. The CFBC, with its large external recirculation and internal structure of solid particles, is an excellent system to handle any solids. These CFBC advantages enable a uniform bed temperature, thus operation of the reactors is isothermal. One major advantage of CFBCs is their ability to desulphurize the combustion gases, allowing environmental standards to be met. Since protecting the environment is an important concern, national, international and regional standards are being defined. Therefore, this feature makes CFBCs an attractive alternative to conventional solid combustion processes.

This study focuses on the modelling CFBCs using the ASPEN PLUS process simulator. ASPEN PLUS has been largely accepted in the chemical industry as a design tool because of its ability to simulate a variety of steady state processes ranging from single unit operation units to complex processes involving many units. In addition, ASPEN PLUS has the flexibility to allow the insertion of Fortran codes into the simulation. Some related work has been performed using the ASPEN PLUS simulator in the past. A brief review of using ASPEN, and its applicability can be found in Douglas and Young (1991). A number of complex processes including a Coal conversion simulation, a Methanol synthesis, the Tri-state indirect-liquefaction process, a pressurized fluidized bed combustion process for electric power generation and modelling and simulation of an Atmospheric Fluidized Bed Combustion (AFBC) have been modelled using ASPEN or ASPEN PLUS. Combustion Engineering Inc. (Wysk, 1982) also used ASPEN in modelling a Lurgi circulating fluid bed. The approach used here has a low level of complexity, the goal being the calculation of the mass and energy balances for the CFBC. This is the same approach that was used by Young (1986). There are many more

examples in the chemical industry showing the vast application of ASPEN PLUS. For these reasons, ASPEN PLUS was chosen as a framework for the development of a CFBC process simulation.

This work will be described over five chapters. The first chapter covers some classical concepts regarding reaction models and chemistry. For the purpose of the simulation, the chemical reactions are classified in term of the main steps describing the main phenomena associated with coal combustion. Chapter 2 is intended to place the hydrodynamic modelling of CFBCs in proper perspective . The information provided in this chapter can be coupled with the reaction models developed in chapter 1 to yield a comprehensive simulation model for CFBCs. Chapter 3 concerns the development of a CFBC simulation model, beginning with the review of some previous works. The development of a simulation model and the required data for the ASPEN PLUS simulation are then presented. The fourth chapter deals with simulation results and model validation, it focuses on the model simulation, validation and studies the emission levels of nitrogen oxides, sulphur dioxide and carbon monoxide. The last chapter provides the conclusion and recommendations for future work. The Appendices contain the ASPEN PLUS input file as well as the computer programs comprising the char particle residence time block, hydrodynamic block, SO_2 capture block and user-supplied kinetics subroutines coded in Fortran.

CHAPTER 1

REACTION MODELS AND CHEMISTRY

In this chapter, the important reaction steps, that occur during coal combustion are presented. These will serve at the basis for the simulation model development.

1.1 COAL COMBUSTION CHEMISTRY

Most of the earth's coal was produced during the carboniferous geological period almost 325 million years ago. (Culp, 1991). The carbohydrate components formed during this process were then converted into hydrocarbon compounds in the absence of air at very high pressures and temperatures. Coal contains carbon, hydrogen, sulphur, oxygen, inorganic mineral matters and moisture. The inorganic mineral materials such as pyrite, quartz and calcite clays can be found in various amounts.

Coal is classified according to its heating value (kJ/kg) and its fixed carbon, the char, contents. The heating value is referred as the heat released during the complete combustion of one kilogram of coal. Table 1.1 shows the coal classification cased on the heating value and the fixed carbon content. Coal is generally represented using the following three analyses:

- The proximate analysis
- The ultimate analysis
- The sulphur analysis

Table 1.1 Coal Classification Based on the Heating Value and the Fixed Carbon Content

Coal type	Fixed carbon content (%)	Heating value (MJ/kg)
1- Anthracite	86 - 95	31.33 - 36.18
2- Bituminous	69 - 86	33.63 - 36.18
3- High Volatile	46 - 69	25.5 - 34.79
4- Sub- bituminous	46 - 60	19.25 - 30.15
5- Lignite	46 - 60	12.76 - 19.25

The proximate analysis provides information about four important characteristics of the coal:

1- The amount of the moisture in the coal

2- The amount of volatile matter (water, gas, oil and tar) liberated by heating and decomposition of the coal.

3- The fixed carbon content remaining after all the volatile matter has been released.

4- The ash content

The ultimate coal analysis yields the mass fraction of carbon (C), Hydrogen (H_2), Oxygen (O_2), Nitrogen (N_2) and Sulphur (S).

The sulphur analysis gives the sulphur mass fraction in different forms. Sulphur components in the coal exist in inorganic (pyritic and sulphate) and organic forms. Organic sulphur is usually removed by cleaning the coal matrix while pyritic sulphur is completely oxidized in the bed. (Cooper and Ellingson, 1984). Often, the amount of energy released during coal combustion is also included in this analysis.

Coal heated in the absence of oxygen decomposes into two main parts: The first part is rich in volatile matters, while the other, called char, is rich in carbon. Many trace elements are found in the mineral material of the coal. During combustion, the mineral material is converted to ash. The trace elements associated with the mineral matter are potential air pollutants due to their presence in the fly ash.

When coal enters the bed, the devolatilization process takes place. In this process, a large variety of physical and chemical changes take place in the coal matrix. The result is a production of lower molecular weight hydrocarbons and a char residue. The amount of volatile matter produced depends on the coal type and may vary from 20 to 30% by weight of the coal (Speight, 1983). Products of the coal devolatilization process are hydrogen, methane, carbon monoxide, tar and lower weight hydrocarbons (less than C_6). The temperature range during which the devolatilization process occurs, is between 350-660 °C (Speight, 1983). The combustible compounds found in the volatile matter react with oxygen to increase the temperature of the bed. Therefore, the first step in coal combustion is referred to as the devolatilization and volatile combustion process.

The large amount of heat generated from the reacting gases is then transferred to the char particles to help their combustion. Consequently, the char particles ignite and

burn slowly. As the reaction may occur on both the outer and the inner surface of the particles, the kinetics of both the heterogeneous and the homogeneous reactions are important in char combustion modelling. Parameters contributing to combustion effectiveness are the furnace temperature, the size and the form of the char, the residence time of the char particles and the oxygen concentration in the bed. The time required to burn the volatile matter of a 80 μm coal particle is about 0.1 seconds, while the time required to consume the char particles is significantly longer (1-3 seconds) (Cooper and Ellingson, 1984). The amount of heat released during the char combustion depends on the carbon and oxygen concentrations in the bed. Therefore, most of the heat released in the combustion process is related to the conversion of carbon to carbon monoxide and carbon monoxide to carbon dioxide.

The theoretical oxygen demand to promote complete conversion of carbon can be calculated for any coal, although in practice more oxygen than theoretically required is necessary. Combustion in the CFBC takes place with an excess air of 10 to 30%. The amount of air needed for the combustion process depends on the coal type and the bed temperature. If the excess air is too low, the combustion efficiency will decrease. High excess air rates have two different effects on NO_x formation. First, they increase the amount of the combustion gases, thus more NO_x formation is expected. Second, they decrease the bed temperature, for which less NO_x formation is expected.

To burn coal in a CFBC, its temperature must be raised to the ignition temperature. At this point, coal added to the bed will ignite spontaneously. To control the temperature and to close the energy balance, heat is transferred through heat exchange tubes to produce steam.

Most of the bed material is made up of noncombustibles such as ash and residual products from the combustion process. The CFBC temperature is normally kept between 550-900 °C. The lower temperature limit is fixed to obtain more effective combustion while the upper temperature is maintained below the ash melting point.

NO_x and N_2O formation in combustion processes result from an oxidation of nitrogen in the combustion air and in the fuel. The formation of NO_x is highly dependent upon temperature and excess air. The nitrogen oxides include several nitrogen-based air pollutants. The most important of these are NO, NO_2 and N_2O. NO is produced from its elements at the high temperatures found in the CFBC. The reactions concerning NOx formation take place slowly and therefore attain a lower overall conversion (Robinson, 1986). In addition, the emission of NO_2 is normally low when compared to NO emissions. This is because only a small portion of NO oxide react to form NO_2 in the CFBC (Robinson, 1986). At very high temperatures, the dominant source of NO_x is thermal generation, which concerns the reactions between air nitrogen and oxygen. At low temperatures, the dominant source of NO_x is fuel nitrogen oxidation. As reported in the CFBC literature, at the conditions found in CFBCs, between ten and fifty percent of the coal nitrogen is converted to nitrogen oxides during combustion (Speight, 1983). Almost 80% of the nitrogen contained in these oxides is associated with fuel bond nitrogen (Meyers, 1981). Thus, only a small part of the air nitrogen participates in the combustion process. Low NO_x emissions can be achieved using staged combustion. In staged combustion, the air used for the combustion is divided into two parts; the first part is supplied through the air distributor and the secondary air stream is injected at the bottom of the upper region. Some published data suggest that NO_x emissions could be controlled by adding chemical components such as carbon monoxide, char, hydrogen, ammonia and

unburned hydrocarbons (Zhao, 1992; Furusawa et al., 1985). Nevertheless, staged combustion is an acceptable method for reducing NO_x emissions in various combustion systems.

Nitrous oxide (N_2O) emissions have been recognized as a harmful air pollutant. Recently, more comprehensive studies have been performed in regards to the N_2O emissions from CFBCs (Hiltunen et al. 1991, Amend et al. 1991, Wojtowicz et al. 1991). In coal combustion processes, the N_2O emission concentration was reported to be between 30-120 ppm (3% O_2-dry basis) (Hiltunen et al., 1991). It has been mentioned that N_2O contributes to the greenhouse effect. Being a stable component, it is transported to the upper atmosphere where it participates in the ozone layer depletion.

During coal combustion, sulphur oxides are produced from the sulphur in the coal. Sulphur dioxide emissions may be captured by injecting limestone into the bed. The sulphur oxides react to form calcium sulphate and exit the bed with the waste solids. Sulphur dioxide produced during coal combustion can also react with water and oxygen to yield sulphuric acid.

$$S(coal) + O_2 \Rightarrow SO_2$$

1.2 REACTION MODELS

Coal combustion is very complex and cannot be characterized by simple reactions. However, for simulation purposes, the combustion of coal particles can be modelled using the following reactions:

1- Devolatilization and volatile combustion

2- Char combustion

3- NO_x formation

4- SO_2 absorption by added limestone or dolomite

1.2.1 Devolatilization and volatile combustion

When coal is introduced into the bed, it decomposes into two parts: hydrogen-rich volatiles and char. The char remains in the bed and is burned slowly as it moves. Based on the plume model, coal devolatilization and complete combustion of the volatile occurs at the feed entry point (LaNauze, 1985), because its residence time in the bed is less than 5 seconds (Turnbull and Davidson, 1984). Two steps will be considered in the simulation:

a) Decomposition

b) Volatile combustion

- Decomposition

Representing coal with a general formula of $C_xH_yO_zS_\alpha N_\beta$.ASH, the following reaction is considered to take place:

$$C_xH_yO_zS_\alpha N_\beta.ASH \Rightarrow xC + \tfrac{1}{2}yH_2 + \tfrac{1}{2}zO_2 + \alpha S + \tfrac{1}{2}\beta N_2 + ASH$$

- Volatile combustion

To simulate the volatile combustion step, three common reactions are considered in the simulation:

$$C + \tfrac{1}{2}O_2 \Rightarrow CO$$

$$S + O_2 \Rightarrow SO_2$$

$$H_2 + \frac{1}{2}O_2 \Rightarrow H_2O$$

Burning of the volatile products gives CO and H_2O, while the SO_2 release rate is proportional to the char combustion rate (Rajan et al., 1978). For instance, it is assumed that the SO_2 released at the feed entry point.

1.2.2 Char combustion

The char particles, resulting from the devolatilization process, are burned to produce a mixture of CO and CO_2. Three main reactions for char combustion are considered here (Gordon and Amundson, 1976):

$$C + \frac{1}{2}O_2 \Rightarrow CO$$

$$CO + \frac{1}{2}O_2 \Rightarrow CO_2$$

$$C + CO_2 \Rightarrow 2CO$$

The first and third reactions are heterogeneous and the second is homogeneous. Since the temperature of the burning particles in the CFBC is not sufficiently high, the effect of the third reaction on the combustion rate is low (LaNauze, 1985), and this reaction has been neglected in the simulation. For all relevant reactions in the model, the reaction rate expressions must be developed carefully. The reaction rates depend on the physical and chemical properties of the char, the hydrodynamic parameters, the mass transfer resistance, the temperature, the reactive concentration and the particle size distribution (PSD). The mathematical kinetic expressions for both char combustion and CO combustion are developed in the next chapter.

1.2.3 NO_x formation

Three main reactions are used to represent the formation of NO_x in the simulation:

$$\frac{1}{2}N_2 + \frac{1}{2}O_2 \Rightarrow NO$$

$$\frac{1}{2}N_2 + O_2 \Rightarrow NO_2$$

$$N_2 + \frac{1}{2}O_2 \Rightarrow N_2O$$

The equilibrium concentrations of NO_x and N_2O are computed based on equilibrium conditions.

1.2.4 SO_2 capture

The SO_2 capture by limestone can be represented by the following reactions:

$$CaCO_3 \Rightarrow CaO + CO_2$$

$$CaO + SO_2 + \frac{1}{2}O_2 \Rightarrow CaSO_4$$

The fractional conversion of SO_2 (η_{SO2}) is strongly affected by the physical and chemical properties of limestone, hydrodynamic parameters, mass transfer resistance, temperature, reactive concentration, the particle size distribution (PSD) and the operating conditions. The mathematical expression for the fractional conversion of SO_2 is developed in chapter 3.

CHAPTER 2

HYDRODYNAMIC MODELLING

2.1 INTRODUCTION

The hydrodynamic model enables the distribution of the gas and solids in the CFBC to be determined. Circulating fluidized bed hydrodynamic is affected not only by physical properties of coal, ash and limestone particles, but also by the superficial gas velocity. The hydrodynamics of circulating fluidized beds are commonly characterized by the variation of the void fraction with height in the riser section. The void fraction is an important parameter affecting the gas/solid contact efficiency within the CFBC. A good understanding of the hydrodynamic behaviour of a CFBC is essential when studying the coal combustion phenomena in CFBCs.

The hydrodynamics of circulating fluidized beds have been studied in experimental units in order to determine the gas/solid efficiency. These experimental findings show a significant difference between hydrodynamics of CFBCs and those of bubbling fluidized beds (Zhao, 1992). Most of the experimental studies are limited to small risers. The majority of studies have confirmed the existence of core-annulus models (Zhao, 1992). A recent review of circulating fluidized bed hydrodynamics has been presented by Berruti et al, (1993). Hydrodynamic modelling, as proposed in most CFBC literature, is based on either the Core-annulus model or the Cluster model (Wong, 1991). In models based

on the Core-annulus structure, a dilute flow of rising gas/solid mixture is surrounded by a denser annulus of a downward flowing mixture. In models based on the Cluster phenomena, discrete particles are considered in a dilute media as upward and downward moving solid packets. There are some empirical correlations based on experimental data that consider the riser of the CFBC as the freeboard of a bubbling fluidized bed. One such model which uses this approach is that of Kunii and Levenspiel (1991(b)).

2.2 MODEL FORMULATION

We have attempted to use the ASPEN PLUS simulator as the framework for our simulation. The hydrodynamic model used in our simulation, provides the mean voidage in the CFBC. A differential method, which would involve the linkage of an infinite number of intervals by ASPEN PLUS, is nearly impossible to achieve. Considering this, we have decided to employ a lumped method for our simulation. Although there are many possible lumped methods to choose from, we have chosen one, which is relatively simple and comprehensive, and thus easily interacts with ASPEN PLUS. Therefore, for the purpose of modelling, the concept defined by Kunii and Levenspiel (1991(a)) has been used in conjunction with the work of Patience and Chaouki (1993) in order to define the hydrodynamics of CFBCs. In the proposed model, the CFBC is divided into two regions: a lower region and an upper one. The lower region is fluidized by the fluidizing air and the upper region is suspended both by combustion gases from the lower region and the secondary air supply.

2.2.1 Lower region of the CFBC

In the lower region, perfect mixing between the solid and the gas phases is assumed. Under these conditions, the mean voidage of the dense region ($\epsilon_{d,avg}$) can be considered constant and may be obtained using the correlation proposed by Kunii and Levenspiel (1991(a)), presented on figure 2.1. Considering U_1=3.7 m/sec , we obtain:

$$\epsilon_{d,avg}=0.82 \tag{2.1}$$

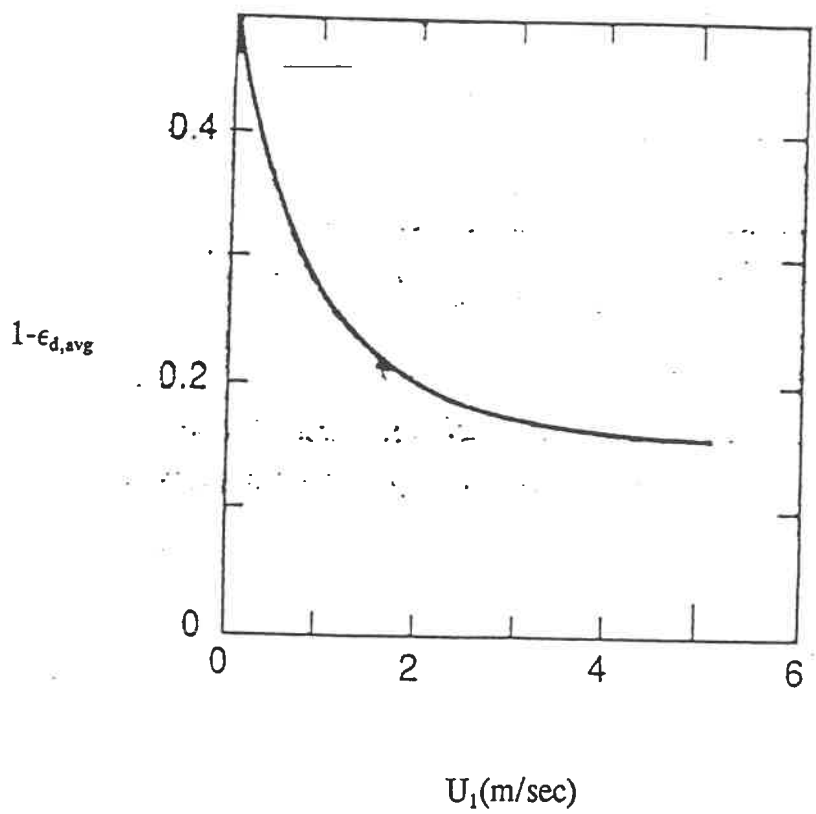

Figure 2.1 Mean Voidage of the Dense Bed of the CFBC as a Function of Superficial gas Velocities

2.2.2 Upper region of the CFBC

In order to predict the mean voidage profile in the upper region of the CFBC, the proposed model assumes that the upper region consists of two zones: an acceleration zone and a fully developed zone. In the fully developed zone the mean voidage is calculated using the Patience (1990) correlation.

$$\Phi = 1 + \frac{5.6}{F_r} + 0.47 F_{rt}^{0.41} \tag{2.2}$$

$$F_r = \frac{U_2}{\sqrt{g.D_r}} \tag{2.3}$$

$$F_{rt} = \frac{U_t}{\sqrt{g.D_r}} \tag{2.4}$$

where:

F_r : Froude number

F_{rt} : Particle Froude number

U_2 : Superficial gas velocity in the dilute bed, m/sec

U_t : Terminal velocity of particles, m/sec

g : Acceleration due to gravity, m/sec^2

D_r : Riser diameter, m

The terminal velocity required in the above equations can be calculated using the following equations (Kunii and Levenspiel, 1991(a)):

$$d_p^* = d_p \left[\frac{\rho_g.(\rho_s - \rho_g).g}{\mu^2} \right]^{\frac{1}{3}} \tag{2.5}$$

$$U_t^* = \left[\frac{18}{d_p^{*2}} + \frac{2.335 - 1.744\varphi_s}{d_p^{*0.5}} \right]^{0.5} \tag{2.6}$$

$$U_t = U_t^* \left[\frac{\mu.(\rho_g - \rho_g).g}{\rho_g^2} \right]^{-\frac{1}{3}} \tag{2.7}$$

where:

μ : Viscosity of gaseous combustion product, kg/m.sec

ϕ_s: Sphericity

ρ_g : Density of gaseous combustion product, kg/m^3

ρ_s : Density of bed solids particles, kg/m^3

d_p : Average particle diameter of bed particles, m

From this information, the mean axial voidage in the fully developed zone is then estimated by the following equation:

$$\epsilon_{u,3,avg} = \frac{1}{1 + \frac{\Phi . G_s}{U_2 \cdot \rho_s}} \tag{2.8}$$

where:

G_s : Net solids circulation flux, $kg/m^2_{riser}.sec$

$\epsilon_{u,3,avg}$: Mean axial voidage in the fully developed zone

The length of the fully developed region is obtained once the length of the acceleration zone is known. In this zone, the axial voidage decreases with the vertical position along the riser (Kunii and Levenspiel, 1991(b)):

$$\frac{\epsilon^* - \epsilon_u}{\epsilon^* - \epsilon_{d,avg}} = \exp^{-a.Z} \tag{2.9}$$

where:

ϵ_u : axial voidage in the acceleration zone

ϵ^* : axial voidage at saturated conditions

a : decay constant, m^{-1}

Z : distance above the lower region,m

The value of the parameter a may by obtained using the correlation of Kunii and Levenspiel (1991(b)):

$$a=\frac{5}{U_2} \tag{2.10}$$

Since the axial voidage at the end of the acceleration zone is the same as in the fully developed zone, the length of the acceleration zone can be calculated using equation (2.9):

$$Z_{ac}=-\frac{1}{a}.\ln\left(\frac{\epsilon^*-\epsilon_u}{\epsilon^*-\epsilon_{d,avg}}\right) \tag{2.11}$$

where:

Z_{ac} : the length of the acceleration zone,m

In the entire upper region, plug flow in both the gas and solid phase is assumed. The modelling of this region is achieved by dividing it into discrete intervals. For instance, n may equal to two. The mean value of the axial voidage in the nith interval of the upper region of the CFBC ($\epsilon_{u,ni,avg}$) may be evaluated as follows:

$$\epsilon_{u,ni,avg} = \frac{\int \epsilon_u . dz}{\Delta L} \tag{2.12}$$

where:

ΔL : Height of the nith interval, m

By integrating Eq. (2.12) between Z_{ni-1} and Z_{ni} the following expression for the average axial voidage in each interval can be obtained:

$$\epsilon_{u,ni,avg} = \epsilon^* - \frac{1}{a.\Delta L}.(\epsilon_{d,avg} - \epsilon^*).(\exp(-a.Z_{ni}) - \exp(-a.Z_{ni-1})) \tag{2.13}$$

where:

Z_{ni} and Z_{ni-1} are the corresponding distances for the ni and ni-1th interval above the lower region,m

The variation of void fraction with length in the CFBC is illustrated in Figure 2.2. As shown in Figure 2.2 , the riser is divided into four sections. Each section is considered as a separate reactor with specific reactions occurring at a mean voidage. The information provided by the hydrodynamic model can be coupled with the reaction steps identified in chapter 1 to yield a complete simulation model for CFBCs.

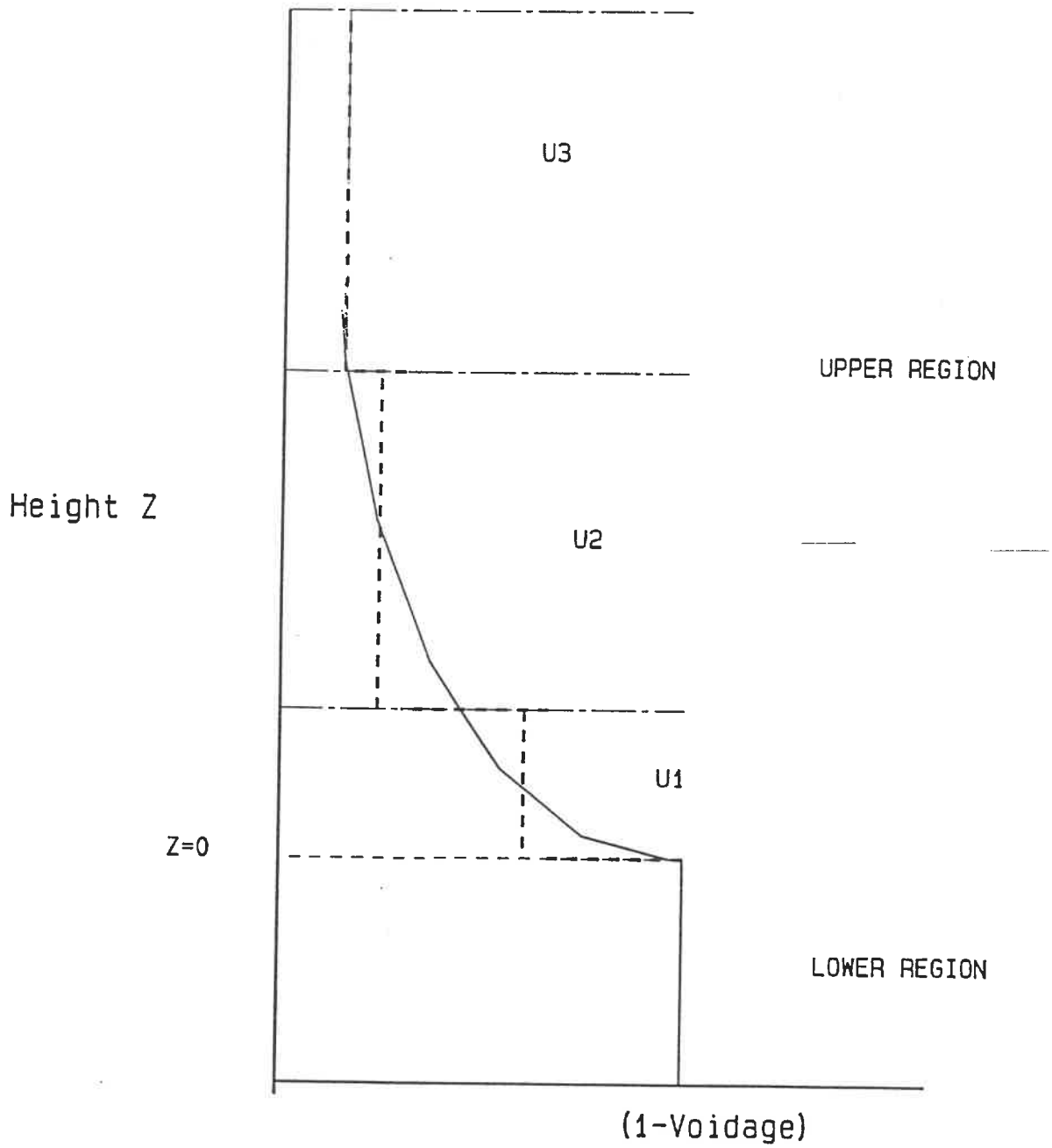

Figure 2.2 The Variation of Void Fraction with Height in the CFBC

CHAPTER 3

DEVELOPMENT OF A CFBC SIMULATION MODEL

In order to develop a simulation model for a CFBC, the hydrodynamic model must be treated simultaneously with the reaction models. The development of a simulation model, the concept and the applications of a process simulator, and a detailed description of the method in which the CFBC has been modelled, as well as the required data for the ASPEN PLUS simulation program are presented here.

3.1 PREVIOUS WORK

During the last two decades, a number of detailed studies on the simulation of the CFBCs have been performed. Furthermore, some aspects of Atmospheric Fluidized Bed Combustion (AFBC) have been studied extensively. Reviewing simulation works from AFBC has been useful due to the fundamental similarity between AFBCs and CFBCs. A detailed review of published models will not be included here; instead the capabilities of certain models will be discussed briefly.

3.1.1 The work of Young (1986) on AFBC

This work entails the modelling and simulation of AFBCs using ASPEN. In this work, the "Black box" approach with one reactor type (RSTOIC) was used to calculate the mass balances based on a given combustion efficiency and a sulphur capture efficiency.

Since there were no links between the coal combustion reaction rates and the hydrodynamic parameters, no predictive capability was possible. FORTRAN Blocks were used to compute several parameters required for the mass balances. They were also used for calculations of the Particle Size Distribution (PSD) in the different solid sub-streams based on standard methods and empirical expressions. The following phenomena were also considered in the model:

- Elutriation rate
- Segregation rate
- Limestone abrasion rate
- Cyclone capture efficiency

It should be mentioned that other important simulation aspects, such as sensitivity of key components as well as an economic analysis, were also included. The difference reported in the material and energy balances were within 10% of those found using experimental data. It can be then concluded that this is a simplified representation of the AFBC.

3.1.2 CFBC simulation work at CERCHAR (Paffenbarger, 1991)

The main objective of the work was to provide the technical information required for the evaluation and the optimisation of CFBCs under steady state conditions. The approach used here is similar to that of Young's, but was extended to cover CFBCs. For the simulation, a detailed hydrodynamic model was developed to predict the PSD in the riser and the resulting heat transfer coefficients. The study of the emissions such as SO_2, NO_x, and N_2O as well as the ash composition leaving the CFBC were not included in this

simulation program; instead some ASPEN PLUS user subroutines were used in order to study the hydrodynamic, combustion and heat transfer phenomena in the bed. The structure for a complete CFBC model using a process analysis program (ASPEN) was indeed established but the work was interrupted before the simulation program could be developed. ASPEN's capacity to process user-supplied kinetic subroutines, in their reaction models utilized RCSTR and RPLUG, was not used here. Rather than using these reactors, the combustion reactions were simulated using RSTOIC reactors. For this purpose, a Fortran block was written to determine the fractional component of certain key components which was then used to execute several RSTOIC reactors.

3.1.3 CFBC simulation work in Calgary (Wong, 1991)

This work centres on modelling the hydrodynamics of circulating fluidized bed risers. The main objective of this work was to develop a CFBC simulation model by examining the hydrodynamics of CFBC risers. Both experimental and theoretical efforts have been made in order to characterise the effect of the internal flow structure within the riser, the particle size, the density and the operating conditions on CFBC behaviour. To estimate the axial voidage profile, a core-annulus structure was developed. The predictive hydrodynamic model was then applied to the CFBC reactor design. The SO_2 and NO_x emissions were also studied.

3.1.4 Lumped-modelling approach for a CFBC (Arena et al.,1990)

In this approach, the CFBC riser was divided into four blocks, each one corresponding to a reactor block. Three of these blocks relate to the CFBC riser. Perfect mixing of solids is assumed for the riser blocks, while the for gas phases, a plug flow regime was assumed. The hydrodynamic parameters were considered uniform throughout each section. Simplifying assumptions were made concerning the CFBC hydrodynamic and reaction models. This model considered reaction rate expressions, chemical and diffusion rate resistance, the char particle size distribution and its variations caused by attrition. Experimental data were compared with the model predictions and satisfactory agreement was reported. Most CFBC simulations only provide the emission data at the output of the CFBC, while, this model goes further as it predicts oxygen concentration within the CFBC. This approach was used as the basis for our simulation model.

3.2 GENERAL HYPOTHESES OF THE SIMULATION MODEL

In order to develop a simulation model for a CFBC, the hydrodynamic model must be treated simultaneously with the combustion model. For steady state conditions, the assumptions regarding the hydrodynamic and combustion models are detailed below:

3.2.1 Hydrodynamic

1- The CFBC is divided into two hydrodynamic regions (Kunii and Levenspiel, 1991(b)):

- A lower region (dense bed)
- An upper region (dilute bed)

The upper region is also divided into two zones; an acceleration zone and a fully developed zone.

2- There is perfect mixing of solids (individual ash, char particles and sorbents) and gas phase in the lower region (Grace, 1986). This assumption is justified by the high internal and external recirculation of solids in the bed.

3- Plug flow regime for both the gas and solids is assumed in the upper region (Grace, 1986).

4- The gas velocity throughout the bed is uniform and constant for each region of the bed.

5- For a given superficial gas velocity, the mean voidage in the lower region of the CFBC is constant (Kunii and Levenspiel, 1991(a)).

6- In the upper region of the CFBC, the voidage decreases with the vertical position along the riser (Kunii and Levenspiel, 1991(a)).

7- The CFBC is assumed to be isothermal and isobaric (Wong, 1991). A CFBC with its large external recirculation and internal structure of solid particles allows the heat generated from the combustion reactions to be quickly transferred to the water tubes along the riser. Under such a high extent of mixing, it is reasonable to assume isothermal bed conditions. Experimental studies performed by CANMET-ERL have largely confirmed this hypothesis (Desai et al, 1991) and the presence of only a small temperature gradient in the bed was confirmed by Grace (1986).

8- The flow is one dimensional.

9- End effects are neglected.

3.2.2 Combustion

1- The coal and limestone are fed constantly into the bottom of the bed at a uniform temperature (Couturier, 1986). This is largely encountered in industrial units operating at high feed rate, because in these conditions, the temperature gradient within the feed is negligible.

2- The oxidation of atmospheric nitrogen is negligible, as only a small percentage of air nitrogen participates in the combustion process at CFBC temperatures (Meyers et al. 1981).

3- The attrition rate constant for char particles in the CFBC varies between $0.8*10^{-7}$ and $8.4*10^{-7}$ (Arena et al., 1991), and hence the effect of attrition is small. Therefore, the attrition-assisted combustion rate is deemed negligible.

4- The effects of the primary fragmentation of coal and the secondary fragmentation of char in the overall coal combustion process are neglected (Arena et al. 1991).

5- Any char particle size reduction caused by ash particles or the walls of the CFBC are neglected.

6- The contribution of the cyclone, the L-valve, the circulation loop and the control valve to the overall combustion rate is neglected. Arena et al (1991) have considered the cyclone as the reaction block for their simulation. Due to the small residence time and the lack of excessive oxygen for the particles in the cyclone, L-valve and recirculation loop, the hypothesis appears to be reasonable.

7- Since the time required for volatile combustion is very short, the devolatilization process is considered to be instantaneous and to take place at the bottom of the bed

(Congalidis and Georgakis, 1981).

8- The gas-particle heat transfer is assumed to be very fast, hence the particle temperature will be equal to the bed temperature.

9- Since char combustion is slower, it is assumed to occur after all the volatile products have been burned (Rajan et al, 1978). This is an acceptable hypothesis considering the very short time required for volatile combustion.

10- Char particles in the CFBC are assumed to burn with constant diameters. Since the amount of char particles within the bed is extremely high, compared to those in the coal feed stream, this hypotheses seems justified.

11- The fraction of char is uniformly distributed throughout the entire CFBC.

It should be mentioned that the special hypotheses related to the performance of each unit operation block will be listed later.

3.3 STEPS INVOLVED IN THE SIMULATION OF A CFBC USING ASPEN PLUS

In order to develop an ASPEN PLUS flowsheet for a CFBC, the following steps are followed:

1- Define the aim of the process flowsheet.

2- Select the measurement units for both input and output variables.

3- Characterize all components presented in the process.

4- Select the convenient data banks and define the user data bank.

5- Describe the NC (Non Conventional) components such as coal by its attributes (proximate, ultimate and sulphur analyses).

6- Choose an enthalpy and a density model for NC.

7- Use the convenient methods and models for calculating the physical properties.

8- Define the stream structure.

9- Represent the CFBC flowsheet with unit operation blocks.

10- Specify the feed streams and block specifications.

11- Insert the user Fortran codes and subroutines into the simulation.

12- Set up any design specifications, sensitivity analyses and case studies.

The detailed descriptions of these steps can be found in ASPEN TECHNOLOGY, (1988(b)).

3.4 MODEL DEVELOPMENT AND SIMULATION FLOWSHEET

To simulate the operation of a CFBC, four ASPEN PLUS reactor blocks are employed in accordance with the phenomena identified in the coal combustion process in chapter 1. Table 3.1 illustrates the reactor models specification utilized in the simulation as well as the input variables.

Table 3.1 The Reactor Models Specification Utilized in the Simulation

BLOCK NAME	INPUT VARIABLES	PHENOMENA
1- RYIELD	T_b, P, F(y)	Devolatilization and volatile combustion
2- RSTOIC	T_b, P, $X_{C,d}$, $X_{H2,d}$, $X_{S,,d}$ Chemical reactions	
3- RCSTR	T_b, P, $r_{11,i}$, $r_{12,i}$ Chemical reactions	Char combustion
4- REQUIL	T_b, P Chemical reactions	NOx Formation
5- RSTOIC-1	T_b, P,X_{CaCO3}, $\eta_{SO2,i}$ Chemical reactions	SO2 Capture

where:

T_b : Bed temperature, K

P : Bed pressure, atm

F(y) : Yield distribution vector

$X_{C,d}$: Fractional conversion of carbon in the volatile combustion

$X_{H2,d}$:Fractional conversion of hydrogen in the volatile combustion

$X_{S,,d}$: Fractional conversion of sulphur in the volatile combustion

$r_{11,i}$: Char combustion rate, kmole/m^3.sec

$r_{12,i}$: CO combustion rate, kmole/m^3.sec

X_{CaCO3} : Fractional conversion of $CaSO_4$ in the dense bed

$\eta_{SO2,i}$: Fractional conversion of SO_2 in the nith interval of the bed

This section provides an outline of the layout of the unit operation blocks and the mathematical expressions needed to integrate those blocks into the overall flowsheet when required. Certain unit operation blocks including reactors, mixers and separators are used in the simulation. Four ASPEN PLUS reactor models, RYIELD, RSTOIC, RCSTR and REQUIL are used here. RSTOIC inputs include a given reaction stoichiometry, the fractional conversion of key components, reactor temperature and pressure. RSTOIC then computes the composition of the outlet stream and the heat generated or absorbed by the reactions. This model is very useful when the fractional conversion of the key components are known. The fractional conversion of the key components can also be calculated using user-supplied Fortran blocks. These parameters are then inset into the ASPEN plus input

file so that they are available to the specified block that functions as desired (ASPEN TECHNOLOGY, 1988(b)). RYIELD simulates a reactor by specifying reaction yields for each component. An RYIELD model is used when the reaction stoichiometry or kinetics are unknown, but yield distribution data or correlations are available. The reactor temperature or pressure must also be specified. (ASPEN TECHNOLOGY, 1988(b)). RCSTR models a Continuous Stirred Tank Reactor (CSTR) when the reaction kinetics, reactor volume, temperature and pressure are known. In the case of reactions involving solids, user-supplied kinetics subroutines are required. REQUIL simulates the equilibrium conditions when the reaction stoichiometry is known. The user should also specify the bed temperature and pressure.

Taking into account the hydrodynamic model and the reaction models, the CFBC flowsheet is easily divided into three sub-flowsheets:

- Lower sub-flowsheet
- Upper sub-flowsheet
- Sep sub-flowsheet

The first sub-flowsheet represents the dilute region of the CFBC where the phenomena associated with coal combustion , devolatilization and volatile combustion, char combustion, NO_x formation and SO_2 capture take place. The order of occurrence of these phenomena is presented below:

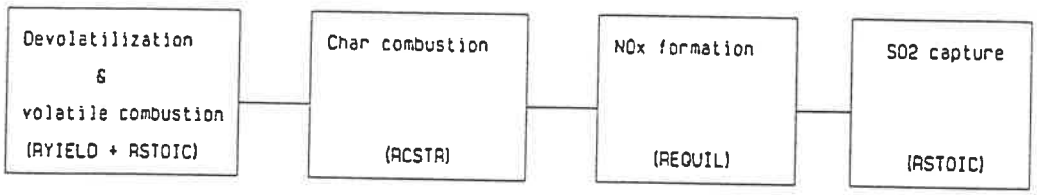

The second sub-flowsheet represents the dilute region of the CFBC. As stated previously, the dilute region is divided into three sections (U1, U2 and U3), two of them represents the acceleration zone, while the third section relates to the fully developed zone. Since the time required for the devolatilization and volatile combustion process is very short, this process is assumed to occur exclusively in the lower region. Therefore, for each section in the upper region the char combustion, NO_x formation and SO_2 capture are considered to occur in the following order:

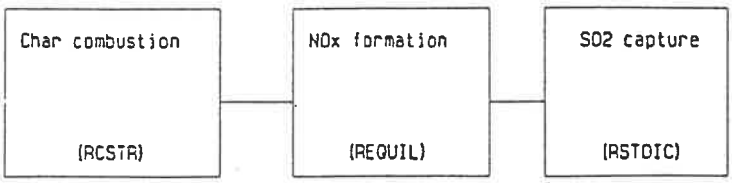

The last sub-flowsheet contains two unit operation blocks; CYCLONE and FSPLIT. Cyclone is used for the gas/solid separation at the riser outlet. In order to satisfy the material balance in the CFBC, a solid drain valve, FSPLIT, is used. The simulation diagram for the CFBC is illustrated in figure 3.1.

As Figure 3.1 shows, Coal (stream F) enters RYIELD (B1). Here, the coal is converted to its constituents. The resultant stream (S1) along with limestone (Fl) and the primary air flow (FA1) enter RSTOIC (B2), where the volatile combustion process takes place. The yield stream (S2) then enters RCSTR (B3). In this block, the main combustion reactions take place and the outlet stream is fed to REQUIL (B4), where the NOx formation process is modelled. The resultant streams are sent to RSTOIC (B5) in order to capture the SO_2 formed during the previous operations. The output stream leaving the dense bed is mixed with the secondary air flow (FA2) upon entering the upper region. As mentioned earlier, the upper region is divided into three sections. Unit operation blocks B7, B8 and B9 are used to model the combustion phenomena such as the char combustion, NO_x formation and SO_2 capture in the first section. Blocks B10, B11 and B12 are used to model the combustion phenomena in the second section of the upper region. In the third section, the combustion phenomena are modelled using blocks B13, B14 and B15. The outlet stream leaving the riser is sent to CYCLONE (B16), where a nearly complete separation of gas/solid takes place. The stream S20, which consist of the combustion gases, exits the system. The resulting solid stream is divided into two parts via FSPLIT (B17). A large amount of solids (FASH) are recycled into the lower

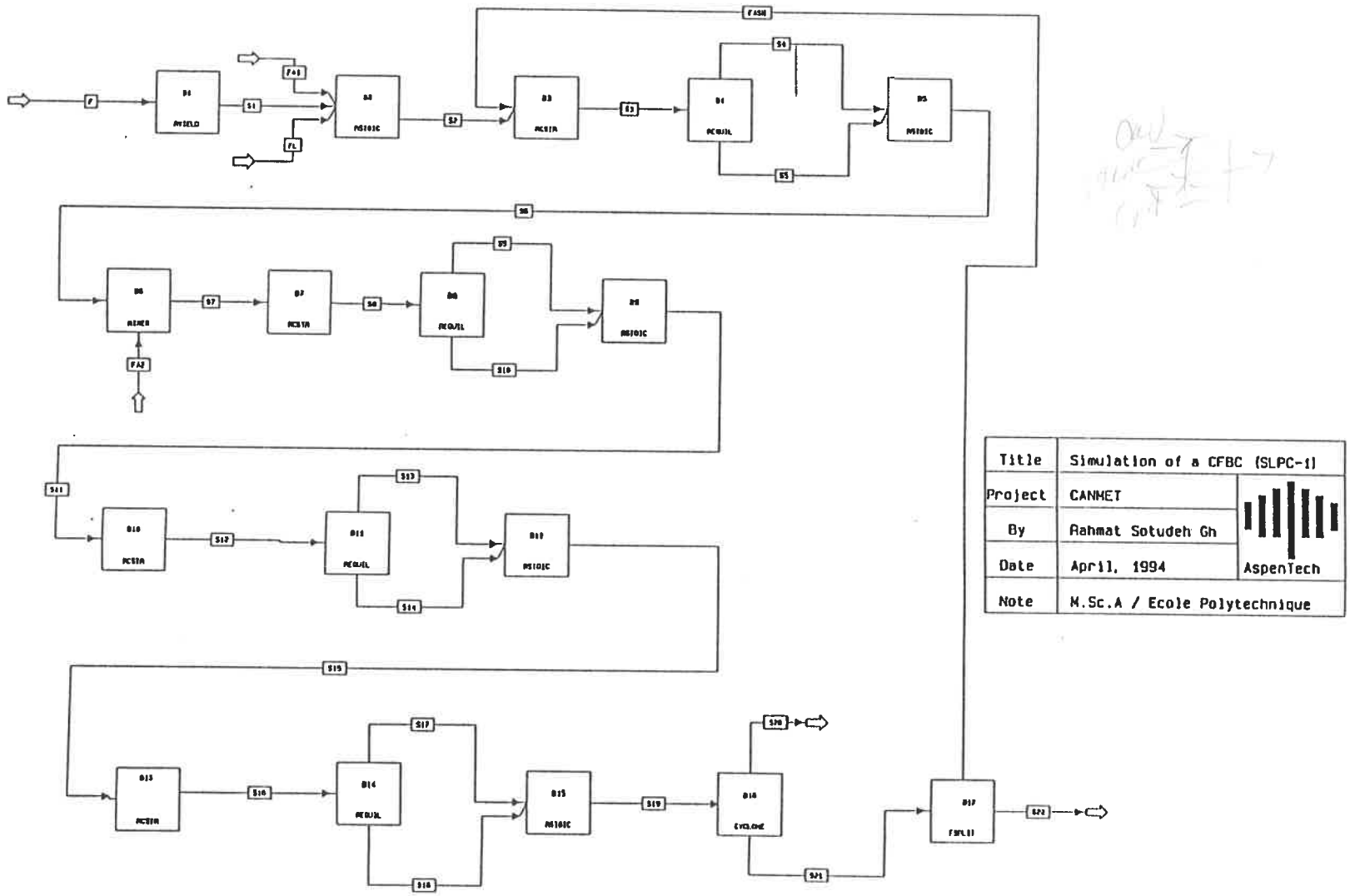

Figure 3.1 A Simulation Diagram for the CFBC

region (B3) to simulate the solids recirculation loop in the CFBC. A detailed description of the unit operation blocks as well as the input data are discussed in detail throughout this chapter. All the sub-flowsheets have a SOLID stream structure, including the NCPSD (Non Conventional components with Particle Size Distribution), CIPSD (Conventional Inert components with Particle Size Distribution) and MIXED sub-streams. In order to consider the PSD (Particle Size Distribution), the number of discrete intervals and their size limits must be specified.

3.4.1 Lower sub-flowsheet

The lower sub-flowsheet represents the dilute region of the CFBC where the phenomena associated with coal combustion , devolatilization and volatile combustion, char combustion, NO_x formation and SO_2 capture take place. The detailed description of unit operation blocks used to model this sub-flowsheet as well as the input data are detailed below:

3.4.1.1 Block RYIELD

RYIELD (Yield reactor) is used to model a reactor by specifying the yield distribution vector.

$$F(y)=[ASH, C, H_2, N_2, S, O_2]$$

The ultimate analysis of coal (Table 3.4) is used as the mass yield vector. ASPEN PLUS

uses elemental enthalpy reference to calculate the heats of formation.

- Block hypotheses

- RYIELD is used to convert coal(NC) to its constituent components such as NC, CISOLID (Conventional Inert SOLID) and MIXED.

3.4.1.2 Block RSTOIC

RSTOIC (Stoichiometric reactor) is used to simulate the volatile combustion process. The following reactions will be considered in the block.

$M_d(R_i)$	J	$X_{j,d}$
i=1 $C + ½O_2 \Rightarrow CO$	C	0.31
i=2 $S + O_2 \Rightarrow SO_2$	S	1.00
i=3 $H_2 + ½O_2 \Rightarrow H_2O$	H_2	1.00

where:

i: Reaction number

$M_d(R_i)$: Reaction matrices in the devolatilization process

j: j^{th} key component

$X_{j,d}$: Fractional conversion of key component in the devolatilization process.

- Block hypotheses

- As shown in the proximate analysis of coal (table 3.4) nearly 35 percent of the coal is volatile matter. Considering that four percent of this volatile matter is H_2, 31 percent can be considered as the fractional conversion for carbon in the devolatilization process.
- All sulphur, hydrogen and oxygen present in the coal will be consumed in the devolatilization process.
- All carbon present in the volatile matter reacts completely to form CO.
- All H_2O as moisture in the coal will be vaporized into H_2O vapour.

3.4.1.3 Block RCSTR

RCSTR (CSTR reactor) is used to model a Continuous Stirred Tank Reactor with known reaction kinetics. As mentioned earlier, the burning of coal particles proceeds in the following basic Steps:

1- Devolatilization and volatile combustion

2- Char combustion

3- NO_x formation

4- SO_2 absorption

The first was discussed earlier, the char combustion process will be presented in this block and the rest will be discussed later.

- Kinetic model for RCSTR

The first reaction is a gas-solid reaction and the chemical changes take place on both the external and the internal surface of the char particles (Congalidis and Georgakis, 1981). The rate of reaction can be assumed first order with respect to oxygen (LaNauze, 1985). The following expression can be obtained for the reaction rate:

$$N_c = K_c . C_{O2} \tag{3.1}$$

where:

N_C : Char reaction rate, kmole/ m^2.sec

K_C : Overall rate constant, m/sec

C_{O2} : Concentration of oxygen, kmole/m^3

The rate expression for char combustion per particle is as follows:

$$R_{char} = 4\pi r_C^2 . K_C . C_{O2} \tag{3.2}$$

where:

R_{char} : Rate expression for char combustion per particle, kmole/(sec.particle)

r_C : Mean coal particle radius, m

Since the amount of char particles within the CFBC is extremely high compared to those in the coal feed stream, the mean char particle radius is calculated based on the particle size distribution in the recirculation stream. The following equation is used to calculate the mean particle radius:

$$r_C = \frac{1}{\sum \frac{P_k(r_C(K))}{r_C(K)}} \tag{3.3}$$

where:

$r_C(K)$: Coal particle radius vector, m

$P_K(r_C(K))$: Weight fraction vector of char particles in the recirculation stream

Our ASPEN PLUS simulation program thus assumes that the char particles within the bed are burned at a constant diameter, as the particle size distribution at the riser outlet is the same as that in the recirculation stream. A typical calculation for r_C is presented in Appendix A.4

The overall rate constant is a function of a chemical reaction constant and a diffusion rate constant as follows:

$$\frac{1}{K_C}=\frac{1}{k_{cr}}+\frac{1}{k_{cd}} \tag{3.4}$$

where:

k_{cr}: Chemical reaction rate constant,m/sec

k_{cd}: Diffusion rate constant,m/sec

The diffusion rate constant depends on the external and internal diffusion. The effect of a stagnant gas film around the particle through which O_2 has to diffuse in order to arrive at the particle surface is neglected. For calculating the internal effect, the effectiveness factor (η_{O2}) is used:

$$K_C=\eta_{O2}.k_{cr} \tag{3.5}$$

For spherical particles(Bird et al., 1960):

$$\eta_{O2}=\frac{3}{K^2}.(K.\coth K-1) \tag{3.6}$$

$$K=\sqrt{\frac{k_{cr}.a_s}{D_{eff}}}.r_C \tag{3.7}$$

$$a_s=\frac{3}{r_C} \tag{3.8}$$

where:

K : Dimensionless group

a_s : External surface area per unit volume of char, m^{-1}

D_{eff}: Effective diffusivity of O_2 in porous char, m^2/sec

We now substitute Eq. (3.5) into (3.2) to obtain:

$$R_{char}=4\pi r_C^2.\eta_{O2}.k_{cr}.C_{O2} \tag{3.9}$$

k_{cr} can be expressed by an Arrhenius form as follows:

$$k_{cr}=k_{01}.\exp\left(-\frac{E_1}{R_g.T_p}\right) \tag{3.10}$$

where:

k_{01} : Pre-exponential factor,m/sec

E_1 : Apparent activation energy,J/kmole

R_g : Universal gas constant,J/(kmole-K)

T_p : Temperature of the char particles, K

As mentioned earlier, the char particle temperature is the same as that of the bed. The values of parameters k_{01}, E_1 and R_g are listed in table 3.3. In Eq. (3.9) the rate expression of char combustion was calculated per particle. To generalize this equation to all char particles, the number of char particles in the bed must be calculated:

$$N_{char,1} = \frac{M_{char}}{m_{char}} \tag{3.11}$$

$$M_{char} = T_{solid} \cdot F_{char,1} \tag{3.12}$$

$$T_{solid} = \frac{V_C \cdot (1 - \epsilon_{d,avg})}{F_{solid,1}} \tag{3.13}$$

$$m_{char} = \frac{4}{3} \cdot \pi \cdot r_C^3 \cdot \rho_{char} \cdot (1 - \epsilon_C) \tag{3.14}$$

where:

$N_{char,1}$: Number of char particles in the dense bed

M_{char} : Total mass of the char particles in the bed, kg

T_{solid} : Mean residence time of solids in the dense bed, sec

$F_{char,1}$: Flux of the char particles entering the dense bed, kg/sec

V_C : Volume of the lower region, m^3

$\epsilon_{d,avg}$: Mean voidage of the lower region

$F_{solid,1}$: Flux of solids entering the dense bed, m^3/sec

ρ_{char} : Density of char particles,kg/m^3

ϵ_C : Char porosity

A: Cross-sectional area of bed,m^2

L_1 : Height of dense bed,m

m_{char} :Weight of a single particle, kg

Generalization of Eq. (3.9) to all particles gives the following expression for the char combustion rate per unit volume of the dense bed:

$$r_{11,1} = \frac{3.\eta_{O2}.k_{cr}.F_{char,1}.(1-\epsilon_{d,avg})}{\rho_{char}.r_C.(1-\epsilon_C).F_{solid,1}}.C_{O2} \qquad (3.15)$$

where:

$r_{11,1}$: Char combustion rate per unit volume of the dense bed, kmole/(m^3.sec)

Defining $k_{11,1}$ as the volumetric rate constant for char combustion, we have:

$$k_{11,1}=\frac{3.\eta_{O2}.k_{cr}.F_{char,1}.(1-\epsilon_{d,avg})}{\rho_{char}.r_{C}.(1-\epsilon_{C}).F_{solid,1}} \tag{3.16}$$

$$r_{11,1}=k_{11,1}.C_{O2} \tag{3.17}$$

where:

$k_{11,1}$: Volumetric rate constant for the char combustion, sec^{-1}

Note that the required data vector units for the kinetic subroutine are kmole/(m^3.sec) (ASPEN TECHNOLOGY, 1985).

The second combusting reaction is the homogeneous reaction of CO and O_2. The emission level of CO from CFBCs is strongly related to the temperature and reactive concentrations. The following expression is postulated for the CO combustion rate in the simulation model (Robinson, 1986).

$$r_{CO,1}=1.18*10^{13}.f_{CO}.f_{O2}^{0.5}.f_{H2O}^{0.5}.\left(\frac{P}{R.T_b}\right).\exp\left(-\frac{2500}{R_1.T_b}\right).C.\epsilon_{d,avg} \tag{3.18}$$

where:

f_{CO}, f_{O2} and f_{H2O} : The mole fractions of CO, O_2, and H_2O, respectively

P : Bed pressure, atm

t : Time, sec

R : Universal gas constant, (1.987 kcal/(kmole/.sec))

R_1 : Universal gas constant, (82.06 m.cm^3/(gmole.K))

C : Combustion gas concentration, kmole/m^3

$r_{CO,1}$: Reaction rate per unit volume of the dense bed, kmole/(m^3.sec)

The CO combustion rate has been studied by several researchers. The validity of the proposed model based on these studies is presented in chapter 4.

3.4.1.4 Block REQUIL

NO_x chemistry in CFBCs is quite complex. Herein, we intend to model the corresponding reactions using equilibrium conditions. Two ASPEN PLUS unit operation blocks, REQUIL and RGIBBS, may be used to compute chemical equilibrium. REQUIL simulates equilibrium with respect to reaction stoichiometry and phase equilibrium equations, while RGIBBS minimizes the Gibbs free energy with respect to atom balance constraints. REQUIL is used when the reaction stoichiometry is known and when only certain reactions approach equilibrium. Equilibrium constants are calculated from the Gibbs free energy. RGIBBS is only convenient for general equilibrium calculations, when the entire system approaches equilibrium. For this reason, we have decided to use

REQUIL for our simulation. Three NO_x formation reactions are used for the model. Possible reactions occurring due to the products formed from these three reactions were also studied. It was concluded that the consideration of these extra-product reactions led to lower NO_x emissions than those predicted using only the three initial reactions. REQUIL is used to model the formation of NO_x in the simulation including three main reactions:

$$\tfrac{1}{2}N_2 + \tfrac{1}{2}O_2 \Rightarrow NO$$

$$\tfrac{1}{2}N_2 + O_2 \Rightarrow NO_2$$

$$N_2 + \tfrac{1}{2}O_2 \Rightarrow N_2O$$

The equilibrium concentrations of NO_x and N_2O are computed based on equilibrium conditions.

3.4.1.5 Block RSTOIC

This block is used to model the capture of sulphur in the CFBC. The SO_2 capture by limestone can be represented by the following reactions:

	Reaction $M_a(R_i)$	j	$X_{j,a}$
i=1	$CaCO_3 \Rightarrow CaO + CO_2$	$CaCO_3$	1.00
i=2	$CaO + SO_2 + \tfrac{1}{2}O_2 \Rightarrow CaSO_4$	SO_2	$\eta_{SO2,1}$

where:

$M_a(R_i)$: Reaction matrices in the absorption process

Since the absorption of sulphur dioxide occurs throughout the bed, two stoichiometric reactors (RSTOIC) will be considered for the absorption process. The first reactor is nested in the dense zone and the other is at the top of the bed. RSTOIC is used to model a reactor with unknown reaction kinetics but with known reaction stoichiometry (ASPEN TECHNOLOGY, 1988(a)). For each reaction the conversion of a key component must be specified.

- Block hypotheses

- The sorbent particles are well mixed in the dense bed and radially mixed in the dilute bed.
- Calcination of limestone is instantaneous and takes place only in the dense bed, so the fractional conversion of $CaCO_3$ is equal to one (Couturier, 1986).
- The sulphation of CaO can be considered first order with respect to SO_2 (Couturier, 1986).
- SO_2 is well mixed in the dense bed and is in a plug flow regime in the dilute phase.
- All of the sulphur present in the coal is consumed in the bottom of the bed to form SO_2.

Another parameter which is required to run the ASPEN PLUS simulation is the fractional conversion of SO_2 ($\eta_{SO2,1}$) in the lower region of the CFBC. This parameter is calculated using a Fortran block according the model presented below:

- **Model development for SO_2 absorption in the dense bed**

To begin the model development, we will define some of the necessary parameters. To model a sulphur capture block, the superficial gas velocity and the fractional conversion of sorbent particles must be known. A mass balance on sulphur dioxide must also be completed.

Superficial gas velocity

The superficial gas velocity U_1 in the lower region of the CFBC, is as follows:

$$n_{air-1} = \frac{F_{air-1}}{29 * 3600} \tag{3.19}$$

$$U_1 = \frac{n_{air-1}}{A.C} \tag{3.20}$$

where:

F_{air-1} : Mass flowrate of primary air,kg/hr

n_{air-1}: Molar flowrate of primary air,kmole/sec

C : Total gas concentration,kmole/m^3

U_1 : Superficial gas velocity,m/sec

Let us now consider the ideal gas law for the combustion products in the CFBC. The total gas concentration is given by:

$$C=\frac{P}{R_1.T_b} \tag{3.21}$$

Mass balance on SO_2

The rate of SO_2 generation per unit volume of dense bed is constant and given by:

$$R_{SO_2,1}=\frac{F_c.W_s}{32.V_C} \tag{3.22}$$

$$F_c=\frac{F_{coal}}{3600} \tag{3.23}$$

where:

$R_{SO2,1}$: Rate of SO_2 generation per unit volume of dense bed,kmole/m^3.sec

F_C : Mass flowrate of coal,kg/sec

W_s : Sulphur weight fraction in the coal (dry basis)

F_{coal} : Mass flowrate of coal,kg/hr

Fractional conversion of sorbent particles

The sulphation rate of individual sorbent particles can be expressed by (Couturier, 1986):

$$\frac{dX_{CaO}}{dt} = \frac{V_{CaO}}{1-\epsilon_I} \cdot \frac{C_{SO_2}}{\frac{(e^{a_1 \cdot t}-1).C_{SO_2}}{K_V} + \frac{R_S(m)}{3.\alpha}} \tag{3.24}$$

where:

X_{CaO}: Fractional conversion of CaO in the dense bed

V_{CaO}: Molar volume of CaO,m_3/kmole

ϵ_I: Porosity of particle after the calcination

C_{SO2}: The SO_2 concentration in the surrounding gas,kmole/m^3

a_1: Parameter defined in Eq. (3.26),sec^{-1}

k_V: volumetric rate constant,kmole/(m^3-sec)

t: Time,sec

α: External mass transfer coefficient,cm/sec

$R_S(m)$: Sorbent particle radius vector,cm

n_L : Number of discrete interval for the sorbent particles as defined for PSD.

The values of parameters a_1, K_v and α may be written as (Couturier, 1986):

$$K_V = 8 * 10^{-4} \tag{3.25}$$

$$a_1 = 3.33 * 10^{-4} . e^{-0.0226.R_s} \tag{3.26}$$

$$\alpha = 35 * D_p^{0.3} \tag{3.27}$$

where:

D_P : Average sorbent surface particle diameter,cm

R_S : Mean sorbent particle radius,cm

$$D_p = \frac{1}{\sum_{1}^{n_l} \frac{P_m(R_s(m))}{2.R_s(m)}} \tag{3.28}$$

where:

$P_m(R_S(m))$: Weight fraction vector of the sorbent particles with diameter $R_S(m)$

Attrition of limestone particles

In a circulating fluidized bed combustor, the limestone fines produced due to attrition is considerable. Douglas and Young (1991) measured the attrition constant β using plant data and developed relationships between the fines and the coarse size fractions. It is assumed that the attrition of the coarse particles may produce a decrease in these fractions and an increase in the fine particle fractions. Considering that the loss of mass caused by the attrition of coarse particles results in a gain of mass to the fines. Therefore, we propose the following expression for the limestone particle attrition.

New fines PSD

$$P_m(R_s(m)) = P_{m,0}(R_s(m)) + \frac{\beta}{n_f}.P_{n-m,0}(R_s(n_l - m)) \tag{3.29}$$

$(R_s(m) < 0.0075 \text{ cm}, \quad m = 1,2,3,\ldots,n_f)$

New coarse PSD

$$P_m(R_s(m)) = \left(1 - \frac{\beta}{n_c}\right).P_{m,0}(R_s(m)) \tag{3.30}$$

$(R_s(m) \geq 0.0075 \text{ cm}, \quad m = n_f+1, n_f+2, n_f+3, \ldots, n_L)$

$$n_f + n_c = n_L \tag{3.31}$$

where:

n_c : Number of discrete intervals for the coarse particles

n_f : Number of discrete intervals for the fines particles

$P_{m,0}(R_{s(m)})$: Initial weight fraction vector of sorbent particles

β : attrition constant

By integrating Eq. (3.24), we obtain the fractional conversion of CaO in the dense bed: (Couturier, 1986)

$$X_{CaO}=\frac{V_{CaO}}{1-\epsilon_I}.\left[\frac{t_1-\frac{1}{a_1}.\ln(1+\frac{3.\alpha.C.Y_{SO_2,L1}}{R_s.K_V}.(e^{a_1.t_1}-1))}{\frac{R_s}{3.\alpha.C.Y_{SO_2,L}}-\frac{1}{K_V}}\right] \tag{3.32}$$

Using Eq. (3.32) the moles of SO_2 removed per unit volume becomes:

$$r_{SO_2,1}=\frac{V_{CaO}.F_{lime}}{(1-\epsilon_I).V_C*100}.\left[\frac{t_1-\frac{1}{a_1}.\ln(1+\frac{3.\alpha.C.Y_{SO_2,L1}}{R_s.K_V}.(e^{a_1.t_1}-1))}{\frac{R_s}{3.\alpha.C.Y_{SO_2,L}}-\frac{1}{K_V}}\right] \tag{3.33}$$

where:

$r_{SO2,1}$: Rate of removal of SO_2 per unit volume of dense bed,kmole/(m^3.sec)

t_1: mean residence time of sorbent particles in the lower region of bed,sec

σ_{SP} : volume fraction occupied by sorbent particles

$Y_{SO2,L1}$: mole fraction of SO_2 in the dense bed

X_{CaO} : Fractional conversion of CaO in the dense bed

If the sorbent particles in the bed are well mixed, their residence time is independent of particle size (Couturier, 1986). Hence, the mean residence time is expressed by:

$$t_1 = \frac{\rho_l \cdot \sigma_{sp} A.L_1}{F_L} \tag{3.34}$$

$$F_L = \frac{F_{Lime}}{3600} \tag{3.35}$$

where:

ρ_L : density of limestone particles,kg/m^3

F_{Lime} : mass flowrate of limestone in the feed,kg/hr

F_L : mass flowrate of limestone in the feed,kg/sec

Since SO_2 is well mixed in the dense bed, an overall SO_2 balance on the dense bed gives:

$$A.U_1.C.Y_{SO_2,L1}=(R_{SO_2,1}-r_{SO_2,1}).V_C \tag{3.36}$$

Division of Eq. (3.36) by AU_1C causes A to be eliminated, and thereby we get $Y_{SO2,L1}$ in terms of other parameters:

$$Y_{SO_2,L1}=\frac{L_1.(R_{SO_2,1}-r_{SO_2,1})}{C.U_1} \tag{3.37}$$

Our convergence problem is to find a value of $Y_{SO2,L1}$ satisfying Eq. (3.37). The procedure is as follow:

1)- Guess a $Y_{SO2,L1}$

2)- Calculate $r_{SO2,1}$ from Eq. (3.33)

3)- Calculate a value of $Y_{SO2,L1}$ from Eq. (3.37)

4)- If the calculated $Y_{SO2,L1}$ does not agree with the guessed value, a new guess for $Y_{SO2,L1}$ is made. The same procedure is repeated until satisfactory agreement between the calculated and guessed value is obtained.

The fractional sulphur capture in the dense bed $\eta_{SO2,1}$ can be evaluated as follows:

$$\eta_{SO_2,1} = 1 - \left[\frac{\textit{sulphur leaving with combustion product in the dense bed}}{\textit{sulphur in feed}} \right] \quad (3.38)$$

$$\eta_{SO_2,1} = 1 - \left[\frac{Y_{SO_2,LI} \cdot C.U_1.A}{F_C \cdot \frac{W_S}{32}} \right] \quad (3.39)$$

Once the $\eta_{SO2,1}$ is calculated for the lower region of bed, it will be used as the fractional conversion of the key component for the RSTOIC reactors. Note that the SO_2 model, as Fortran code, is then nested in the ASPEN PLUS input file so that the SO_2 absorbing block may be executed.

3.4.2 Upper sub-flowsheet

Plug flow regime for both gas and solid phases is assumed in the upper region of the CFBC. To model this region, the dilute bed is divided into n discrete intervals. A number of reactors including RCSTR, REQUIL and RSTOIC are used in order to simulate the corresponding phenomena in each interval. Calculations are carried out in the direction shown in Figure (3.2). Here, we will develop the calculation procedure for the ni^{th} interval in general forms. One can use the same equations considering ni = 1,2,3,...n for the other intervals starting from the bottom of the upper region to the top of the bed.

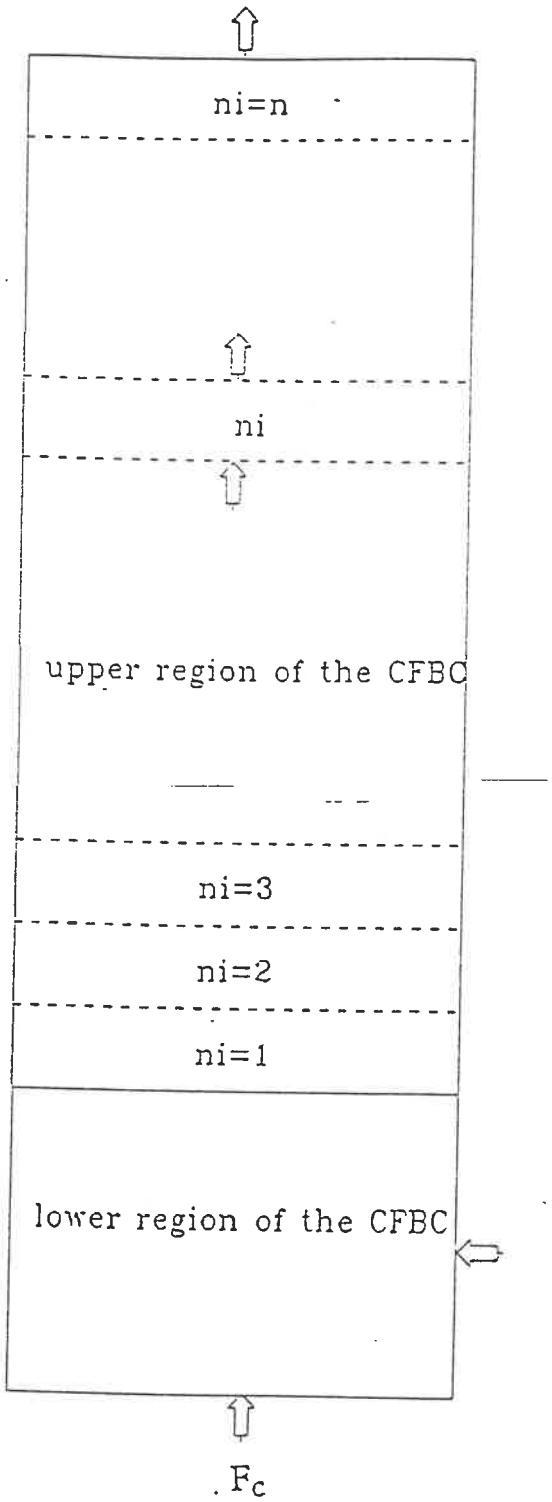

Figure 3.2 Direction for Making Simulation in the Entire CFBC

3.4.2.1 Block RCSTR

To model char combustion in each interval of the upper region, RCSTR is considered. This type of reactor is used to model a reactor with a known kinetic expression.

- **Kinetic models for RCSTR**

As before, two dominant reactions are assumed in RCSTR. The reaction rate formulas can be achieved using the same procedure as developed previously.

$$k_{21,ni}=\frac{3.\eta_{O2}.k_{cr}.F_{char,ni}.(1-\epsilon_{u,ni,avg})}{\rho_{char}.r_{C}.(1-\epsilon_{C}).F_{solid,ni}} \tag{3.40}$$

$$r_{21,ni}=k_{21,ni}.C_{O_2} \tag{3.41}$$

where:

$F_{char,ni}$: Flux of the char particles entering the nith interval, kg/sec

$F_{solid,ni}$: Flux of solids entering the nith interval, m^3/sec

$\epsilon_{u,ni,avg}$: mean axial voidage in the nith interval of the upper region of the CFBC

ni : interval number in the upper region of the CFBC

$k_{21,ni}$: volumetric rate constant for the char combustion in the nith interval of the upper region, sec^{-1}

$r_{21,ni}$: char combustion rate per unit volume of the nith interval of the dilute bed,

kmole/(m^3.sec)

The reaction rate expression for the second reaction $r_{22,ni}$ in the nith interval in the combustion process is the same as that previously (Robinson, 1986). So we have:

$$r_{CO,ni}=1.18*10^{13}.f_{CO}.f_{O2}^{0.5}.f_{H2O}^{0.5}.\left(\frac{P}{R.T_b}\right).\exp\left(-\frac{2500}{R_1.T_b}\right).C.\varepsilon_{u,ni,avg} \qquad (3.42)$$

where:

$r_{CO,ni}$: CO combustion rate per unit volume of the nith interval,kg/(m^3.sec)

- **Block hypotheses**

RCSTR is operated under isothermal and isobaric conditions.

3.4.2.2 Block REQUIL

The purpose of this block is exactly the same as the REQUIL in the dense bed and the same input and output data, and operating conditions are applied here.

3.4.2.3 Block RSTOIC

This block is used to model the SO_2 capture in the nith interval of the dilute bed of the CFBC. The following reaction can be considered to occur in the block:

$$CaO + SO_2 + \frac{1}{2}O_2 \Rightarrow CaSO_4$$

It should be emphasized that $CaCO_3$ is unstable at CFBC conditions so the calcination process is assumed to occur instantaneously and completely in the lower region of the bed and any calcination in the upper region may be neglected. As was mentioned for the lower region, we need to develop the sulphur capture efficiency model, as Fortran code, for the nith interval of the upper region of the CFBC ($\eta_{SO2,ni,2}$). The user Fortran coded program can be inserted into the flowsheet computation. The following approach is used to calculate the $\eta_{SO2,ni,2}$.

- Model development for SO_2 absorption in the dilute bed

In the dense bed section of the bed, some parameters were formulated from mass balance, mean residence time of sorbent particles and physical properties of the components. In this section we will show how this procedure can be applied for each interval of the upper region of the CFBC.

Superficial gas velocity

At the base of the dilute zone, secondary air is added, thus making it is necessary to consider the additional amount of fluidizing gas in the material balance. Consequently, the superficial gas velocity in the upper region is:

$$n_{air-2}=\frac{F_{air-1}}{29*3600} \tag{3.43}$$

$$A.U_2.C=A.U_1.C+n_{air-2} \tag{3.44}$$

$$U_2=U_1+\frac{n_{air-2}}{A.C} \tag{3.45}$$

where:

F_{air-2}: The molar flowrate of secondary air,kg/hr

n_{air-2}: The molar flowrate of secondary air,kmole/sec

U_2 : superficial gas velocity in the dilute bed,m/sec

Mass balance on SO_2

The sulphur capture efficiency in the lower region was calculated and thus the rate of SO_2 per unit volume of the nith interval is constant and given by:

$$R_{SO_2,ni,2}=\frac{(1-\eta_{SO_2,ni-1}).F_C.W_S}{32.A.\Delta L} \tag{3.46}$$

where:

$R_{SO2,ni,2}$: Rate of SO_2 per unit volume of the nith interval in the upper region of the CFBC,kmole/(m^3.sec)

$\eta_{SO2,ni-1}$: Fractional sulphur capture in the bed with the height of L_1+Z_{ni-1}

For the first interval (ni=1), we have:

$$\eta_{SO_2,ni,2}=\eta_{SO_2,1} \tag{3.47}$$

$$Y_{SO_2,ni-1,u}=Y_{SO_2,L1} \tag{3.48}$$

where:

$Y_{SO2,ni-1,u}$: mole fraction of SO_2 entering the nith interval of the upper region

For the other intervals:

$$\eta_{SO_2,ni-1}=1-\left[\frac{Y_{SO_2,ni-1,u}.C.U_2.A}{F_C.\frac{W_S}{32}}\right] \tag{3.49}$$

Eqs. (3.29) and (3.30) may be used here to calculate the effect of attrition. By integrating

Eq. (3.24) and considering the average concentration for SO_2 in each interval, we obtain the fractional conversion of CaO in each interval as follows:

$$X_{CaO,ni,2}=\frac{V_{CaO}}{1-\epsilon_I}.\left[\frac{t_{ni,2}-\frac{1}{a_1}.\ln(1+\frac{3.\alpha.C.Y_{SO_2,ni,\mu}}{R_s.K_V}.(e^{a_1.t_{ni,2}}-1))}{\frac{R_s}{3.\alpha.C.Y_{SO_2,ni,\mu}}-\frac{1}{K_V}}\right] \tag{3.50}$$

where:

$X_{CaO,ni,2}$: fractional conversion of CaO in the nith interval

The mean residence time of sorbent particles in the interval, $t_{ni,2}$, is given by:

$$t_{ni,2}=\frac{\rho_l.\sigma_{sp}.A.\Delta L}{F_L.\left(1-\sum_1^n X_{CaO,ni-1,2}\right)} \tag{3.51}$$

For the first interval(ni=1):

$$\sum_{1}^{n} X_{CaO,ni-1,2} = X_{CaO} \tag{3.52}$$

The rate of SO_2 removed per unit volume of the interval can be expressed by:

$$r_{SO_2,ni,2} = \frac{V_{CaO}.F_{lime}}{(1-\epsilon_l).A.\Delta L*100}.\left[\frac{t_{ni,2} - \frac{1}{a_1}.\ln(1+\frac{3.\alpha.C.Y_{SO_2,ni,u}}{R_s.K_V}.(e^{a_1.t_{ni,2}}-1))}{\frac{R_s}{3.\alpha.C.Y_{SO_2,ni,u}} - \frac{1}{K_V}}\right] \tag{3.53}$$

where:

$r_{SO2,ni,2}$: Mole of SO_2 removed per unit volume of the nith interval,Kmole/(m^3.sec)

$t_{ni,2}$: Mean residence time of sorbent particles in the nith interval,sec

$Y_{SO2,ni,u}$: Mole fraction of SO_2 in the nith interval

Since SO_2 is well mixed in the nith interval, an overall SO_2 balance on the interval gives:

$$A.U_1.C.Y_{SO_2,ni,u} = (R_{SO_2,ni,2} - r_{SO_2,ni,2}).A.\Delta L \tag{3.54}$$

Division of Eq. (3.54) by AU_1C causes A to be eliminated, and thereby we get $Y_{SO2,ni,u}$ in terms of other parameters:

$$Y_{SO_2,ni,u} = \frac{\Delta L.(R_{SO_2,ni,2} - r_{SO_2,ni,2})}{C.U_2} \tag{3.55}$$

Our convergence problem is to find a value of $Y_{SO2,ni,u}$ satisfying Eq. (3.55). The procedure is as follow:

1)- Guess a $Y_{SO2,ni,u}$

2)- Calculate $r_{SO2,ni,2}$ from Eq. (3.53)

3)- Calculate a value of $Y_{SO2,ni,u}$ from Eq. (3.55)

4)- If the calculated $Y_{SO2,ni,u}$ does not agree with the guessed value, a new guess for $Y_{SO2,ni,u}$ is made. The same procedure is repeated until satisfactory agreement between the calculated and guessed value is obtained.

The fractional sulphur capture in the interval ($\eta_{SO2,ni,2}$) can be evaluated as follows:

$$\eta_{SO_2,ni,2} = 1 - \left[\frac{Y_{SO_2,ni,u}.C.U_2.A}{F_C.\frac{W_S}{32}.(1-\eta_{SO2,ni})} \right] \tag{3.56}$$

Once the $\eta_{SO2,ni,2}$ is calculated for the nith interval of the upper region of bed, it will be used as the fractional conversion of the key component. This value is necessary to run the RSTOIC block in the ASPEN PLUS simulation. As before, the upper section of the bed

is divided into n intervals. In each interval three reactors are employed: RPLUG, RSTOIC and REQUIL. We have developed the corresponding expression and the ASPEN PLUS language for the nith interval. Calculations are therefore started in the first interval and continued upward in order to arrive to the top of the bed.

Upon completing calculations in the bed, the fractional sulphur capture in the upper region of the CFBC $\eta_{SO2,2}$ can be calculated as follows:

$$\eta_{SO_2,2} = 1 - \left[\frac{Y_{SO_2,n,u}.C.U_2.A}{F_C.\frac{W_S}{32}.(1-\eta_{SO_2,1})} \right] \tag{3.57}$$

The value of the overall sulphur capture efficiency (η_{SO2}) can also be obtained with $Y_{SO2,n,u}$ as follow:

$$\eta_{SO_2} = 1 - \left[\frac{Y_{SO_2,n,u}.C.U_2.A}{F_C.\frac{W_S}{32}} \right] \tag{3.58}$$

3.4.3 Sep sub-flowsheet

This sub-flowsheet contains two unit operation blocks; CYCLONE and FSPLIT. Cyclone is used for the gas/solid separation at the riser outlet. In order to satisfy the

material balance in the CFBC, a solid drain valve, FSPLIT, is used.

3.4.3.1 Block CYCLONE

CYCLONE, ASPEN PLUS unit operation block, is used for gas- solid separation in the top of the CFBC to remove almost 100% of the solids from the gas. The following input variables is used in CYCLONE:

D_C : cyclone diameter,m

cyclone type: high efficiency

3.4.3.2 Block FSPLIT

To maintain the required level of solid inventory in the bed, a solid drain valve presented as FSPLIT in ASPEN PLUS is used. The resulting solid stream from CYCLONE is fed to FSPLIT where it is divided into two streams: the first one is recycled into the lower region and the second exits the system in order to satisfy the material balance. Only the fraction of residue (F_R) going to the outlet stream needs to be specified.

3.5 Value of the Fixed Parameters Used in the Simulation

The following fixed parameters, which were taken from the literature, will be used in the simulation model:

Table 3.2 Design Data

Reactor dimension	SOURCE
$A = 0.13\ m^2$	(Desai et al., 1991)
$L = 6.7\ m$	" " " " "
$D_r = 0.405\ m$	" " " " "

Table 3.3 Physico-chemical Properties Used in the Simulation (Desai et al, 1991)

PARAMETER	SOURCE
$D = 1.525*10^{-4}, m^2/sec$	(Zhao, 1992)
$D_{eff} = 1*10^{-5}, m^2/sec$	(Wong, 1991)
$E_1 = 1.247*10^8, J/kmole$	(Gordon and Amundson, 1978)
$k_{01} = 1.55*10^7, m/sec$	" " " " "
$K_V = 8*10^{-4}$, kmole/(m^3-sec)	(Couturier, 1986)
$R_g = 8314$, J/(kmole-sec)	
$R_1 = 8.205*10^{-2}$,(m^3-atm)/(kmole-k)	
$V_{CaO} = 1.69*10^{-2}, m^3/kmole$	(Wong, 1991)
$\beta = 0.16$	(Douglas and Young, 1991)
$\epsilon_C = 0.30$	(Wong, 1991)
$\epsilon_I = 0.52$	
$\rho_{char} = 1500, kg/m^3$	(Wong, 1991)
$\rho_L = 2710, kg/m^3$	(Wong, 1991)
$\rho_S = 800, kg/m^3$	(Gordon and Amundson, 1978)
$\phi_s = 0.806$	

Table 3.4 Coal Analysis (Desai et al, 1991)

PROXIMATE ANALYSIS	Wt%
1- Moisture	5.2
2- Fixed carbon (dry basis)	54.87
3- Volatile matter (dry basis)	35.62
4- Ash	9.51
ULTIMATE ANALYSIS	**F(y)-Wt%**
1- Ash	9.51
2- Carbon (W_C)	75.14
3- Hydrogen (W_H)	4.76
4- Nitrogen (W_N)	1.41
5- Sulphur (W_S)	3.88
6- Oxygen (W_O)	5.30

Table 3.5 Particle Size Distribution of Coal Particles (Desai et al, 1991)

k	Size Ranges (micron)	$R_c(k)$,cm	$r_c(k)$,m	$P_{k,0}(r_c(k))$
1	0-200	0.01	10^{-4}	0.1
2	200-400	0.03	$3*10^{-4}$	0.08
3	400-800	0.06	$6*10^{-4}$	0.12
4	800-1000	0.09	$9*10^{-4}$	0.07
5	1000-2000	0.15	$1.5*10^{-3}$	0.19
6	2000-3000	0.25	$2.5*10^{-3}$	0.14
7	3000-4000	0.35	$3.5*10^{-3}$	0.1
8	4000-5000	0.45	$4.5*10^{-3}$	0.1
9	5000-6000	0.45	$5.5*10^{-3}$	0.08
10	6000-10000	0.8	$8*10^{-3}$	0.02

Table 3.6 Particle Size Distribution of Sorbent Particles (Desai et al, 1991)

m	Size Ranges (micron)	$R_s(m)$,cm	$r_s(m)$,m	$P_{m,0}(R_s(m))$
1	0-40	0.002	$2*10^{-5}$	0.1
2	40-80	0.006	$6*10^{-5}$	0.1
3	80-100	0.009	$9*10^{-5}$	0.1
4	100-200	0.015	$1.5*10^{-4}$	0.4
5	200-300	0.025	$2.5*10^{-4}$	0.15
6	300-400	0.035	$3.5*10^{-4}$	0.08
7	400-750	0.0575	$7*10^{-4}$	0.04
8	750-1000	0.088	$1.5*10^{-3}$	0.02
9	1000-2000	0.15	$2.5*10^{-3}$	0.10
10	2000-4000	0.3	$3.5*10^{-3}$	0.00

CHAPTER 4

SIMULATION RESULTS AND MODEL VALIDATION

In ASPEN PLUS, there is no model capable of simulating CFBC reactors. However, ASPEN PLUS allows users to insert their own models, coded in Fortran, into the simulation. These Fortran programs are used in conjunction with ASPEN PLUS unit operation blocks to simulate the CFBC. There are generally two different approaches to model a CFBC. The first approach, known as the " BLACK BOX", uses a given reaction stoichiometry, fractional conversion of key components, bed temperature and pressure to compute the outlet stream compositions and the heat generated by the reactions. This model is useful to predict the output variables as well as the heat generated by the coal combustion. This approach is also helpful as it gives the order of magnitude for the heat generated by the coal combustion reactions. This approach, however, fails to provide information regarding the emissions of NO_x, N_2O, CO and SO_2 as well as the heat transfer phenomena within the CFBC. This is without a doubt, a major disadvantages of this types of model. For this reason, a second approach is usually used to model CFBC units. This second approach considers the different physical aspects regarding the kinetics of chemical reactions, the hydrodynamic model and other phenomena associated with the modelling of CFBCs. Our approach, which falls into this category, will be referred to as the SLPC-1 (Sotudeh, Legros, Paris and Chaouki) simulation model.

Fourteen different sets of operating data from several CANMET runs were used in our simulation. A detailed description of the CANMET 0.8 MWth CFBC pilot plant

is presented in Appendix A.5.

4.1 BLACK BOX APPROACH

As mentioned previously, several studies regarding CFBCs have considered the entire CFBC system as a BLACK BOX (Young, 1986). This approach is useful when the calculation of output variables is the only requirement. Herein, we have also used this approach to get an idea of the output variables. To do so, the entire CFBC system was considered as a BLACK BOX and modelled using a RSTOIC reactor as shown below:

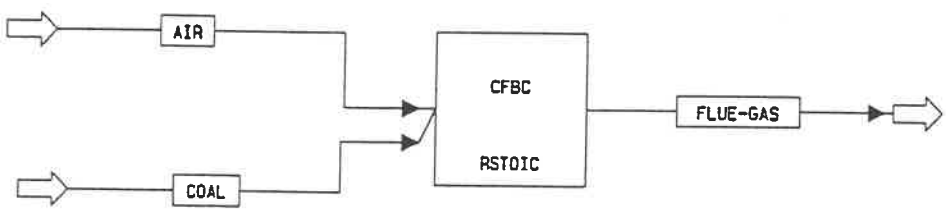

4.1.1 Model Hypotheses

This approach is based on the following hypotheses:

1- The following reactions were considered to attain complete in the simulation:

1) $C + O_2 \Rightarrow CO_2$

2) $S + O_2 \Rightarrow SO_2$

3) $H_2 + \frac{1}{2}O_2 \Rightarrow H_2O$

4) $CaCO_3 \Rightarrow CaO + CO_2$

5) $CaO + SO_2 + \frac{1}{2}O_2 \Rightarrow CaSO_4$

2. There are no intermediate products, such as CO, formed.

3. There is no NO_x formation from the fuel nitrogen and from the air.

4.1.2 Simulation results

The entire CFBC was modelled using one RSTOIC reactor. Coal and air streams serve as the input streams to the RSTOIC. Operating data from CANMET runs were used as a basis for the calculation and included the model variables included the oxygen, nitrogen, carbon monoxide, CaO, $CaSO_4$ and H_2O fluxes (Desai et al, 1991). As stated previously, no information regarding the NO_x, N_2O, CO and SO_2 emissions are obtained with this model. This approach, however, gives the order of magnitude for the O_2, N_2, and CO_2 concentrations in the flue gases considering complete conversion. Once calculated, the output variables from the BLACK BOX simulation, can be used as a comparison basis for similar parameters obtained using the SLPC-1 simulation. Table 4.1 shows the BLACK BOX simulation results for run # 1 of CANMET data.

Table 4.1 BLACK BOX simulation results

STREAM ID / FLUX (KMOLE/HR)	INPUT	OUTPUT
COAL	6.2013	0.00
O_2	5.8159	0.654
N_2	21.9802	21.982
CO_2	0.00	4.596
LIME	0.1918	0.00
CaO	0.00	0.119
$CaSO_4$	0.00	7.3082E-2
H_2O	0.00	1.5143
TOTAL	34.1892	28.9384

4.2 SLPC-1 APPROACH

In chapter 3, we discussed in detail the CFBC process simulation model development. Our model links together the hydrodynamic parameters and the reaction models, which include the kinetic subroutines and internal Fortran blocks nested in the input file. The developed algorithms allow the parameters used by the ASPEN PLUS simulation program to be calculated. In order to simulate the CFBC, several ASPEN PLUS reactor models are assembled to represent the phenomena identified in the coal combustion process in chapter 1. Fortran blocks, integrated with the ASPEN PLUS input file, provide required information for the operation of the ASPEN PLUS reactor models. It is interesting to note that most fluidized bed models reported in the CFBC literature have a level of complexity which varies with the model's applicability. Detailed studies usually predict various parameters such as reactive concentration profiles, heat transfer and temperature profiles, attrition effects, particle size distribution, combustion heat release and NO_x emissions as well as the factors leading to NO_x formation and destruction. Since our model was developed for process simulation purposes, the predictions are based on a lumped approach, instead of a differential approach as in the more complex models. However, our model still provide prediction capabilities as a result of its innovative utilization of kinetic models and ASPEN PLUS reactor models. The internal details and operation procedures for the SLPC-1 simulation program are now presented:

4.2.1 Simulation diagram for the CANMET CFBC unit

Along with the unit operation blocks provided by ASPEN PLUS, several complete Fortran programs, an external subroutine for the kinetic models, and internal fortran blocks were used in the simulation. A comprehensive simulation diagram for the CFBC is illustrated in Figure 4.1. The required data necessary to execute the Fortran blocks

were collected from the ASPEN PLUS streams. The Fortran codes contain the following four blocks which are required to accurately model CFBCs. The first block, "SUM.FOR", is the external kinetic subroutine developed from the simulation model in chapter 3 for both gas/solid and gas/gas reactions. The information needed for this block is obtained from the ASPEN PLUS subroutines and the user Fortran blocks. The developed kinetic model in Fortran code is presented in Appendix A.2.

The second Fortran block, called "F-1", when integrated with the ASPEN PLUS input file, calculates the residence time of char particles in the CFBC. This calculation is required in order to execute the external subroutine as mentioned above. The program is presented in Appendix A.3.

The third block, "HYDRO", is inserted into the ASPEN PLUS input file to calculate the mean void fraction in each section of the upper region and in the dense bed of the CFBC. The program can be found in Appendix A.3.

The fourth block of Fortran codes, "SO2", calculates the sulphur capture efficiency in each section of the upper region and in the dense bed. This program is nested in ASPEN PLUS input file so that all the RSTOIC reactors used to model the SO_2 capture in the bed can be executed. The program is presented in Appendix A.3.

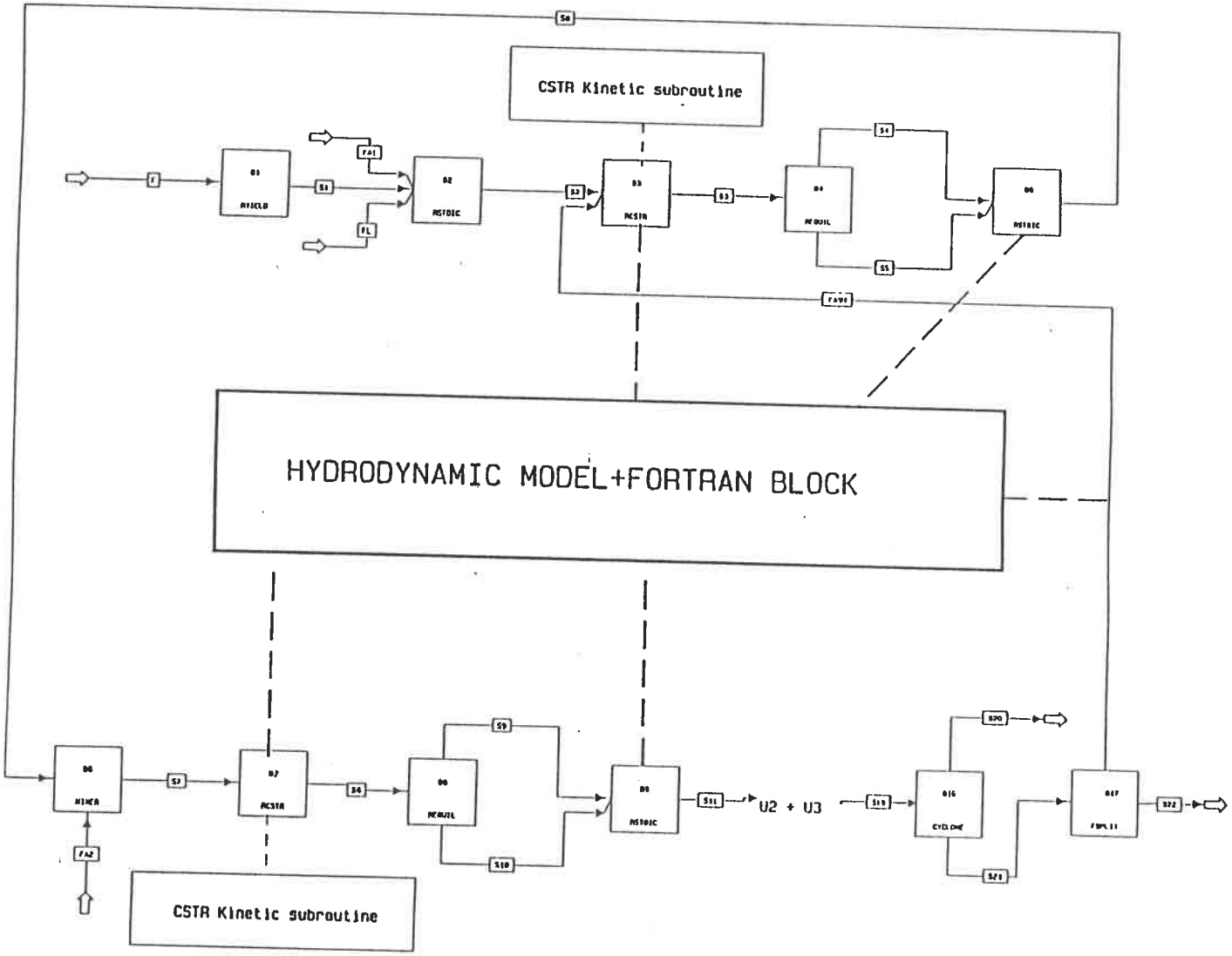

Figure 4.1 A Comprehensive Simulation Diagram For the CFBC

4.2.2 Simulation convergence

As discussed previously, one of the goals of the CFBC is to promote complete combustion by recirculating the solids captured by the cyclone back to the base of the riser. For this reason, the flowsheet contains only one recycle loop. The simulation flowsheet containing the recycle loop must be solved iteratively and the tear streams, convergence methods and calculation sequence must be specified. ASPEN PLUS can perform all of these functions automatically or the user can supply them. Some options are available for converging recycle loop in ASPEN PLUS (ASPEN TECHNOLOGY, 1988(b)). To converge the recirculation stream in the simulation, we have used the classical bounded Wegstein method, which almost always converges rapidly (ASPEN TECHNOLOGY, 1988(b)).

It should be mentioned that in order for convergence to occur, the value of the tear stream variables should be correctly initialized. Such as initialization will enable a rapid convergence of the tear streams. In order to initialize the tear stream variables (FASH), a value greater than G_s was considered for the initial tear stream flux. Since the combustion efficiency through one pass is less than 10%, the amount of char in the tear stream was approximately taken to attain 100% combustion efficiency. The composition of other constituents in the tear stream can be found automatically during convergence. Sometimes, a direct convergence method, which converges slowly but surely, can be used to approximate the tear stream variable composition. The initialization of the parameters whose values are calculated by either Fortran blocks or convergence blocks is extremely important. The ASPEN PLUS input file for the simulation of the CFBC is presented in Appendix A.1.

4.2.3 Simulation results

Herein, the values predicted using our simulation model are compared to those calculated using the BLACK BOX approach (table 4.2). Operating data from CANMET runs were used as basis for simulation calculations (Desai et al, 1991). It can be seen that the SLPC-1 model has a predictive capability as it calculates the coal combustion efficiency, instead of using a given value as for the simple BLACK BOX model. The small differences in the oxygen concentration between the two approaches, can be related to the combustion efficiency. For the BLACK BOX approach, the combustion efficiency was assumed to be 100%, while for the SLPC-1 simulation, this value was calculated to be 98%.

Table 4.2 The Comparison Between Simulation Results for BLACK BOX Approach and "SLPC-1" Approach

STREAM ID Kmole/hr	INPUT	OUTPUT (BLACK BOX)	OUTPUT (SLPC-1)
COAL	6.2013	0.00	0.00
O_2	5.8159	0.654	0.676
N_2	21.9802	21.982	21.98
C	0.0	0.00	1.665E-3
SO_2	0.0	0.00	0.0187
CO	0.0	0.00	1.226E-3
CO_2	0.0	4.596	4.5824
NO	0.0	0.00	1.285E-3
NO_2	0.0	0.00	9.378E-6
N_2O	0.0	0.00	8.578E-8
LIME	0.1918	0.00	0.0
CAO	0.0	0.1198	0.068
$CASO_4$	0.0	7.3082E-2	0.009
H_2O	0.0	1.5143	1.5143
TOTAL	34.1892	28.9384	28.853

4.3 CARBON MONOXIDE COMBUSTION RATE

Carbon monoxide is produced during the incomplete combustion of char or as an intermediate combustion product in the bed. Factors contributing to CO emission levels are the bed temperature, O_2, CO and H_2O concentration. The CO combustion rate has been studied by several researchers and the most important of them are presented below:

$$r_{CO}=1.30*10^{11}.\exp\left(-\frac{3000}{R.T_b}\right).C_{CO}.C_{O2}^{0.5}.C_{H2O}^{0.5} \tag{4.1}$$

(Congalidis and Georgakis, 1981)

$$r_{CO}=3.09*10^{8}.\exp\left(\frac{-1.2*10^{-4}}{T_b}\right).C_{O_2}.C_{CO} \tag{4.2}$$

(Gordon and Amundson, 1976)

$$r_{CO}=3.0*10^{10}.\exp\left(\frac{-6.699*10^{7}}{R.T_b}\right).\left(\frac{P}{R_g.T_b}\right)^{1.8}.f_{H_2O}^{0.5}.f_{CO}.*\left(\frac{17.5*f_{O_2}}{1+f_{O2}}\right).C \tag{4.3}$$

(Wong, 1991)

$$r_{CO}=1.20*10^{11}.f_{CO}.f_{O2}^{0.3}.f_{H2O}^{0.5}.\left(\frac{P}{R.T_b}\right)^{0.8}.\exp\left(-\frac{16000}{R.T_b}\right).C \tag{4.4}$$

(Robinson, 1986)

$$r_{CO}=1.18*10^{13}.f_{CO}.f_{O2}^{0.5}.f_{H2O}^{0.5}.\left(\frac{P}{R.T_b}\right).\exp\left(-\frac{25000}{R_1.T_b}\right).C \tag{4.5}$$

(Robinson, 1986)

The validity of proposed CO combustion rates were determined by inserting the above expressions into the simulation program. The simulation was then executed for the conditions of Run # 1 (Desai et al, 1991) using each of the above rate expressions and the CO yields are presented below:

Equation	4.1	4.2	4.3	4.4	4.5
CO (ppm)	1.00	12000	00.0	11.4	45.00

Although CO combustion rates have been widely studied, the usefulness of these expressions pertaining to CFBCs is limited. Considering the above results, the equation number 4.5 closely compares to the CO range reported by Desai et al (1991). Therefore, this expression has been used in the simulation of the experimental conditions throughout runs #1 to # 14.

4.4 MODEL VALIDATION

In order to validate the proposed model, data from various CANMET runs (Desai et al. 1991) were used to cover a wide range of conditions as shown in table 4.3. So far, the results of the simulation were obtained for the condition Run #1. The experimental parameters for each run included emission data, combustion efficiency and sulphur capture efficiency. These experimental results were compared with those obtained from our simulation model. Unfortunately, the material balances for the experimental data do not close and in some cases the error is more than 3 percent. Therefore, it is difficult to justify the experimental error when the sources of error for the experimental data are unknown. However, the main difference between the simulation results and experimental data is related to the oxygen level, which has been corrected for the experimental data in order to satisfy the material balances. The comparison between the simulation results and the experimental data are provided, through the different parameters presented in table 4.4, in tables 4.5 through 4.18.

Table 4.3 The CFBC Operating Conditions (Desai et al, 1991)

Data / RUN	T_b K	F_{coal} kg/hr	F_{lime} kg/hr	Ca/S	F_{air} kg/hr	S/P	L1 m
1	1140	67.30	19.20	2.28	799.0	0.45	1.37
2	1106	70.20	15.90	1.70	832.0	0.43	2.59
3	1146	64.60	13.20	1.61	778.0	0.43	2.59
4A	1155	74.90	23.50	2.38	807.0	0.43	1.37
4B	1155	62.10	16.10	1.97	796.0	0.43	1.37
5	1187	61.20	17.60	2.13	757.0	0.42	1.37
6	1180	60.40	16.60	2.07	749.0	0.41	2.59
7	1192	65.10	17.90	2.10	768.0	0.85	2.59
8	1183	63.30	17.80	2.10	773.0	0.85	1.37
9	1155	66.60	17.90	2.10	792.0	0.86	1.37
10	1152	66.30	18.10	2.06	791.0	0.86	2.59
11	1109	70.00	18.20	1.91	836.0	0.84	2.59
12A	1105	69.80	18.00	2.08	734.0	0.85	1.37
12B	1104	70.00	18.70	2.15	831.0	0.85	1.37

Table 4.4 Parameters Utilized to Compare Predicted and Experimental Results Using the CANMET Runs Operating Conditions

PARAMETER	DESCRIPTION	UNITS
W_{N2}^*	Amount of N_2 in dry flue gas	%
W_{SO2}^*	Amount of SO_2 in dry flue gas	ppm
W_{CO}^*	Amount of CO in dry flue gas	ppm
W_{CO2}^*	Amount of CO_2 in dry flue gas	%
W_{NOx}^*	Amount of NO_x in dry flue gas	ppm
W_{N2O}^*	Amount of N_2O in dry flue gas	ppm
η_C	Combustion efficiency	---
η_{SO2}	Sulphur capture efficiency	---

* corrected to 3% O_2 in dry flue gas

Table 4.5 Comparison Between SLPC-1 Simulation Results for RUN1 and Experimental Data

Emissions		SLPC-1 Model	Experimental data
O_2 (%)		2.48	3.58
N_2 (%)	Corrected to 3% O_2	80.21	80.97
SO_2 (ppm)		681.00	802.00
CO (ppm)		45.00	208.00
CO_2 (%)		16.70	15.90
NO_x (ppm)		46.00	203.00
N_2O (ppm)		00.00	----
Combustion Efficiency (%)		98.34	95.64
SO2 Capture Efficiency (%)		74.45	75.62

Table 4.6 Comparison Between SLPC-1 Simulation Results for RUN2 and Experimental Data

Emissions		SLPC-1 Model	Experimental data
O_2 (%)		1.71	3.77
N_2 (%)	Corrected to 3% O_2	79.78	81.12
SO_2 (ppm)		88.80	43.40
CO (ppm)		152.00	270.00
CO_2 (%)		17.20	15.96
NO_x (ppm)		28.60	167.60
N_2O (ppm)		00.00	118.00
Combustion Efficiency (%)		100.00	96.00
SO2 Capture Efficiency (%)		96.70	98.70

Table 4.7 Comparison Between SLPC-1 Simulation Results for RUN3 and Experimental Data

Emissions		SLPC-1 Model	Experimental data
O_2 (%)		2.87	3.79
N_2 (%)	Corrected to 3% O_2	80.70	81.50
SO_2 (ppm)		160.30	161.30
CO (ppm)		54.73	233.00
CO_2 (%)		16.28	15.40
NO_x (ppm)		52.60	156.30
N_2O (ppm)		00.00	89.00
Combustion Efficiency (%)		98.84	97.11
SO2 Capture Efficiency (%)		94.00	94.63

Table 4.8 Comparison Between SLPC-1 Simulation Results for RUN4A and Experimental Data

Emissions		SLPC-1 Model	Experimental data
O_2 (%)		2.65	3.79
N_2 (%)	Corrected to 3% O_2	79.95	81.45
SO_2 (ppm)		719.00	609.30
CO (ppm)		29.00	156.00
CO_2 (%)		16.96	15.40
NO_x (ppm)		47.00	176.00
N_2O (ppm)		00.00	80.00
Combustion Efficiency (%)		97.72	96.60
SO2 Capture Efficiency (%)		75.34	74.62

Table 4.9 Comparison Between SLPC-1 Simulation Results for RUN4B and Experimental Data

Emissions		SLPC-1 Model	Experimental data
O_2 (%)		3.57	3.63
N_2 (%)	Corrected to 3% O_2	81.02	81.23
SO_2 (ppm)		679.00	718.00
CO (ppm)		34.00	173.00
CO_2 (%)		15.90	15.60
NO_x (ppm)		63.00	144.00
N_2O (ppm)		00.00	79.00
Combustion Efficiency (%)		100.00	96.64
SO2 Capture Efficiency (%)		72.68	74.62

Table 4.10 Comparison Between SLPC-1 Simulation Results for RUN5 and Experimental Data

Emissions		SLPC-1 Model	Experimental data
O_2 (%)		4.20	3.86
N_2 (%)	Corrected to 3% O_2	81.68	81.50
SO_2 (ppm)		68.00	154.00
CO (ppm)		10.00	112.00
CO_2 (%)		15.30	15.44
NO_x (ppm)		89.00	309.00
N_2O (ppm)		00.00	51.00
Combustion Efficiency (%)		96.24	97.05
SO2 Capture Efficiency (%)		97.44	95.56

Table 4.11 Comparison Between SLPC-1 Simulation Results for RUN6 and Experimental Data

Emissions		SLPC-1 Model	Experimental data
O_2 (%)		6.50	4.50
N_2 (%)	Corrected to 3% O_2	83.46	82.20
SO_2 (ppm)		489.00	459.00
CO (ppm)		3.00	147.00
CO_2 (%)		13.25	14.70
NO_x (ppm)		122.00	150.00
N_2O (ppm)		00.00	-----
Combustion Efficiency (%)		87.40	97.45
SO2 Capture Efficiency (%)		81.60	85.11

Table 4.12 Comparison Between SLPC-1 Simulation Results for RUN7 and Experimental Data

Emissions		SLPC-1 Model	Experimental data
O_2 (%)		6.73	4.90
N_2 (%)	Corrected to 3% O_2	83.94	82.20
SO_2 (ppm)		72.00	2126.00
CO (ppm)		18.00	189.00
CO_2 (%)		13.03	14.60
NO_x (ppm)		115.00	111.00
N_2O (ppm)		00.00	-----
Combustion Efficiency (%)		97.54	-----
SO2 Capture Efficiency (%)		97.44	28.50

Table 4.13 Comparison Between SLPC-1 Simulation Results for RUN8 and Experimental data

Emissions		SLPC-1 Model	Experimental data
O_2 (%)		6.6	4.00
N_2 (%)	Corrected to 3% O_2	85.40	81.40
SO_2 (ppm)		1252.80	1044.00
CO (ppm)		6.50	154.00
CO_2 (%)		12.98	15.60
NO_x (ppm)		111.00	145.60
N_2O (ppm)		00.00	54.00
Combustion Efficiency (%)		99.995	98.90
SO2 Capture Efficiency (%)		55.00	64.70

Table 4.14 Comparison Between SLPC-1 Simulation Results for RUN9 and Experimental data

Emissions		SLPC-1 Model	Experimental data
O_2		3.16	3.62
N_2 (%)	Corrected to 3% O_2	80.86	80.82
SO_2 (ppm)		330.00	289.00
CO (ppm)		32.00	184.00
CO_2 (%)		16.10	16.10
NO_x (ppm)		59.00	155.00
N_2O (ppm)		00.00	88.00
Combustion Efficiency (%)		98.10	97.30
SO2 Capture Efficiency (%)		87.79	89.80

Table 4.15 Comparison Between SLPC-1 Simulation Results for RUN10 and Experimental Data

Emissions		SLPC-1 Model	Experimental data
O_2 (%)		3.87	4.46
N_2 (%)	Corrected to 3% O_2	81.50	81.70
SO_2 (ppm)		422.00	424.00
CO (ppm)		54.00	216.00
CO_2 (%)		15.40	15.23
NO_x (ppm)		65.60	107.62
N_2O (ppm)		00.00	90.00
Combustion Efficiency (%)		98.16	97.20
SO2 Capture Efficiency (%)		84.53	85.60

Table 4.16 Comparison Between SLPC-1 Simulation Results for RUN11 and Experimental Data

Emissions	SLPC-1 Model	Experimental data
O_2	2.45	3.79
N_2 (%)	80.22	81.40
SO_2 (ppm)	184.00	118.00
CO (ppm)	82.50	316.00
CO_2 (%)	16.70	15.53
NO_x (ppm)	35.00	107.00
N_2O (ppm)	00.00	117.00
Combustion Efficiency (%)	99.00	97.00
SO2 Capture Efficiency (%)	93.13	96.00

Corrected to 3% O_2

Table 4.17 Comparison Between SLPC-1 Simulation Results for RUN12A and Experimental Data

Emissions		SLPC-1 Model	Experimental data
O_2		0.8	3.80
N_2 (%)	Corrected to 3% O_2	79.20	81.10
SO_2 (ppm)		106.00	72.00
CO (ppm)		92.00	262.00
CO_2 (%)		17.80	15.80
NO_x (ppm)		18.00	143.00
N_2O (ppm)		00.00	110.00
Combustion Efficiency (%)		97.90	96.50
SO2 Capture Efficiency (%)		96.45	97.40

Table 4.18 Comparison Between SLPC-1 Simulation Results for RUN12B and Experimental Data

Emissions	SLPC-1 Model	Experimental data
O_2 (%)	1.11	3.83
N_2 (%)	79.18	81.10
SO_2 (ppm)	131.00	40.00
CO (ppm)	139.00	245.00
CO_2 (%)	17.80	15.90
NO_x (ppm)	23.00	255.00
N_2O (ppm)	00.00	116.00
Combustion Efficiency (%)	100.00	96.50
SO2 Capture Efficiency (%)	95.04	98.50

Corrected to 3% O_2

4.4.1 Simulation result analysis

The predicted simulation results regarding the emission levels of CO_2, NO_x, CO and SO_2 are compared with those of experimental data. The results are detailed below:

4.4.1.1 CO_2 content in the flue gas

The notable difference between the simulation model results and the experimental data is related to the higher combustion efficiency predicted by the simulation model. Considering this, the CO_2 content in the flue gas predicted by the simulation model is in good agreement with that of the experimental data.

4.4.1.2 NO_x emission levels

The predicted NO_x emission levels ranged from 28.3 to 122 ppm. The following parameters have been found to effect the NO_x emission levels (Desai et al, 1991):

a) Temperature

b) Secondary air to primary air ratio (S/P)

c) Secondary air elevation

d) O2 content of the flue gas

All the studies agree that an increase in reactor temperature causes an increase in the NO_x emission levels. We found that the increase in NO_x emission levels due to a change in reactor temperature is not considerable. Figure 4.2 shows the comparison between the predicted and experimental NO_x. It should be mentioned that only equilibrium conditions were considered in the modelling of NO_x emissions. NO_x emissions for the experimental

CFBC ranged from 106-307 ppm (Desai et al, 1991), initially we expected that the SLPC-1 simulation model would predict higher NO_x emissions than those observed experimentally. As it turned out, the SLPC-1 emissions were consistently lower than for the experimental data. This can be related to the fact that the NO_x formation model does not take into account all the formation mechanism of NO_x from the fuel nitrogen. More studies should be undertaken in order to fully describe this phenomena under CFBC conditions.

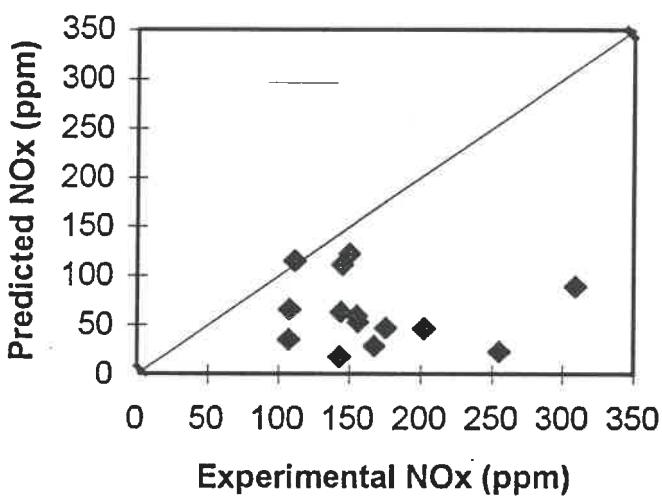

Figure 4.2 Comparison Between the Predicted and Experimental NO_x

The secondary air to primary air ratio had an effect on the NO_x emission levels. Both the experimental data and model prediction indicated that lower NO_x levels are related to the higher secondary to primary air ratio, as presented in Figure 4.3

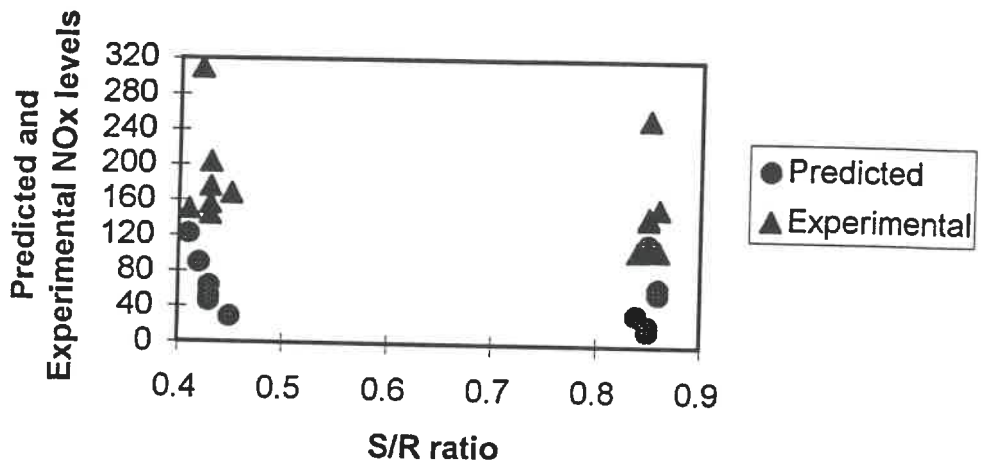

Figure 4.3 The Predicted and Experimental NO_x in Different S/P ratios

4.4.1.3 CO emission levels

The CO emission levels predicted by the SLPC-1 model ranged from 3 to 152 ppm, while those for the experimental data varied from 111-267 ppm. We found that the following parameters had an effect on the CO emission levels:

a) Temperature

b) O_2, and H_2O contents in the flue gas

c) S/P ratio

d) Hydrodynamic parameters

At high S/P ratios, CO emissions were found to increase slightly (Desai et al., 1991). Both the simulation results and the experimental data indicated that CO emission levels

decrease when the combustor temperature increases. The comparison between the predicted and experimental CO is presented in Figure 4.4. The difference between the experimental data and simulation results can be attributed to the fact that the models used to predict CO emission levels were not totally suited to CFBC conditions.

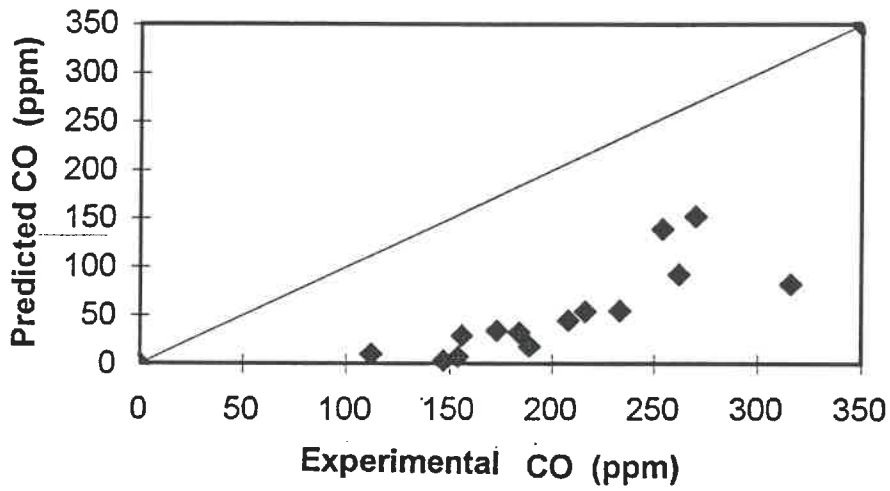

Figure 4.4 Comparison Between the Predicted and Experimental CO

4.4.1.4 SO2 emission levels

The Ca/S molar ratio ranged between 1.6 and 2.3 for the various runs considered here. Such values of Ca/S are usually considered sufficient in order to obtain a reasonable sulphur capture efficiencies. The following variables have been found to effect the sulphur capture efficiency (Desai et al, 1991):

a) Ca/S ratio

b) Bed temperature

c) S/P ratio and the secondary air elevation

d) O_2 content of the flue gas

c) Volumetric percentage of CaO in the bed

Although a definite relation between sulphur capture efficiency and Ca/S molar ratio can be noted, it is difficult to quantify this relation from the simulation due to the small range in Ca/S values used during the experimental runs. An increase in temperature was found to cause a decrease in the sulphur capture efficiency. A detailed analysis of the experimental data was provided by Desai et al (1991). Figure 4.5 shows the comparison between the predicted and experimental SO_2. The predicted simulation results correlated well with those of experimental.

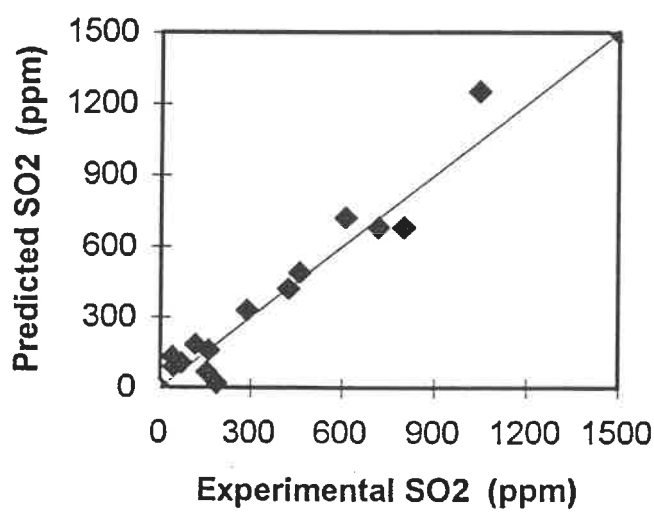

Figure 4.5 Comparison Between the Predicted and Experimental SO_2

4.4.1.5 Combustion efficiency

In order to estimate the combustion efficiency, the SLPC-1 model is considered as a black box. The two outlet streams, S20 and S22 (Figure 4.1), contain small amount of unburnt char particles compared to the concentration of char in the bed. However, this small fraction of char particles controls the combustion efficiency. The combustion efficiency (η_C) is defined as:

$$\eta_C = \frac{\textit{Total rate of carbon in the outlet stream}}{\textit{Total rate of carbon in the feed stream}}$$

The combustion efficiency predicted by the SLPC-1 model is compared in Figure 4.6 with the experimental values.

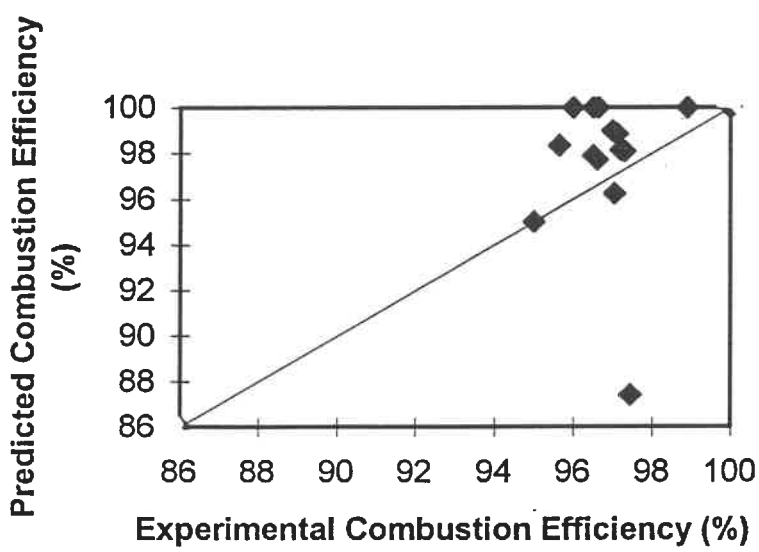

Figure 4.6 Comparison Between the Predicted and Experimental Combustion Efficiency

Herein, the differences do not appear to be large when considering the error caused by simulating all unit operation blocks in series. This assumption is somewhat erroneous as in a real CFBC the phenomena associated with coal combustion occur simultaneously and not in series.

4.4.1.6 O_2 and CO concentration profiles within the CFBC

The CANMET CFBC pilot plant allows measurement of the emission data at the output of the CFBC only. It is not possible to obtain the information regarding the O_2 and CO concentration profiles along the riser. Our simulation model goes one step further as it predicts oxygen and carbon monoxide concentrations within the CFBC. The CANMET CFBC pilot plant does not provide the data necessary for the simulation model justification in that way. However, the predicted concentration profiles have been compared qualitatively with data from the literature. The comparison of experimental data at a given riser height are in close agreement with those predicted by the SLPC-1 model. In the lower region, a significant change in the oxygen concentration is found, while in the upper region, there is a gradual decrease in the oxygen concentration. The CO concentration is constantly high in the lower region, while it sharply decreases in the upper region due to the injection of secondary air. Typical O_2 and CO concentration profiles provided by Hansen et al. (1991), presented in Figure 4.7, and experimental data reported by Brereton et al. (1991) and Grace et al. (1989), presented in Figures 4.8 and 4.9, are in close agreement with those obtained by the SLPC-1 model.

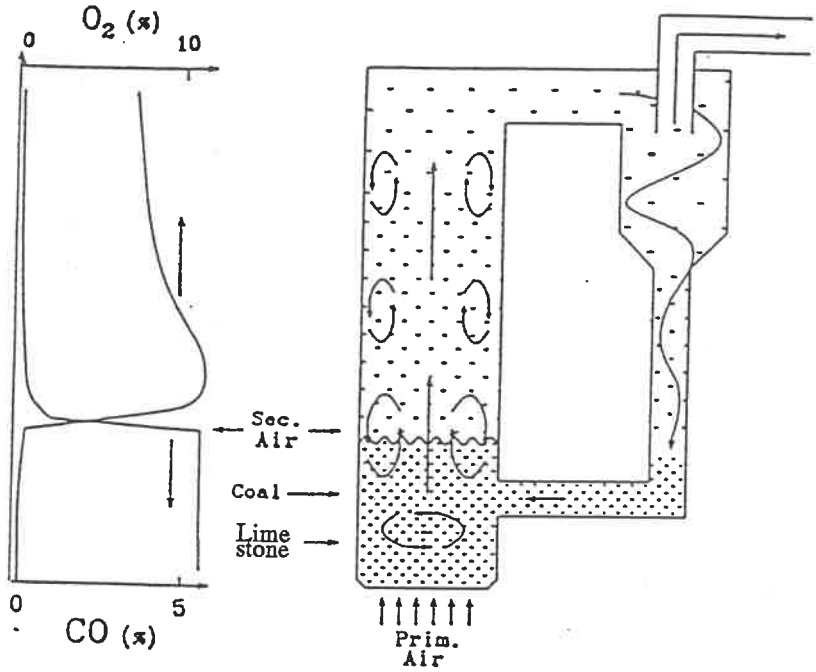

Figure 4.7 Typical Concentration Profiles for Oxygen and Carbon Monoxide within the CFBC (Hansen et al., 1991)

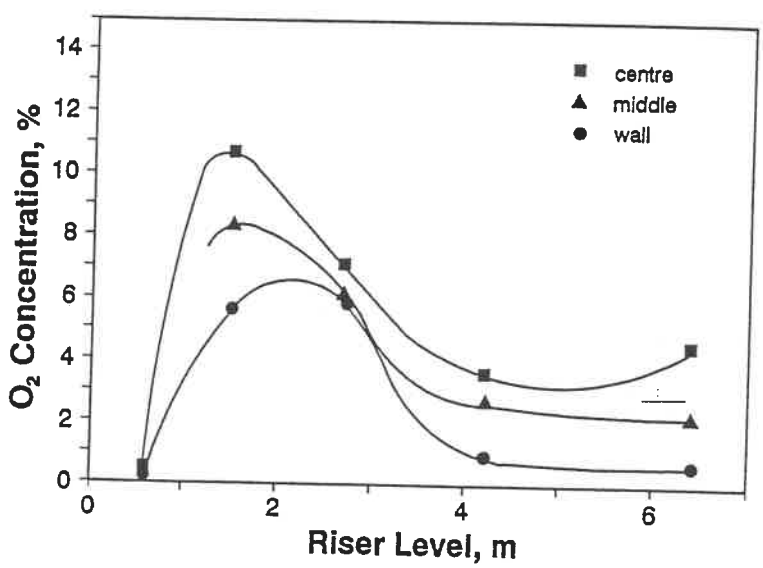

Figure 4.8 O_2 Concentration Profile as a Function of Height within the CFBC (Brereton et al., 1991)

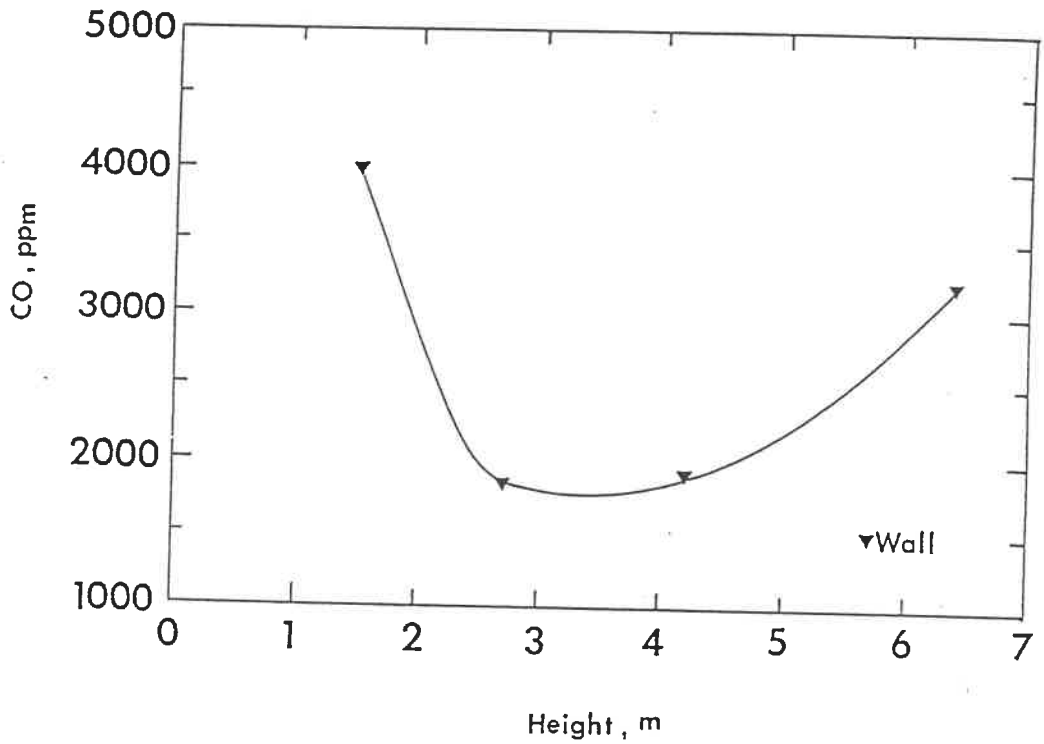

Figure 4.9 CO Concentration Profile as a Function of Height within the UBC-CFBC (Grace et al., 1989)

Due to the relatively dense bed found at the bottom of the CFBC, measurements of the O_2 and CO concentration in the lower region of the bed were very difficult. Therefore, the experimental data pertaining to O_2 and CO concentration have only been reported for the upper region. The comparison of the experimental data provided from the upper region with those of the SLPC-1 model, presented in Figures 4.10 and 4.11, shows reasonable agreement.

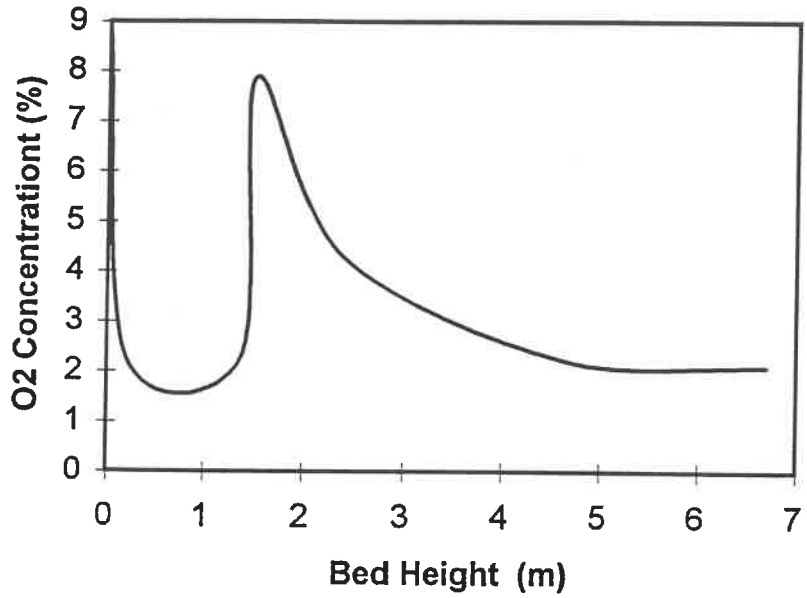

Figure 4.10 O_2 Concentration Profile within the CFBC Predicted by SLPC-1

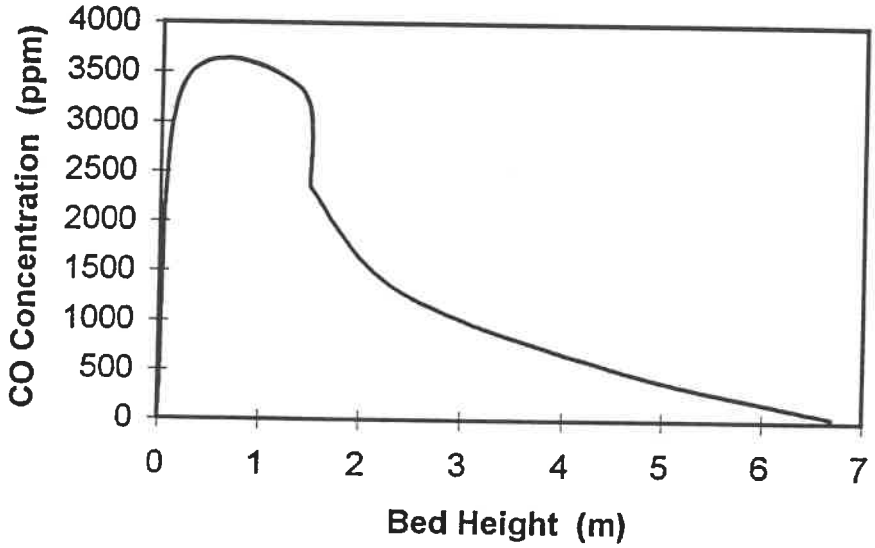

Figure 4.11 CO Concentration Profile within the CFBC Predicted by SLPC-1

4.4.1.7 Conclusion

In order to improve the simulation model, several parameters in the simulation model could be tuned through a optimisation process, but this is outside the scope of this work. In general, our model is capable of predicting output variables which correspond closely to those of the experimental data. Herein, the CFBC has been modelled using two distinct regions. The lower region is considered perfectly mixed while the upper region is assumed to operate under plug flow conditions. For the modelling of the plug flow regime, discrete intervals, each perfectly mixed, were considered. Obviously, the model capability could be enhanced by considering a higher number of discrete intervals. The increase in the number of discrete intervals required could be optimised in accordance with the hydrodynamic model. Overall, our study has accomplished the following:

1- Linking between hydrodynamic and reaction models

2- Modelling of reaction kinetics for gas/solid and gas/gas reactions

3- Prediction of sulphur capture efficiency and overall combustion efficiency

4- Prediction of NO_x emission levels

5- Calculation of particle size distribution

CHAPTER 5

CONCLUSIONS AND RECOMMENDATIONS FOR FUTURE WORK

5.1 CONCLUSIONS

A simulation model was developed for the combustion of coal in a circulating fluidized bed. For this purpose, a two-region hydrodynamic model was integrated with the coal combustion reaction models. The proposed hydrodynamic model which, calculates the bed voidage along the riser, is based on the Kunii-Levenspiel model and the Patience-Chaouki correlation. To insure that the required information for the flowsheet is provided, the hydrodynamic model was developed using a Fortran code nested in the ASPEN PLUS input file.

The reaction models consider four important aspects of coal combustion:

- The devolatilization and volatile combustion process
- The char combustion process
- The NOx formation process
- The SO2 capture process by limestone particles

These aspects were modelled using four reactor models; RYIELD, RSTOIC, RCSTR and

REQUIL. For all the RCSTR in the lower and in each section of the upper region, the kinetic models were developed using data from the literature. The developed kinetic models were inserted into the flowsheet calculations as a subroutine for each RCSTR block. For the RSTOIC reactors, which model SO_2 capture, a mathematical model was developed. This model was derived from mass balance equations and the corresponding kinetic expressions from the literature, the hydrodynamic parameters and the simplification hypotheses. The model, developed using Fortran code, was nested in the ASPEN PLUS input file in order to calculate the SO_2 capture efficiency required by the RSTOIC reactor blocks during the simulation.

Our simulation model integrates the hydrodynamic parameters, the reaction models, the kinetic subroutines, and the Fortran Blocks. The prediction from various models published in the literature regarding CO combustion rates were also studied.

The validity of the proposed model was demonstrated using fourteen different sets of operating conditions for the CANMET 0.8 MWth CFBC pilot plant. The predicted and the experimental parameters that were compared included emission data, combustion efficiency and sulphur capture efficiency. It was found that the predicted simulation results correlated well with the data from the experimental CFBC.

NO_x chemistry is an important concern in the CFBC modelling effort and most of the work has been done in the last decade. Herein, we have modelled this process at

equilibrium conditions using three different reactions. In all cases, the amount of NO_x and N_2O formation reported for the CFBC pilot plant is greater than predicted by the simulation. This is an interesting point since we have initially expected to predict more NO_x than those of experimental data, but the predicted calculated values for NO_x emission levels were consistently lower than those for the experimental data.

5.2 RECOMMENDATIONS FOR FUTURE WORK

There is no doubt that our model can certainly serve as a basis for further studies. Since this has been the first attempt to simulate CFBCs using ASPEN PLUS, further studies should be performed in order to make the model more comprehensive. These studies should increase the model applicability over a wide range of conditions. Further studies are suggested in the following areas:

1. Extending and validating the model on an industrial scale while considering operation at various circulation rates, operating conditions and pressures for both coal combustion and for other solid fuels.
2. Inserting more sophisticated hydrodynamic model into the flowsheet.
3. Determining NO_x levels, and factors leading to its formation and destruction by increasing the number of discrete intervals in the bed and by including all possible chemical reactions.
4. Studying the sensibility of the key parameters influencing CFBC operation.
5. Proposing the best model to predict CO combustion rate in CFBCs.

REFERENCES

AMAND L.E., B. LECKNER, S. ANDERSSON, and L. GUSTAVSSON, "N_2O form Circulating Fluidized Bed Boilers", Paper presented at LNET1/EPA/IFP European Workshop on N_2O emissions, Lisbon, 1991.

ARENA U., A. MALANDRINO and L. MASSIMILLA, "Modelling of Circulating Fluidized Bed Combustion of a Char", Can. J. Chem. Eng., Volume 69, August, 1991.

ASPEN TECHNOLOGY, Inc., " ModelManager",Cambridge,U.S.A., 1991.

ASPEN TECHNOLOGY, Inc., "ASPEN PLUS User Guide", Cambridge, U.S.A.,August, 1988(a).

ASPEN TECHNOLOGY, Inc., "ASPEN PLUS Solids Manual", Cambridge, U.S.A., August, 1988(b).

ASPEN TECHNOLOGY, Inc., "ASPEN PLUS Notes on Interfaces and User Models ", Cambridge, U.S.A., December, 1985.

BERRUTI F., L.GODFROY and J. CHAOUKI, "The Hydrodynamics of Circulating Fluidized Beds: A Review", CHISA'93, Prague, 1993.

BIRD, R.B., W.E. STEWART and E.N. LIGHTFOOT, " Transport Phenomena ", John Wiley, 1960.

BRERETON C., J.R. GRACE, C.J. LIM, J. ZHU, R. LEGROS, J.R. MUIR, J. ZHAO, R.C. SENIOR, A. LUCKOS, N.INUMARU, J. ZHANG and I. HWANG, "Environmental Aspects, Control and Scale-up of Circulating Fluidized Bed Combustion for Application in Western Canada", The university of British Columbia, Final report, prepared for Energy, Mines and Resources Canada, December 1991.

COOPER B.R. and W.A. ELLINGSON, "The Science and Technology of Coal and Coal Utilization", Plenum press, 1984.

CONGALIDIS J.P. and C. GEORGAKIS," Multiplicity Patterns in Atmospheric Fluidized Bed Coal Combustors ", Chemical Engineering Science, Vol. 36, No.9 pp.1529-1546, 1981.

COUTURIER M.F.,"Sulphur Dioxide Removal in Fluidized Bed Combustors", Ph.D Dissertation, Queen's University,Kingston, Ontario, Canada, 1986.

CULP A.W., "Principles of Energy Conversion", McGraw-Hill, U.S.A., 1991.

DESAI D.L., F.D. FRIEDRICH and G.K. LEE, "Pilot-Scale Circulating Fluidized Bed Combustion Research Facility at Combustion and Carbonization Research Laboratory", CANMET, Ottawa.

DESAI D.L., I. LAU and E.J. ANTHONY, "Study of N_2O Formation in CRL's Circulating Fluidized Bed Combustor", Final report, ENERGY RESEARCH LABORATORIES, CANMET, Ottawa, 1991.

DOUGLAS P.L. and B.E. YOUNG," Modelling and Simulation of an AFBC Steam Heating Plant Using ASPEN/SP ", Fuel Vol.70, pp. 145-154, February,1991.

FURUSAWA T., M. KOYAMA and M. TSUJIMURA, "Nitric Oxide Reduction by Carbon Monoxide over Calcined Limestone Enhanced by Simultaneous Sulphur Retention.", Fuel, Vol. 64, pp.413-415, March 1985.

GORDON A.L. and N.R. AMUNDSON," Modelling of Fluidized Bed Reactor-IV", Chemical Engineering Science, Vol.31, pp.1163-1178, 1978.

GRACE, J.R., "Contacting Modes and Behaviour Classification of Gas-Solid and Other Two Phase Suspensions", Can. J. Chem. Eng., 64, 1986.

GRACE J.R., C.M.H BRERETON, C.J. LIM, R. LEGROS, J. ZHAO, R.C. SENIOR, R.L. WU, J.R. MUIR and R. ENGMAN, "Circulating Fluidized Bed Combustion of Western Canadian fuels", The university of British Columbia, Final report, prepared for Energy, Mines and Resources Canada, August 1989.

HANSEN P.F.B, K. DAM-JOHANSEN, L.H. BANK and K. OSTERGAARD, "Sulphur Retention on Limestone Under Fluidized Bed Combustion Conditions - an Experimental Study", Proc. 11th Int. Conf. on Fluidized Bed Combustion., ed. E.J. Anthony, ASME, Montreal, 1991

HILTUNEN M., P. KILPINEN, M. HUPA and Yam Y. LEE, "N_2O Emissions From CFB Boilers: Experimental Results and Chemical Interpretation." Proc. 11th Int. Conf. on Fluidized Bed Combustion., ed. E.J. ANTHONY, ASME, Montreal, 1991

KUNII D. and O. LEVENSPIEL, "Fluidization Engineering", 2nd. edition, Butterworth-Heinemann, 1991(a).

KUNII D. and O. LEVENSPIEL," Flow Modelling of Fast Fluidized Beds", in P.Basu, M.Horio and M.Hasatani eds., Circulating Fluidized Bed Technology III, pp.91-98,Pergamon press, Oxford, 1991(b).

LANAUZE R.D., "Fundamentals of Coal Combustion",in Fluidization, 2nd ed. J.F.Davidson, R. Clift and D. Harrison eds., Academic press, London, pp.631-674, 1985.

LECKNER B., M. KARLESSON, M. MJORNEL and U. HAGMAN, "Emissions From a 165 MW^{th} Circulating Fluidised-Bed Boiler", Journal of the Institute of Energy, 65, September 1992.

MEYERS R.A., "Coal Handbook", Marcel Dekker, U.S.A, 1981.

PAFFENBARGER, J., "Analyse des Procédés à Lit Fluidisé avec ASPEN et USRFBC", CERCHAR, FRANCE, 1991.

PATIENCE G.S. "Circulating Fluidized Bed: Hydrodynamics and Reactor Modelling", Ph.D. Dissertation, École Polytechnique de Montréal,1990.

PATIENCE G.S. and J. CHAOUKI, " Gas Phase Hydrodynamic in the Riser of a Circulating Fluidized Bed", Chemical Engineering Science, Vol.48, No.18,1993.

RAJAN R., R. KRIISHNAN and C.Y. WEN, "Simulation of Fluidized Bed Combustors-PART II", in Fluidization /Application to Coal Conversion Process,AICHE Symposium Series, No.176, Vol.74, 1978.

ROBINSON W.D., "The Solid Waste Handbook: a Practical Guide", John Wiley & Sons, 1986.

SPEIGHT J.G., "The Chemistry and Technology of Coal", Marcel Dekker, 1983.

TURNBULL E. and J.F. DAVIDSON," Fluidized Combustion of Char and Volatile from Coal", AICHE Journal Vol.30,No.6, pp.881, November,1984.

WOJTOWICZ M.A., J.A. OUDE LOHUIS J.A., P.J.J TROMP and J.A. MOULIJN, "N_2O Formation In Fluidised Bed Combustion of Coal", Proc. 11th Int. Conf. on Fluidized Bed Combustion., ed. E.J. ANTHONY, ASME, Montreal, 1991

WONG R.," Modelling the Hydrodynamic of Circulating Fluidized Bed Risers", M.A.Sc Thesis, the University of Calgary, Calgary, Canada,1991.

WYSK S.R., "Modelling a LURGI Circulating Fluid Bed Using ASPEN", ASA 82-11, Combustion Engineering,Inc., Windsor,1982.

YOUNG B.E.,"Technico-economic Evaluation of Atmospheric Fluidized Bed Combustion in Steam Production ", M.Sc.A Thesis, Queen's University, Kingston,Ontario,Canada, 1986.

ZHAO J.," Nitrogen Oxide Emissions from Circulating Fluidized Bed Combustion ",Ph.D Dissertation, the University of British Columbia, Vancouver, Canada, 1992.

APPENDICES

A.1 ASPEN PLUS input file

The following input file, which has been created by Modelmanager Rel. 3.3-4, is used to simulate a CFBC. A detailed description of steps involved in this output file can be found in ASPEN TECHNOLOGY (1988(a), 1988(b) and 1991).

```
IN-UNITS MET
DEF-STREAMS SOLID ALL
SYS-OPTIONS REUSE=NO TRACE=YES
RUN-CONTROL MAX-TIME=3600 MAX-ERRORS=200
DATABANKS ASPENPCD / SOLIDS
PROP-SOURCES ASPENPCD / SOLIDS
COMPONENTS
  H2 H2 H2 /
  O2 O2 O2 /
  N2 N2 N2 /
  C C C /
  S S S /
  COAL * COAL /
  ASH * ASH /
```

```
    SO2 O2S SO2 /
    CO CO CO /
    CO2 CO2 CO2 /
    NO NO NO /
    NO2 NO2 NO2 /
    N2O N2O N2O /
    LIME CACO3-2 LIME /
    CAO CAO CAO /
    CASO4 CASO4 CASO4 /
    H2O H2O H2O

FLOWSHEET LOWER
    BLOCK B1 IN=F OUT=S1
    BLOCK B2 IN=S1 FA1 FL OUT=S2
    BLOCK B3 IN=S2 FASH OUT=S3
    BLOCK B4 IN=S3 OUT=S4 S5
    BLOCK B5 IN=S4 S5 OUT=S6

DEF-STREAMS SOLID LOWER

FLOWSHEET SEP
    BLOCK B16 IN=S19 OUT=S20 S21
```

```
    BLOCK B17 IN=S21 OUT=S22 FASH

DEF-STREAMS SOLID SEP

FLOWSHEET UPPER
    BLOCK B6 IN=S6 FA2 OUT=S7
    BLOCK B7 IN=S7 OUT=S8
    BLOCK B8 IN=S8 OUT=S9 S10
    BLOCK B9 IN=S9 S10 OUT=S11
    BLOCK B10 IN=S11 OUT=S12
    BLOCK B11 IN=S12 OUT=S13 S14
    BLOCK B12 IN=S13 S14 OUT=S15
    BLOCK B13 IN=S15 OUT=S16
    BLOCK B14 IN=S16 OUT=S17 S18
    BLOCK B15 IN=S17 S18 OUT=S19

DEF-STREAMS SOLID UPPER
PROPERTIES SYSOP0
NC-COMPS COAL PROXANAL ULTANAL SULFANAL
NC-PROPS COAL ENTHALPY HCOALGEN / DENSITY DCOALIGT
NC-COMPS ASH PROXANAL ULTANAL SULFANAL
NC-PROPS ASH ENTHALPY HCOALGEN / DENSITY DCOALIGT
```

```
DEF-SUBS-ATTR PSD PSD
   INTERVALS 10
   SIZE-LIMITS 0.0 / 2.00000E-4 / 4.00000E-4 / 8.00000E-4 /  &
      1.00000E-3 / 2.00000E-3 / 3.00000E-3 / 4.00000E-3 /  &
      5.00000E-3 / 6.00000E-3 / .0100000

DEF-SUBS-ATTR PSDLIM PSD
   INTERVALS 10
   SIZE-LIMITS 150 <MU> / 250 <MU> / 350 <MU> / 450 <MU> /  &
      600 <MU> / 800 <MU> / 1000 <MU> / 1500 <MU> /  &
      2000 <MU> / 3000 <MU> / 5000 <MU>

DEF-SUBS CIPSD CIPSD

DEF-SUBS-CLA CIPSD

   DEF TYPE=CISOLID ATTR=PSDLIM

DEF-SUBS CIPSD1 CIPSD1

DEF-SUBS-CLA CIPSD1
   DEF TYPE=CISOLID ATTR=PSD
```

```
DEF-STREAM-C SOLID MIXED CIPSD1 CIPSD NCPSD

STREAM F
   SUBSTREAM MIXED TEMP=298 <K> PRES=1.05
   MASS-FLOW H2O 3.7
   SUBSTREAM NCPSD TEMP=298 <K> PRES=1.05
   MASS-FLOW COAL 67.3
   COMP-ATTR COAL PROXANAL ( 5.2 54.87 35.62 9 )
   COMP-ATTR COAL ULTANAL ( 9 74.5 4.3 4 0.0 3.3 5.3 )
   COMP-ATTR COAL SULFANAL ( 1.97 .08 2.6 )
   SUBS-ATTR PSD ( 0.1 0.08 0.12 0.07 0.19 0.14 0.1 0.1  &
      0.08 0.02 )

STREAM FA1
   SUBSTREAM MIXED TEMP=298 PRES=1.05 MASS-FLOW=551.0000  &
      NPHASE=1
   MOLE-FRAC O2 0.21 / N2 0.79

STREAM FA2
   SUBSTREAM MIXED TEMP=298 PRES=1.05 MASS-FLOW=248.0000  &
      NPHASE=1
   MOLE-FRAC O2 0.21 / N2 0.79
```

```
STREAM FASH
   SUBSTREAM MIXED TEMP=1140.000 PRES=1.050000
   SUBSTREAM CIPSD1 TEMP=1140.000 PRES=1.050000
   MOLE-FLOW C 57.42036
   SUBS-ATTR PSD ( 0.1 0.08 0.12 0.07 0.19 0.14 0.1 0.1  &
      0.08 0.02 )
   SUBSTREAM CIPSD TEMP=1140.000 PRES=1.050000
   MOLE-FLOW CAO 8.218800 / CASO4 4.627404
   SUBS-ATTR PSDLIM ( 0.1 0.1 0.1 0.4 0.15 0.08 0.04 0.02  &
      0.1 0.0 )
   SUBSTREAM NCPSD TEMP=1140.000 PRES=1.050000
   MASS-FLOW ASH 26000
   COMP-ATTR ASH PROXANAL ( 0 0 0 100 )
   COMP-ATTR ASH ULTANAL ( 100 0 0 0 0 0 0 )
   COMP-ATTR ASH SULFANAL ( 0 0 0 )
   SUBS-ATTR PSD ( 0.05 0.03 0.03 0.03 0.035 0.045 0.045  &
      0.09 0.335 0.31 )

STREAM FL
   SUBSTREAM CIPSD TEMP=298.1500 PRES=1.05
   MASS-FLOW LIME 19.2
   SUBS-ATTR PSDLIM ( 0.003 0.0045 0.0073 0.0172 0.033  &
```

```
    0.135 0.36 0.24 0.168 0.032 )

BLOCK B6 MIXER
  PARAM PRES=0

BLOCK B17 FSPLIT
  PARAM MAXIT=300
  MASS-FLOW FASH 23400

BLOCK B12 RSTOIC
  PARAM TEMP=1140 <K> PRES=1.05 MAXIT=300
  STOIC 1 CIPSD CAO -1 / MIXED SO2 -1 / O2 -0.5 /  &
    CIPSD CASO4 1
  CONV 1 MIXED SO2 0.6

BLOCK B15 RSTOIC
  PARAM TEMP=1140 <K> PRES=1.05 NPHASE=1 MAXIT=300
  STOIC 1 CIPSD CAO -1 / MIXED SO2 -1 / O2 -0.5 /  &
    CIPSD CASO4 1
  CONV 1 MIXED SO2 0.6

BLOCK B2 RSTOIC
```

```
    PARAM TEMP=1140.000 PRES=1.05 NPHASE=1 MAXIT=200 TOL=0.001
    STOIC 1 CIPSD1 C -1 / MIXED O2 -0.5 / CO 1
    STOIC 2 CIPSD1 S -1 / MIXED O2 -1 / SO2 1
    STOIC 3 MIXED H2 -1 / O2 -0.5 / H2O 1
    CONV 1 CIPSD1 C 0.3132
    CONV 2 CIPSD1 S 1.0
    CONV 3 MIXED H2 1

BLOCK B5 RSTOIC
    PARAM TEMP=1140.000 PRES=1.05 NPHASE=1 SERIES=YES MAXIT=200
&
       TOL=0.001
    STOIC 1 CIPSD LIME -1 / CAO 1 / MIXED CO2 1
    STOIC 2 CIPSD CAO -1 / MIXED SO2 -1 / O2 -0.5 /  &
       CIPSD CASO4 1
    CONV 1 CIPSD LIME 1
    CONV 2 MIXED SO2 0.6

BLOCK B9 RSTOIC
    PARAM TEMP=1140 <K> PRES=1.05 NPHASE=1
    STOIC 1 CIPSD CAO -1 / MIXED SO2 -1 / O2 -0.5 /  &
       CIPSD CASO4 1
```

```
CONV 1 MIXED SO2 0.6

BLOCK B1 RYIELD
  PARAM TEMP=1140 PRES=1.05 NPHASE=1 MAXIT=200 TOL=0.001
  MASS-YIELD MIXED H2 0.043 / N2 0.04 / O2 0.049 /  &
    CIPSD1 C 0.745 / S 0.033 / NCPSD ASH 0.09
  COMP-ATTR NCPSD ASH PROXANAL ( 0 0 0 100 )
  COMP-ATTR NCPSD ASH ULTANAL ( 100 0 0 0 0 0 0 )
  COMP-ATTR NCPSD ASH SULFANAL ( 0 0 0 )

BLOCK B11 REQUIL
  PARAM NREAC=3 TEMP=1140 <K> PRES=1.05 CHEM-MAXIT=300  &
    MAXIT=300
  STOIC 1 N2 -0.5 * / O2 -1 * / NO2 1 *
  STOIC 2 N2 -1 * / O2 -0.5 * / N2O 1 *
  STOIC 3 N2 -1 * / O2 -1 * / NO 2 *
  FRAC CIPSD1
  FRAC CIPSD
  FRAC NCPSD

BLOCK B14 REQUIL
  PARAM NREAC=3 TEMP=1140 <K> PRES=1.05 CHEM-MAXIT=300  &
```

```
    MAXIT=300
  STOIC 1 N2 -0.5 * / O2 -1 * / NO2 1 *
  STOIC 2 N2 -1 * / O2 -0.5 * / N2O 1 *
  STOIC 3 N2 -1 * / O2 -1 * / NO 2 *
  FRAC CIPSD1
  FRAC CIPSD
  FRAC NCPSD

BLOCK B4 REQUIL
  PARAM NREAC=3 TEMP=1140 <K> PRES=1.05 NPHASE=1 &
    CHEM-MAXIT=500 MAXIT=500
  STOIC 1 N2 -0.5 * / O2 -1 * / NO2 1 *
  STOIC 2 N2 -1 * / O2 -0.5 * / N2O 1 *
  STOIC 3 N2 -1 * / O2 -1 * / NO 2 *
  FRAC CIPSD1
  FRAC CIPSD
  FRAC NCPSD

BLOCK B8 REQUIL
  PARAM NREAC=3 TEMP=1140 <K> PRES=1.05 NPHASE=1 &
    CHEM-MAXIT=300 MAXIT=100
  STOIC 1 N2 -0.5 * / O2 -1 * / NO2 1 *
```

```
STOIC 2 N2 -1 * / O2 -0.5 * / N2O 1 *
STOIC 3 N2 -1 * / O2 -1 * / NO 2 *
FRAC CIPSD1
FRAC CIPSD
FRAC NCPSD

BLOCK B10 RCSTR
SUBROUTINE KINETICS=SUM
USER-VECS NREAL=4
INT VALUE-LIST=0
REAL VALUE-LIST=1.121E-3 200.0 23.0 0.9718
PARAM VOL=275.0 TEMP=1140.000 PRES=1.050000 MB-MAXIT=300
STOIC 1 CIPSD1 C -1 / MIXED O2 -0.5 / CO 1
STOIC 2 MIXED CO -1 / O2 -0.5 / CO2 1

BLOCK B13 RCSTR
SUBROUTINE KINETICS=SUM
USER-VECS NREAL=4
INT VALUE-LIST=0
REAL VALUE-LIST=1.121E-3 300.0 23.0 0.976
PARAM VOL=274.4 TEMP=1140 <K> PRES=1.05 MB-MAXIT=300
STOIC 1 CIPSD1 C -1 / MIXED O2 -0.5 / CO 1
```

```
    STOIC 2 MIXED CO -1 / O2 -0.5 / CO2 1

BLOCK B3 RCSTR
    SUBROUTINE KINETICS=SUM
    USER-VECS NREAL=4
    INT VALUE-LIST=0
    REAL VALUE-LIST=1.121E-3 200.0 23.0 0.82
    PARAM VOL=178.1 TEMP=1140.000 PRES=1.05 MB-MAXIT=300
    STOIC 1 CIPSD1 C -1 / MIXED O2 -0.5 / CO 1
    STOIC 2 MIXED CO -1 / O2 -0.5 / CO2 1

BLOCK B7 RCSTR
    SUBROUTINE KINETICS=SUM
    USER-VECS NREAL=4
    INT VALUE-LIST=0
    REAL VALUE-LIST=1.121E-3 300 23.0 0.9165
    PARAM VOL=137.6 TEMP=1140 PRES=1.05 MB-MAXIT=300
    STOIC 1 CIPSD1 C -1 / MIXED O2 -0.5 / CO 1
    STOIC 2 MIXED CO -1 / O2 -0.5 / CO2 1

BLOCK B16 CYCLONE
    SIMULATION DIAM=0.61
```

CONV-OPTIONS

PARAM STATE=H

WEGSTEIN MAXIT=300 WAIT=2 QMIN=-1E10 QMAX=1 ACCELERATE=10

NACCELERATE=0

TEAR

TEAR FASH 0.01 STATE=H

A.2 User-supplied kinetic subroutine (Fortran block SUM.FOR)

This block is the external kinetic subroutine developed from the simulation model in chapter 3. The information needed for the block is obtained from the ASPEN plus subroutines and the Fortran block "F-1"(Appendix A.3). The developed kinetic model in Fortran code is presented below:

```
      SUBROUTINE SUM (SOUT,NSUBS,IDXSUB,ITYPE,NINTK,INTK,NREALK,
     1                REALK,IDS,NPO,NBOPST,NIWK,IWK,NWK,WK,NC,NR,
     2               STOIC,RATES)
C
      IMPLICIT REAL*8(A-H,O-Z)
C
      DIMENSION SOUT(40),IDXSUB(NSUBS),ITYPE(NSUBS),INTK(NINTK),
     1          REALK(NREALK),IDS(2,1),NBOPST(6,NPO),IWK(NIWK),
     2          WK(NWK),STOIC(NSUBS,NC,NR),RATES(32)
C
      COMMON /USER/ RMISS,IMISS,NGBAL,IPASS,IRESTR,ICONVG,LMSG,
     1             LPMSG,KFLAG,NHSTRY,NRPT,NTRMNL
C
      COMMON /NCOMP/ NCC,NNCC,NCQ
      COMMON /IDSCC/ IDSCC(2,1)
      COMMON /IDSNCC/ IDSNCC(2,1)
```

```
      COMMON /MW/ XMW(1)
      COMMON /XFLASHZ/ ALKMAX,AKMAX,AKMIN,ATMAX,ATMIN,
     *                 APMAX,EXPMAX,DLOGMN,XSOLMX,DIVMIN
C
      COMMON /STWORK/ NRETN,NIRETN,NHXF,NHYF,NWYF,NSTW,KK1,KK2,
     1          KZ1,KZ2,KA1,KA2,KRET,KRSC,MF,MX,MX1,MX2,MY,MCS,MNC,
     2            MHXF,MHYF,MWY,MRETN,MIM,MIC,MIN,MPH,MIRETN
C
      COMMON /STWKWK/ NCPM,NCPCS,NCPNC,NTRIAL,IDUM3(2),TCALC,
     *                 PCALC,VCALC,QCALC,BETCAL,RDUM(21),RESLTS(1)
C
      DATA RD/1E-5/,ROCHAR/2267/,EPSIC/0.30/
C
      DIMENSION INDX(1)
      EQUIVALENCE (INDX(1),RESLTS(1))
      DIMENSION CONC(20),F(20)
      TK=SOUT(NCC+2)
C     WRITE(NRPT,*) ' TK=', TK
      PPAS=SOUT(NCC+3)
C
C     WRITE(NRPT,*) 'NCC=',NCC
C     WRITE(NRPT,*) 'S1-2',(SOUT(I),I=1,2)
```

```
C     WRITE(NRPT,*) 'S3-4',(SOUT(I),I=3,4)
C     WRITE(NRPT,*) 'S5-6',(SOUT(I),I=5,6)
C     WRITE(NRPT,*) 'S7-8',(SOUT(I),I=7,8)
C     WRITE(NRPT,*) 'S9-10',(SOUT(I),I=9,10)
C     WRITE(NRPT,*) 'S11-12',(SOUT(I),I=11,12)
C     WRITE(NRPT,*) 'S13-14',(SOUT(I),I=13,14)
C     WRITE(NRPT,*) 'S15',SOUT(15),'S16',SOUT(16)
C     WRITE(NRPT,*) 'SOUT=',(SOUT(I),I=17,18)
C     WRITE(NRPT,*) 'SOUT=',(SOUT(I),I=19,21)
C
      CALL VOLV(TK,PPAS,RESLTS(MY),NCPM,INDX(MIM),NBOPST,3,1,VOLM,
     *          D2,KER)
C
      VOLMIN=1./VOLM
C
C     WRITE(NRPT,*) 'VOLMIN=',VOLMIN,'VOLM=',VOLM
C
      FLOWTN= SOUT(NCC+1)
C     WRITE(NRPT,*) 'FLOWTN=',FLOWTN
C
      DO 200 I=1,NCC
      CONC(I)= SOUT(I)*VOLMIN/FLOWTN
```

```
      F(I)=SOUT(I)/FLOWTN
C     WRITE(NRPT,*) 'F(I)=',F(I)
  200 CONTINUE
C
C     WRITE(NRPT,*) 'CONC=',CONC(2)
C     WRITE(NRPT,*) 'CONC=',CONC(7)
C     WRITE(NRPT,*) 'CONC=',CONC(15)
C     WRITE(NRPT,*) 'CONC=',(CONC(I),I=10,12)
C     WRITE(NRPT,*) 'CONC=',(CONC(I),I=13,15)
C     WRITE(NRPT,*) 'CONC=',(CONC(I),I=16,20)
C
      RKCR=1.55E7*DEXP(-1.5E4/TK)
C
      RC=REALK(1)
      A=(3*RKCR*RC/RD)**0.5
      PIE=3.141592654
      A1=(2.*PIE*A)/360.
C
      ETAO2=DABS((3./(A**2))*(A/DTAN(A1)-1))
C
      FCHAR=REALK(2)
      S2TOT=REALK(3)
```

```
      EPSILON=REALK(4)
C
      R123=3*ETAO2*RKCR*(1-EPSILON)*FCHAR*CONC(2)/
     1     (ROCHAR*RC*(1-EPSIC)*S2TOT)
C
      R223=1.8E13*DEXP(-12588.12/TK)*(F(2)**0.5)
     1     *F(7)*(F(15)**0.5)*VOLMIN*(0.013/TK)*EPSILON
C
C     WRITE(NRPT,*) 'EPSILON=',REALK(4)
C     WRITE(NRPT,*) '1-R123=',R123
C     WRITE(NRPT,*) '1-R223=',R223
C
C
C     REACTION RATES IN MIXED-FLOW
C
      RATES(1)=0.0
      RATES(2)=-0.5*(R123+R223)
      RATES(3)=0.0
      RATES(4)=0.0
      RATES(5)=0.0
      RATES(6)=0.0
      RATES(7)=R123-R223
```

```
      RATES(8)=R223
      RATES(9)=0.0
      RATES(10)=0.0
      RATES(11)=0.0
      RATES(12)=0.0
      RATES(13)=0.0
      RATES(14)=0.0
      RATES(15)=0.0
C
C
C     REACTION RATES IN SOLID-FLOW (CIPSD1)
C
      RATES(16)=0.0
      RATES(17)=0.0
      RATES(18)=0.0
      RATES(19)=-R123
      RATES(20)=0.0
      RATES(21)=0.0
      RATES(22)=0.0
      RATES(23)=0.0
      RATES(24)=0.0
      RATES(25)=0.0
```

```
      RATES(26)=0.0
      RATES(27)=0.0
      RATES(28)=0.0
      RATES(29)=0.0
      RATES(30)=0.0
C
C
C     REACTION RATES IN SOLID FLOW (CIPSD)
C
      DO 155 I=31,45
      RATES(I)=0.0
  155 CONTINUE
C
C
C     REACTION RATES IN NON CONVENTIONAL STREAM
C
      RATES(46)=0.0
      RATES(47)=0.0
C     WRITE(NRPT,*) 'RATES',(RATES(I),I=1,3)
C     WRITE(NRPT,*) 'RATES',(RATES(I),I=4,6)
C     WRITE(NRPT,*) 'RATES',(RATES(I),I=7,9)
C     WRITE(NRPT,*) 'RATES',(RATES(I),I=10,12)
```

```
C     WRITE(NRPT,*) 'RATES',(RATES(I),I=13,15)
C     WRITE(NRPT,*) 'RATES',(RATES(I),I=16,18)
C     WRITE(NRPT,*) 'RATES',(RATES(I),I=20,21)
C     WRITE(NRPT,*) 'RATES',(RATES(I),I=22,24)
C     WRITE(NRPT,*) 'RATES',(RATES(I),I=24,27)
C     WRITE(NRPT,*) 'RATES',(RATES(I),I=28,30)
C     WRITE(NRPT,*) 'RATES',(RATES(I),I=31,32)
      RETURN
      END
```

A.3 Fortran codes listing

Along with the unit operation blocks provided by ASPEN PLUS, four complete Fortran programs, an external subroutine for the kinetic models, and three internal fortran blocks were used in the simulation. The required data necessary to execute the Fortran blocks were collected from ASPEN PLUS streams. The Fortran codes contain the following four blocks which are required to accurately model CFBCs. The first block, "SUM.FOR", is the external kinetic subroutine developed from the simulation model in chapter 3 for both gas/solid and gas/gas reactions. The developed kinetic model in Fortran code was presented in Appendix A.2.

The second fortran block, called "F-1", when integrated with the ASPEN PLUS input file, calculates the residence time of char particles in the CFBC. This calculation is then required in order to execute the external subroutine as mentioned above. The developed program coded in Fortran is presented below:

```
FORTRAN F-1
  DEFINE FS2C MASS-FLOW STREAM=S2 SUBSTREAM=CIPSD1  &
     COMPONENT=C
  DEFINE FASHC MASS-FLOW STREAM=FASH SUBSTREAM=CIPSD1  &
     COMPONENT=C
  DEFINE FCHAR1 BLOCK-VAR BLOCK=B3 VARIABLE=VALUE-LIST  &
     SENTENCE=REAL ELEMENT=2
```

```
DEFINE S201 STREAM-VAR STREAM=S2 SUBSTREAM=CIPSD1 &
   VARIABLE=MASS-FLOW
DEFINE S202 STREAM-VAR STREAM=S2 SUBSTREAM=CIPSD &
   VARIABLE=MASS-FLOW
DEFINE S203 STREAM-VAR STREAM=S2 SUBSTREAM=NCPSD &
   VARIABLE=MASS-FLOW
DEFINE S202D STREAM-VAR STREAM=S2 SUBSTREAM=CIPSD &
   VARIABLE=MASS-DENSITY
DEFINE SA202 STREAM-VAR STREAM=FASH SUBSTREAM=CIPSD &
   VARIABLE=MASS-FLOW
DEFINE SA203 STREAM-VAR STREAM=FASH SUBSTREAM=NCPSD &
   VARIABLE=MASS-FLOW
DEFINE SA201 STREAM-VAR STREAM=FASH SUBSTREAM=CIPSD1 &
   VARIABLE=MASS-FLOW
DEFINE SA202D STREAM-VAR STREAM=FASH SUBSTREAM=CIPSD &
   VARIABLE=MASS-DENSITY
DEFINE S2TOT BLOCK-VAR BLOCK=B3 VARIABLE=VALUE-LIST &
   SENTENCE=REAL ELEMENT=3
DEFINE FCHAR2 BLOCK-VAR BLOCK=B7 VARIABLE=VALUE-LIST &
   SENTENCE=REAL ELEMENT=2
DEFINE S7TOT BLOCK-VAR BLOCK=B7 VARIABLE=VALUE-LIST &
   SENTENCE=REAL ELEMENT=3
```

```
      DEFINE FCHAR3 BLOCK-VAR BLOCK=B10 VARIABLE=VALUE-LIST  &
        SENTENCE=REAL ELEMENT=2
      DEFINE S11TOT BLOCK-VAR BLOCK=B10 VARIABLE=VALUE-LIST  &
        SENTENCE=REAL ELEMENT=3
      DEFINE FCAHR4 BLOCK-VAR BLOCK=B13 VARIABLE=VALUE-LIST  &
        SENTENCE=REAL ELEMENT=2
      DEFINE S15TOT BLOCK-VAR BLOCK=B13 VARIABLE=VALUE-LIST  &
        SENTENCE=REAL ELEMENT=3
C
C
F     FCHAR1=FS2C+FASHC
F     FCHAR2=FCHAR1
F     FCHAR3=FCHAR1
F     FCHAR4=FCHAR1
C
F     WRITE(NRPT,*) 'FCHAR1=' ,FCHAR1
F     WRITE(NRPT,*) 'FCHAR2=' ,FCHAR2
C
F     ASHD=0.8
F     CHARD=2.267
C
F     S2SUM=0.001*(S201/CHARD+S202/S202D+S203/ASHD)
```

```
C
F     IF(SA201.NE.0.0) GO TO 50
F     IF(SA202.NE.0.0) GO TO 60
F     SASUM=0.001*(SA203/ASHD)
F     GO TO 200
C
F 50  IF(A202.NE.0.0) GO TO 100
F     SASUM=0.001*(SA201/CHARD+SA203/ASHD)
F     GO TO 200
C
F 60  SASUM=0.001*(SA202/SA202D+SA203/ASHD)
F     GO TO 200
C
F 100 SASUM=0.001*(SA201/CHARD+SA202/SA202D+SA203/ASHD)
C
F 200 S2TOT=S2SUM+SASUM
F     S7TOT=S2TOT
F     S11T0T=S2TOT
F     S15TOT=S2TOT
C
F     WRITE(NRPT,*) 'S7TOT=',S7TOT,'S2TOT=',S2TOT
   EXECUTE BEFORE BLOCK B3
```

The third block, "HYDRO", is inserted into the ASPEN PLUS input file to calculate the mean void fraction in each section of the upper region and in the dense bed of the CFBC. The developed program, in Fortran code, is presented below:

```
FORTRAN HYDRO
   DEFINE BEDV BLOCK-VAR BLOCK=B3 VARIABLE=VOL
SENTENCE=PARAM
   DEFINE BEDV1 BLOCK-VAR BLOCK=B7 VARIABLE=VOL
SENTENCE=PARAM
  DEFINE BEDV2 BLOCK-VAR BLOCK=B10 VARIABLE=VOL &
     SENTENCE=PARAM
  DEFINE BEDV3 BLOCK-VAR BLOCK=B13 VARIABLE=VOL &
     SENTENCE=PARAM
  DEFINE VOIDL BLOCK-VAR BLOCK=B3 VARIABLE=VALUE-LIST &
     SENTENCE=REAL ELEMENT=4
  DEFINE VOIDU1 BLOCK-VAR BLOCK=B7 VARIABLE=VALUE-LIST &
     SENTENCE=REAL ELEMENT=4
  DEFINE VOIDU2 BLOCK-VAR BLOCK=B10 VARIABLE=VALUE-LIST &
     SENTENCE=REAL ELEMENT=4
  DEFINE VOIDU3 BLOCK-VAR BLOCK=B13 VARIABLE=VALUE-LIST &
     SENTENCE=REAL ELEMENT=4
C
```

```
F       AREA=3.14159*(BEDD/2.)**2.
F       VOID(1)=0.82
C
C       ----------------------GS {KG/M2.SEC} -----------
C
F       GS=50.0
F       DPDL=DP*(ROG*(ROSL-ROG)*G/VISCO**2.)**(1./3.)
F       UTDL=1./(18.0/(DPDL**2.)+(2.335-1.744*PHIS)/(DPDL**0.5))
F       UT=UTDL*(ROG**2.0/(VISCO*(ROSL-ROG)*G))**(-1./3.)
F       FR= UGAS(4)/(G*BEDD)**0.5
F       FRT= UT/(G*BEDD)**0.5
F       PHI=1.0+5.6/FR+0.47*FRT**0.41
F       VOID(4)=1.0/(PHI*GS/(UGAS(4)*ROSL)+1.0)
F       A=5.0/UGAS(4)
F       BEDZ=-1./A*DLOG((VOIDS-VOID(4))/(VOIDS-VOID(1)))
C
C
F       BDL(1)=BEDV/AREA/1000.
F       BDL(2)=BEDZ/3.
F       BDL(3)=2.*BEDZ/3.
F       BDL(4)=BEDLT-BEDZ-BDL(1)
C
```

```
C
F       BEDVV(1)=BEDV
F       BEDVV(2)=AREA*BDL(2)*1000
F       BEDVV(3)=AREA*BDL(3)*1000
F       BEDVV(4)=AREA*BDL(4)*1000
C
C
F       VOID(2)=VOIDS+(VOIDS-VOID(1))/(BDL(1)*A)*(EXP(-A*BDL(2))-1)
F       VOID(3)=VOIDS+(VOIDS-VOID(1))/(BDL(2)*A)*
F     *         (EXP(-A*BEDZ)-EXP(-A*BDL(2)))
C
C
F       VOIDL =VOID(1)
F       VOIDU1=VOID(2)
F       VOIDU2=VOID(3)
F       VOIDU3=VOID(4)
C
C
F       BEDV1=BEDVV(2)
F       BEDV2=BEDVV(3)
F       BEDV3=BEDVV(4)
C
```

```
F       WRITE(NRPT,*) 'UGAS=',(UGAS(I), I=1,4)
F       WRITE(NRPT,*) 'BEDL(I)=',(BEDL(I), I=1,4)
F       WRITE(NRPT,*) 'BEDVV(4)=',(BEDVV(I),I=1,4)
F       WRITE(NRPT,*) 'VOID(I)=',(VOID(I),I=1,4)
    EXECUTE AFTER BLOCK B3
```

The fourth block of Fortran codes, "SO2", calculates the sulphur capture efficiency in each section of the upper region and in the dense bed. This program is nested in ASPEN PLUS input file so that all the RSTOIC reactors used to model the SO_2 capture in the bed can be executed. The program, coded in Fortran, is presented below:

FORTRAN SO2

```
F       COMMON /USER1/ UGAS
C
F       REAL*8 PMRSB(10,10), PMRSN(10,10), DAVE(10), TAVE(10),
F   1         UGAS(4), BEDL(4),RSO2(10), YSO2(10), ETASO2(10),
F   2         DS(10),XCAO(10),AKL(10),KV,BDL(4),VOID(4),
F   3         BEDVV(4)
C
C
F       DATA DS/0.02,0.03,0.04,0.05,0.07,0.09,0.125,0.175,0.25,0.4/
```

```
F       DATA R/8.205E-2/,ROL/3313.61/,SIGMP/0.001/,BETA/0.16/
F       DATA BEDD/0.405/,BEDLT/6.7/,KV/8E-4/
F       DATA EPSI/0.52/,VCAO/1.69E-2/
F       DATA G/9.8/,ROSL/3350./,ROG/0.313/,VOIDS/0.9999/
F       DATA VISCO/4.45E-4/,DP/1.25E-4/,PHIS/0.806/
F       DATA AKL/3E-3,4.5E-3,7.3E-3,1.72E-2,3.3E-2,0.135,0.36,0.24
F    *          ,0.168,3.2E-2/
C
C
   DEFINE FA1 STREAM-VAR STREAM=FA1 SUBSTREAM=MIXED  &
      VARIABLE=MOLE-FLOW
   DEFINE FA2 STREAM-VAR STREAM=FA2 SUBSTREAM=MIXED  &
      VARIABLE=MOLE-FLOW
   DEFINE FL STREAM-VAR STREAM=FL SUBSTREAM=CIPSD  &
      VARIABLE=MASS-FLOW
   DEFINE FLASH MASS-FLOW STREAM=FASH SUBSTREAM=CIPSD  &
      COMPONENT=CAO
   DEFINE  BEDT  BLOCK-VAR  BLOCK=B3  VARIABLE=TEMP
SENTENCE=PARAM
   DEFINE  BEDV  BLOCK-VAR  BLOCK=B3  VARIABLE=VOL
SENTENCE=PARAM
   DEFINE  BEDV1  BLOCK-VAR  BLOCK=B7  VARIABLE=VOL
```

```
SENTENCE=PARAM
   DEFINE BEDV2 BLOCK-VAR BLOCK=B10 VARIABLE=VOL  &
      SENTENCE=PARAM
   DEFINE FSO2IN MOLE-FLOW STREAM=S2 SUBSTREAM=MIXED  &
      COMPONENT=SO2
   DEFINE  ETAL  BLOCK-VAR  BLOCK=B5  VARIABLE=CONV
SENTENCE=CONV  &
      ID1=2
   DEFINE  ETAU1  BLOCK-VAR  BLOCK=B9  VARIABLE=CONV
SENTENCE=CONV  &
      ID1=1
   DEFINE ETAU2 BLOCK-VAR BLOCK=B12 VARIABLE=CONV  &
      SENTENCE=CONV ID1=1
   DEFINE ETAU3 BLOCK-VAR BLOCK=B15 VARIABLE=CONV  &
      SENTENCE=CONV ID1=1
C
C
C       CALCULATION OF SO2 CAPTURE EFFICIENCY IN THE CFBC
C
C  %%%%%%%%%%%%%% FAIR1,FAIR2,FSO20(KMOLE/SEC) %%%%%%
C
F    FAIR1=FA1/3600
```

```
F     FAIR2=FA2/3600
F     FSO20=FSO2IN/3600
C
C              % % % % % % % % % % % % % % %  F L I M E  (K G / S E C)
%%%%%%%%%%%%%%%%%%%%%%%%%%%%
C
F     FLIME=FL/3600
F     FLS2=FLASH/3600
C
C              % % % % % % % % % % % % % % %  B E D V L  ( C M )
%%%%%%%%%%%%%%%%%%%%%%%%%%%%%%%%
C
F     BEDVL=BEDV/1000
C
C     WRITE(NRPT,*) 'FAIR1=',FAIR1,'FAIR2=',FAIR2
C     WRITE(NRPT,*) 'FLIME=',FLIME
C     WRITE(NRPT,*) 'BEDVL=',BEDVL,'FSO20=',FSO20
C     WRITE(NRPT,*) 'FLS2=',FLS2
C
F     NL=10
F     NF=7
C       %%%%%%%%%%%%%%%%%%%%  BEDP ( BED PRESSURE, ATM)
```

```
%%%%%%%%%%%%%%
F     BEDP=1.05
F     AREA=3.14159*(BEDD/2.)**2.
F     BEDL(1)=BEDVL/AREA
F     BEDL(2)=BEDV1/AREA/1000
F     BEDL(3)=BEDV2/AREA/1000
F     BEDL(4)=BEDLT-(BEDL(1)+BEDL(2)+BEDL(3))
C     WRITE(NRPT,*) 'BEDL=',(BEDL(I),I=1,4)
C
F     CONC=BEDP/(R*BEDT)
C     WRITE(NRPT,*) 'CONC=',CONC
C
F     UGAS(1)=FAIR1/(AREA*CONC)
F     UGAS(2)=UGAS(1)+FAIR2/(AREA*CONC)
F     UGAS(3)=UGAS(2)
F     UGAS(4)=UGAS(3)
C
C     WRITE(NRPT,*) 'UGAS(I)=',(UGAS(I),I=1,4)
C
F     RSO2(1)=FSO20/BEDVL
C
F     YSO2(1)=0.00005
```

```
F     MF=NF+1
C
F     DO 1 I=1,10
F     PMRSB(1,I)=AKL(I)
F  1  CONTINUE
C
C
F     XX=0.0
F     M=2
F     XCAO(1)=0.0
C
F     DO 2 J=1,4
F     SUMST=0.0
C
F     DO 3 I=MF,NL
F     SUMST=SUMST+PMRSB(J,I)
F     PMRSN(J,I)=(1-BETA/(NL-NF))*PMRSB(J,I)
F  3  CONTINUE
C
F     SUMS=SUMST*BETA/((NL-NF)*NF)
C     WRITE(NRPT,*) 'SUMST=',SUMST
C     WRITE(NRPT,*) 'SUMS=',SUMS
```

```
C
F     DO 4 I=1,NF
F     PMRSN(J,I)=PMRSB(J,I)+SUMS
F  4  CONTINUE
C
F     SUMP=0.0
C
F     DO 5 I=1,10
F     SUMP=SUMP+PMRSN(J,I)/DS(I)
F  5  CONTINUE
C
F     DAVE(J)=1.0/SUMP
C
F     DO 10 I=1,10
F     PMRSB(J+1,I)=PMRSN(J,I)
F 10  CONTINUE
F 2   CONTINUE
C
C
C
F     DO 23 J=1,4
F     A1=3.33E-4*DEXP(-0.0113*DAVE(J))
```

```
C     WRITE(NRPT,*) 'A1=',A1
F     ALPHA=35*(DAVE(J))**0.30
C     WRITE(NRPT,*) 'ALPHA=',ALPHA
F     TAVE(J)=ROL*SIGMP*AREA*BEDL(J)/(FLIME*(1-XX))/0.56
C
C
F  8  XCAO1=TAVE(J)-1/A1*DLOG(1+6*ALPHA*CONC
F    *       *YSO2(J)/(DAVE(J)*KV)*(DEXP(A1*TAVE(J))-1))
C
F     XCAO2 = DAVE(J)/(6*ALPHA*CONC*YSO2(J))-1/KV
F     XCAO(M)= VCAO/(1-EPSI)*XCAO1/XCAO2
C     WRITE(NRPT,*) 'XCAO1=',XCAO1,'XCAO2=',XCAO2
C
C     WRITE(NRPT,*) 'XCAO=',XCAO(M)
F     RSO21=XCAO(M)*FLIME*(1-XX)/(100*BEDL(J)*AREA)
C     WRITE(NRPT,*) 'RSO21=',RSO21
F     YSO2JN=ABS(BEDL(J)*(RSO2(J)-RSO21)/(CONC*UGAS(J)))
C     WRITE(NRPT,*) 'YSO2JN=',YSO2JN
F     IF(DABS((YSO2JN-YSO2(J))/YSO2JN).LE.1E-2) GO TO 7
F     YSO2(J)=YSO2JN
F     GO TO 8
C
```

```
F  7  ETASO2(J)=1-YSO2(J)*CONC*UGAS(J)/(RSO2(J)*BEDL(J))
F     IF(J.EQ.4) GO TO 9
C
F     YSO2(J+1)=YSO2(J)
F     RSO2(J+1)=BEDL(J)*(RSO2(J)-RSO21)/BEDL(J+1)
C     WRITE(NRPT,*) 'RSO2(J+1)=',RSO2(J+1)
F     XX=XX+XCAO(M)*(1-XCAO(M-1))
F     M=M+1
C
C
C
F 23  CONTINUE
C
F  9  ETAL = ETASO2(1)
F     ETAU1= ETASO2(2)
F     ETAU2= ETASO2(3)
F     ETAU3= ETASO2(4)
C
C
C     WRITE(NRPT,*) 'ETAL=',ETAL,'ETAU1=',ETAU1
C     WRITE(NRPT,*) 'ETAU2=',ETAU2,'ETAU3=',ETAU3
C     WRITE(NRPT,*) 'DAVE=',(DAVE(I),I=1,4)
```

```
F     WRITE(NRPT,*) 'TAVE=',(TAVE(I),I=1,4)
C     WRITE(NRPT,*) 'RSO2=',(RSO2(I),I=1,4)
F     WRITE(NRPT,*) 'ETASO2=',(ETASO2(I),I=1,4)
C     WRITE(NRPT,*) 'PMRSB=',((PMRSB(J,I),I=1,10),J=1,4)
C     WRITE(NRPT,*) 'PMRSN=',((PMRSN(J,I),I=1,10),J=1,4)
C
C
C
C
      EXECUTE BEFORE BLOCK B3
```

A.4 A typical calculation for r_c

The equation 3.3 is used to calculate the mean radius of the char particles. In order to do so, the weight fraction vector of char particles and char particle radius vector are required.

Table A.4.1 Particle Size Distribution of Char Particles

Interval	$r_c(k)$,m	$P_k(r_c(k))$
1	10^{-4}	0.1
2	$3*10^{-4}$	0.08
3	$6*10^{-4}$	0.12
4	$9*10^{-4}$	0.07
5	$1.5*10^{-3}$	0.19
6	$2.5*10^{-3}$	0.14
7	$3.5*10^{-3}$	0.1
8	$4.5*10^{-3}$	0.1
9	$5.5*10^{-3}$	0.08
10	$8*10^{-3}$	0.02

$$r_C = \frac{1}{\sum \frac{P_k(r_C(K))}{r_C(K)}} \tag{3.3}$$

Using the information given in table A.4.1, the mean radius particle size is calculated by equation 3.3:

$$r_C = 0.557 \text{ mm}$$

During the convergence process, ASPEN PLUS adjusts the value of the $P_k(r_C(k))$ which then used to calculate r_C according to equation 3.3.

A.5 Description of CANMET 0.8 MWth CFBC pilot plant

Pilot-Scale Circulating Fluidized Bed Combustion Research Facility at Combustion and Carbonization Research Laboratory, CANMET

BY

D.L. Desai*, F.D. Friedrich* and G.K. Lee*
* CANMET, Energy, Mines and Resources Canada, Ottawa, Ontario, K1A 0G1

INTRODUCTION

Energy, Mines and Resources Canada has a broad range of inhouse and contract research and demonstration program to expedite the advancement and application of fluidized bed combustion technology in the industrial and utility sectors in Canada. A pilot-scale circulating fluidized bed combustion (CFBC) research facility has been built at the Combustion and Carbonization Research Laboratory (CCRL) at CANMET's Bells Corners Complex as a part of the inhouse R and D program. This state-of-the-art facility is suitable for testing a wide variety of solid and heavy liquid fuels and combustible industrial waste products. In conjunction with the existing bubbling FBC research facility, it will be used to generate data base on the combustion performance of various Canadian fuels, useful for predicting optimum design of full-scale units.

PILOT-SCALE RESEARCH FACILITY

The major components of CCRL's CFBC are shown in Fig. 1. It comprises mainly a combustor, hot cyclone, inclined L-valve, flue gas

cooler, baghouse, fuel and limestone charging and feed systems, and forced and induced draft blowers.

COMBUSTOR AND CYCLONE

The combustor is 7 m high having an id of 405 mm and a cross-sectional area of 0.13 m^2. It is refractory- lined to allow operation up to 1100°C. Four retractable bayonet type cooling tubes penetrating the combustor roof permit the control of combustor temperature at various heat input rates and superficial gas velocities. Varying the penetration depth and the number of tubes permits heat extraction to be varied from 0 to 65% of thermal input.

The air distributor consists of a plate 17 mm thick x 305 mm diam fitted with eighteen 25.4 mm diam. pipes which serve as bubble caps. The primary and secondary air is supplied by a forced draft blower having a capacity of 1300 m^3 at 70 kPag. There is provision to supply secondary air to the combustor at five different elevations. An 1800 MJ/h startup burner fired with propane or natural gas is provided to preheat the combustor with mildly fluidized solids to the ignition temperature of the test fuel.

The cyclone also refractory- lined for operation at up to 1100°C, has an id of 600 mm. It is connected to the combustor via a short refractory- lined duct and an expansion joint. The solids captured in the cyclone are recirculated to the combustor by means of an inclined L-valve. Purge air can be supplied at any one or more of the five locations on the L-valve to initiate, maintain and control the

recirculation of solids.

FLUE GAS COOLER

Flue gas exiting the cyclone passes into a water-to-gas plate-and-shell-type heat exchanger via a refractory lined duct. The heat exchanger is designed to cool the flue gas to 175°C at maximum heat input rate. It is so designed that 50% of the cooling surface can be isolated permitting operation at low loads without excessive flue gas cooling.

BAGHOUSE

The cooled flue gas from the heat exchanger is ducted to a baghouse. An air to cloth ratio of 2.5:1, selected to provide ample capacity to handle high dust loadings. The baghouse product can either be collected in a barrel or recycled pneumatically into the lower section of the combustor to improve the sorbent utilization and combustion efficiency. The flue gas from the baghouse is exhausted to the atmosphere by means of an induced draft fan and a stack.

FUEL AND SORBENT FEED SYSTEM

The fuel and sorbent feed systems are designed to load the feedstocks into their respective bins and inject them into the combustor while controlling and monitoring the feed rates. A bucket

elevator charges the fuel into the fuel bin. The fuel then flows, via a vibrating bin discharger to a variable speed weigh feeder which meters and controls the fuel feed rate. An air lock valve on the discharge side of the feeder prevents the backflow of combustion gases and delivers the fuel to a screw conveyor.

The sorbent is charged into the sorbent bin by means of a vacuum type pneumatic conveying system with bag filters and a cyclone. Sorbent flow is controlled by a variable speed screw prefeeder and metered by a constant speed weigh feeder. The sorbent bin also has a vibrating discharger. As in the fuel feed system a rotary air lock valve at the discharge end of the weigh feeder isolates the weigh feeder from the backflow of combustion gases and delivers the sorbent to the same screw conveyor which accepts the fuel.

The feedstocks from the screw conveyor are fed into the combustor at about 400 mm above the air nozzles via a 100 mm diam inclined feed chute. The chute is purged with combustion air to offset the effect of combustor backpressure and assist the flow of the feedstocks. Alternatively, the feedstocks from the screw conveyor can be discharged into a water cooled screw which would convey the feedstocks directly into the combustor at about 1.52 m above the air nozzles.

INSTRUMENTATION AND CONTROL

The instrument system is designed to monitor and extract all important data and record automatically on a data logger, chart recorders and on a floppy disk using a data acquisition system. The

temperatures and pressures at strategic locations throughout the rig will be monitored using thermocouples and pressure transducers respectively. The air flow rates will be measured by orifice plates and the water flow rates will be measured using electronic turbine flow meters.

The flue gas will be monitored continuously for concentrations of CO, CO_2, SO_2, NOx and O_2.

There will be two basic types of controls; interlocking and modulating. Logic control will provide interlocks for the startup burner, forced and induced draft fans, fuel and sorbent feeders, airlock valves and screw conveyors. Modulating control will regulate the fuel and sorbent rate, fuel-to-air ratio, secondary-to-total-air ratio, sorbent-to-fuel ratio, system draft, cooling water flow and temperature.

SUMMARY

The capabilities of the CFBC at CCRL are summarized in Table 1. It has excellent flexibility in terms of input conditions as well as comprehensive instrumentation, measurement and control capabilities. It is a powerful tool for fostering the rapid implementation of CFBC and to meet challenges presented by the need to utilize new and low grade fuels and sorbents while meeting increasingly stringent environmental emission regulations.

TABLE 1 - RANGE OF OPERATING CONDITIONS

PARAMETER	RANGE
INPUT	
Combustion Temp.	1,100 °C
Heat Input	0.8 MWt
Excess O_2	2 - 10%
Superficial vel.	2 - 8 m/s
Ca/S Molar Ratio	2.5
Primary Air	35 - 80%
Secondary Air	20 - 65%
Loopseal Air	0 - 5%
Cooling Tube Area	0 - 3 m^2
* OUTPUT	
CO_2	10 - 18%
CO	100 - 1,500 ppm
NOx	50 - 300 ppm
SO_2	50 - 7,000 ppm
Solid Streams	
Ash	75 - 100%
Sorbent	0 - 30%
Bed Solids	0 - 10%

* output parameters will be dependant on fuel composition

ÉCOLE POLYTECHNIQUE DE MONTRÉAL
3 9334 00278677 8